



**DEVELOPMENT AND ANALYSIS OF KENAF CORE
CONCRETE FOR ACOUSTICAL AND MECHANICAL
PROPERTIES**

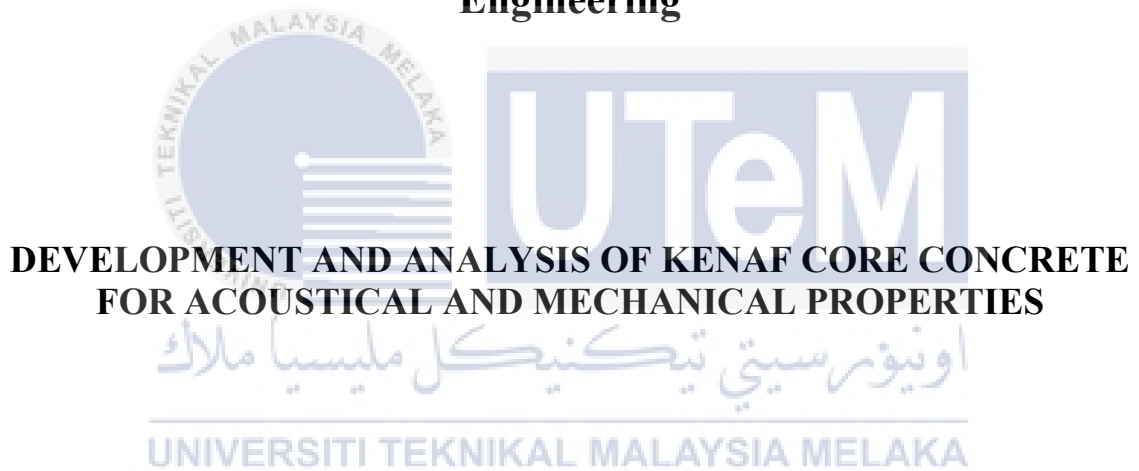


**BACHELOR MANUFACTURING ENGINEERING
TECHNOLOGY(BMMP) HONOURS**

2024



**Faculty of Industrial and Manufacturing Technology and
Engineering**



**DEVELOPMENT AND ANALYSIS OF KENAF CORE CONCRETE
FOR ACOUSTICAL AND MECHANICAL PROPERTIES**

SHAZMIN BINTI SHAHRULZAMAN

Bachelor of Manufacturing Engineering Technology (BMMP) with Honours

2024

**DEVELOPMENT AND ANALYSIS OF KENAF CORE CONCRETE FOR
ACOUSTICAL AND MECHANICAL PROPERTIES**

SHAZMIN BINTI SHAHRULZAMAN

**A thesis submitted
in fulfillment of the requirements for the degree of
Bachelor of Manufacturing Engineering Technology (BMMP) with Honours**



Faculty of Industrial and Manufacturing Technology and Engineering

UNIVERSITI TEKNIKAL MALAYSIA MELAKA

2024

DECLARATION

I declare that this thesis entitled “Development and Analysis of Kenaf Core Concrete for Acoustical and Mechanical Properties” is the result of my own research except as cited in the references. The Choose an item. has not been accepted for any degree and is not concurrently submitted in candidature of any other degree.

Signature

:



Name

:

SHAZMIN BINTI SHAHRULZAMAN

Date

:

10 January 2024

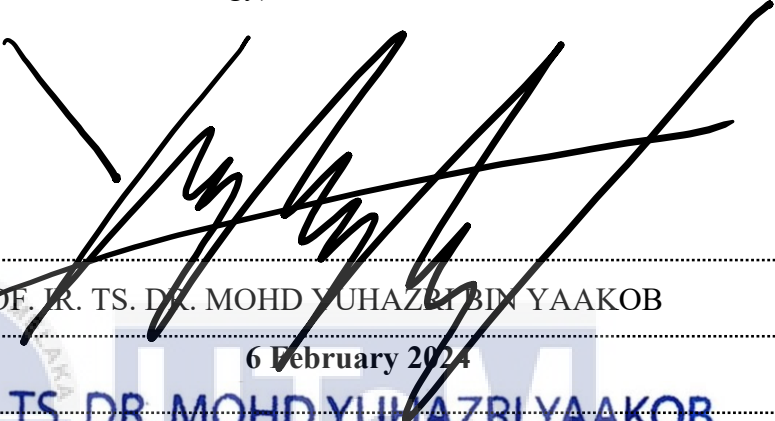
UNIVERSITI TEKNIKAL MALAYSIA MELAKA

اونيورسيتي تيكنيكل مليسيا ملاك



APPROVAL

I hereby declare that I have checked this thesis and in my opinion, this thesis is adequate in terms of scope and quality for the award of the Bachelor of Mechanical and Manufacturing Engineering Technology (Process and Technology) with Honours.

Signature : 
Supervisor Name : PROF. IR. TS. DR. MOHD YUHAZRI BIN YAAKOB
Date : 6 February 2024


IR. TS. DR. MOHD YUHAZRI YAAKOB
Associate Professor
Faculty of Industrial and Manufacturing Technology and Engineering
Universiti Teknikal Malaysia Melaka

اونيورسيتي تيكنيكل مليسيا ملاك
UNIVERSITI TEKNIKAL MALAYSIA MELAKA

DEDICATION

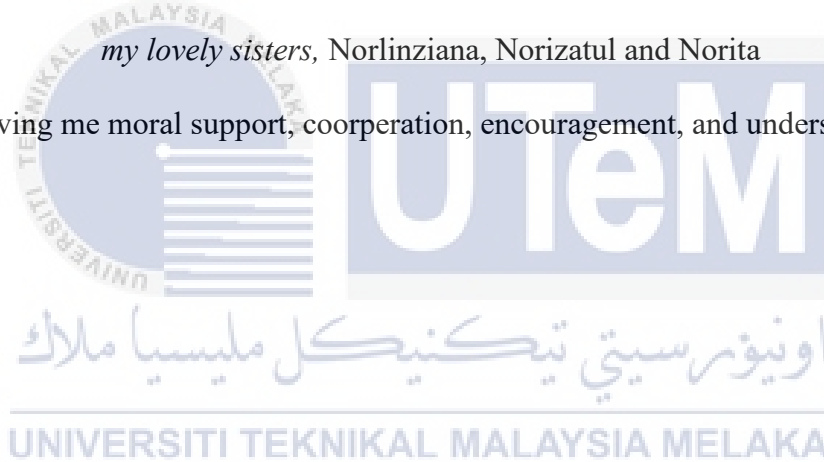
Dedicated to

my beloved father, Shahrulzaman Bin Ramli

my appreciated mother, Nooraini Binti ohd Noor

my lovely sisters, Norlinziana, Norizatul and Norita

for giving me moral support, cooperation, encouragement, and understanding.



ABSTRACT

Natural fibers, including kenaf core, possess significant potential as substitutes for synthetic fibers due to their high absorbency, eco-friendliness, cost-effectiveness, and low density. Consequently, the utilization of natural fibers has garnered considerable interest among researchers, particularly in industries such as aircraft and automotive, where they are employed as reinforcements to create composite materials with superior strength properties. However, despite extensive research on natural fiber-based composites for concrete reinforcement, there have been limited studies exploring the application of kenaf core in acoustical panels. This study aimed to experimentally examine the effects of different sizes of kenaf core in the development of acoustical panels. Five sizes of kenaf core were used, namely 30 mm, 20 mm, 10 mm, 20 mesh, and 40 mesh. The kenaf core served as reinforcement, while concrete served as the matrix. The raw materials were blended according to the matrix composition of kenaf core and concrete and molded using 3D printing technology. The acoustic panels were then subjected to impedance tube testing, which focused on evaluating their performance across low, medium, and high frequency ranges. The fabrication process and testing methods adhered to the ASTM E1050-09 standard, while the mechanical strength test utilized compressive testing based on ASTM 109. The morphological features of the samples were analyzed using a scanning electron microscope (SEM). Overall, kenaf core exhibits tremendous potential for development due to its cost-effectiveness, high performance, and biodegradability. Cement (C) performs well in compressive strength, while C5 shows a substantial 131.58 % improvement over Foam (F) at 30 mm thickness. C3 excels in flexural strength, with a remarkable 178.43 % increase over Foam. In sound absorption, C5 leads at 500 Hz, while C3 outperforms at 1500 Hz. These findings highlight kenaf core's diverse strengths for different applications.

ABSTRAK

Oleh kerana ciri serapan mereka yang tinggi, mesra alam, kos rendah dan ketumpatan rendah, serat semula jadi seperti teras kenaf boleh digunakan sebagai pengganti gentian sintetik. Oleh itu, minat penyelidik terhadap pembangunan serat semula jadi telah meningkat, dan industri pengeluar seperti pesawat dan kenderaan telah menggunakan bahan komposit yang mempunyai sifat kekuatan yang tinggi. Banyak penyelidik juga mengkaji serat semula jadi berasaskan komposit dalam bentuk konkrit, tetapi sedikit kajian telah dijalankan mengenai teras kenaf untuk kegunaan akustik. Siasatan eksperimen kajian ini bertujuan untuk mengkaji teras kenaf yang berbeza yang digunakan dalam pembinaan panel akustik. Dalam kajian ini, lima (5) saiz teras kenaf telah digunakan: 30 mm, 20 mm, 10 mm, 20 mesh dan 40 mesh. Konkrit digunakan sebagai matriks dan keras kenaf digunakan sebagai tetulang. Di dalam mesin acuan 3D, bahan mentah dicampur dengan komposisi matriks kenaf teras yang diisi dengan konkrit. Ujian tiub impedans digunakan untuk menguji panel akustik. Julat frekuensi rendah, sederhana dan tinggi adalah kategori biasa panel akustik. Selain itu, semua kaedah fabrikasi dan ujian adalah berdasarkan piawaian ASTM E1050-09. Walau bagaimanapun, pemeriksaan mekanikal yang digunakan ialah pemeriksaan mampatan berdasarkan ASTM 109. Seterusnya, ciri morfologi dikenal pasti melalui pengimbasan elektron mikroskop (SEM). Pada akhirnya, kajian ini menunjukkan bahawa kenaf mempunyai potensi yang tinggi untuk pembangunan. Simen (C) berprestasi baik dalam kekuatan mampatan, sementara C5 menunjukkan peningkatan yang besar sebanyak 131.58 % berbanding polystyrene foam (F) pada ketebalan 30 mm. C3 unggul dalam kekuatan fleksural, dengan peningkatan yang mengagumkan sebanyak 178.43 % berbanding polystyrene. Dalam penyerapan bunyi, C5 memimpin pada 500 Hz, sementara C3 lebih baik pada 1500 Hz.

UNIVERSITI TEKNIKAL MALAYSIA MELAKA

ACKNOWLEDGEMENTS

In the Name of Allah, the Most Gracious, the Most Merciful

I express my deepest gratitude to Allah the Almighty, my Creator and Sustainer, for the blessings and guidance I have received throughout my life. I would also like to extend my thanks to Universiti Teknologi Malaysia Melaka (UTeM) for providing me with the research platform. Additionally, I am grateful to the Malaysian Ministry of Higher Education (MOHE) for their financial support.

I would like to offer my heartfelt appreciation to my primary supervisor, Prof. Madya Ir. Dr. Ts. Mohd Yuhazri bin Yaakob, for his invaluable assistance, guidance, and inspiration. His unwavering patience in imparting wisdom and providing support will forever be cherished.

I am also deeply grateful to my family, particularly my parents, for their constant love, support, and prayers. Their unwavering belief in me has been a source of strength throughout my journey.

Lastly, I would like to express my gratitude to all those who have helped, supported, and inspired me during my time as a bachelor's degree student. Your contributions have been invaluable in shaping my academic and personal growth.



TABLE OF CONTENTS

	PAGE
DECLARATION	
APPROVAL	
DEDICATION	
ABSTRACT	ii
ABSTRAK	iii
ACKNOWLEDGEMENTS	iv
TABLE OF CONTENTS	v
LIST OF TABLES	viii
LIST OF FIGURES	x
LIST OF SYMBOLS AND ABBREVIATIONS	xv
LIST OF APPENDICES	xvi
CHAPTER 1 INTRODUCTION	1
1.1 Background	1
1.2 Problem Statement	4
1.3 Objectives	6
1.4 Scope of Research	6
CHAPTER 2 LITERATURE REVIEW	7
2.1 Introduction of Composite	7
2.1.1 Natural fibre composites	9
2.1.2 Classification of natural fibre composite	11
2.2 Kenaf	13
2.2.1 Introduction to kenaf fibre and kenaf core	14
2.2.2 Kenaf fibre structural application	16
2.2.3 Application of kenaf in cementitious composite	17
2.3 Concrete	18
2.3.1 Structure	19
2.3.2 Properties	20
2.3.3 Natural fibre-reinforced concrete	21
2.4 Acoustic Panel	22
2.4.1 Synthetic sound absorber	24
2.4.2 Acoustic properties of kenaf fibre	27
2.4.3 Acoustic properties of Kenaf core particleboard	28
2.4.4 Acoustic characterization	29

2.5	Mechanical Properties and Sound Absorbing Testing	30
2.5.1	Compressive strength test	31
2.5.2	Three point flexural testing	32
2.5.3	Impedance tube testing	33
2.6	Summary	35
2.6.1	Natural fibre composites	40
2.6.2	Classification of natural fibre composite	43
CHAPTER 3		45
3.1	Overview of Methodology	45
3.2	Raw Material Preparation	47
3.2.1	Kenaf core as reinforcement material	47
3.2.2	Foam as reinforcement material	49
3.2.3	Cement as matrix material	50
3.3	Preparation of Mould	51
3.4	Fabrication Process	53
3.4.1	3D printing machine	53
3.5	Preparation of the Composition	53
3.6	Curing Process	55
3.7	Cutting Process	56
3.8	Testing	56
3.8.1	Compression test	57
3.8.2	Flexural test	57
3.8.3	Impedence tube test	58
3.9	Scanning Electron Microscope	59
CHAPTER 4		61
4.1	Fabrication and Characteristics of Concrete with Different Composition	61
4.2	Mechanical Properties of Kenaf Core Concrete Sample	65
4.2.1	Flexural performance	65
4.2.2	Compression performance	75
4.3	Summary of Mechanical Properties on Kenaf Core Reinforced Concrete	85
4.4	Sound Absorption Performance of Concrete With Different Air Gap.	86
4.4.1	Sound absorption performance without air gap	86
4.4.2	Sound absorption performance with 10 mm air gap	88
4.4.3	Sound absorption performance with 20 mm air gap	89
4.4.4	Sound absorption performance with 30 mm air gap	91
4.5	Sound Absorption Performance of Different Thickness of Samples	93
4.5.1	Sample C1	93
4.5.2	Sample C2	99
4.5.3	Sample C3	105
4.5.4	Sample C4	112
4.5.5	Sample C5	118
4.5.6	Sample F	124
4.5.7	Sample C	130
4.6	Summary of Performance of Sound Absorption of Kenaf Core Concrete	136
4.7	The best composite composition for sound absorption	138
4.8	Summary	140

CHAPTER 5	143
5.1 Conclusion	143
5.2 Recommendations	145
5.3 Sustainability Element	145
5.4 Commercial Value and Potential	147
5.5 Research Achievement	147
REFERENCES	149
APPENDICES	158



LIST OF TABLES

TABLE	TITLE	PAGE
Table 2.1	Manufacturing techniques and applications of some fibres with their matrix materials (Rajak et al., 2019)	8
Table 2.2	Advantages and disadvantages of natural fibres (Asyraf et al., 2022)	11
Table 2.3	Thickness and mass of the kenaf fibre, (Lim et al., 2018)	15
Table 2.4	Compressive strength of Banana-reinforced concrete (Chandramouli et al.,2019)	22
Table 2.5	5 A summary of raw material fibre sound absorbers (Yang et al., 2020)	26
Table 2.6	Sound absorption coefficient of kenaf fibre (Lim et al., 2018)	28
Table 2.7	Reported work on the application of kenaf	36
Table 2.1	Manufacturing techniques and applications of some fibres with their matrix materials (Rajak et al. 2019)	39
Table 2.2	Advantages and disadvantages of natural fibres (Asyraf et al. 2022)	42
Table 3.1	The properties of kenaf core	47
Table 3.2	Price of kenaf core based on mesh size	48
Table 3.3	The properties of foam beads	50
Table 3.4	Properties of cement	51
Table 3.5	Samples of kenaf core and concrete	54
Table 3.6	ASTM standard for mechanical and sound testing	56

Table 4.1 Cracking pattern and failure mode sample

69

Table 4.2 Form of crack for kenaf core concrete

78



LIST OF FIGURES

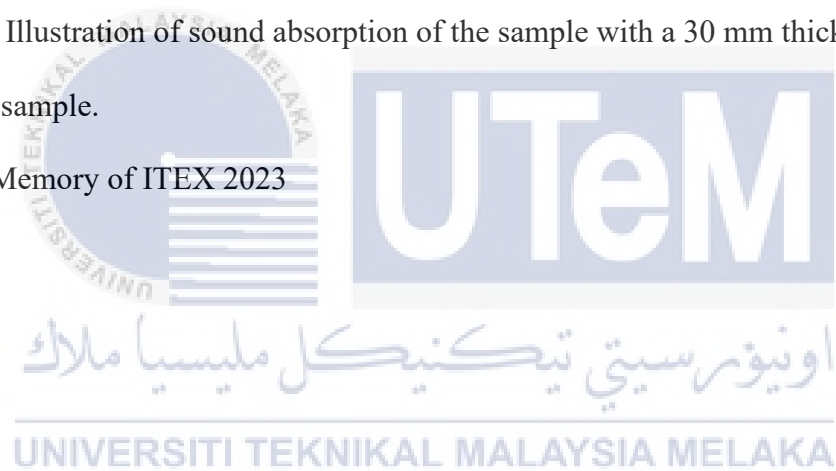
FIGURE	TITLE	PAGE
Figure 2.1	Figure 2.1 Natural fibre (a) kenaf, (b) sisal, (c) coir, (d) wool, (e) jute, (f) hemp (Rajak et al., 2019)	10
Figure 2.2	Classification of Natural Fibres (Noryani et al., 2018)	12
Figure 2.3	Life Cycle of Polymer Composite (Arjmandi et al., 2021)	13
Figure 2.4	Kenaf plant (Afzal et al., 2022)	14
Figure 2.5	: Absorption coefficient of kenaf fibre of varied thickness with constant bulk density of 93.5 kg/m ³ (Lim et al. 2018)	15
Figure 2.6	Kenaf core size (a) 20 mesh, (b) 40 mesh (Radzuan et al., 2019)	16
Figure 2.7	: Kenaf fibre-reinforced concrete (a) 0%, (b) 1%, (c) 1.5%, (d) 2% (Zhou et al., 2020)	18
Figure 2.8	Structures that are made of UHPC concrete (a) Curved panels of the Louis Vuiton Foundation Building in Paris (b) The “fishnet” façade of the Mucem museum in Marseille (Van, 2018)	20
Figure 2.9	Synthetic sound absorber (a) Glass wool (b) Rock wool (Yap et al., 2021)	25
Figure 2.10	Arenga pinnata tree (Yahya et al., 2017)	26
Figure 2.11	Non-woven kenaf fibre (Yuhazri et al., 2018)	28
Figure 2.12	Kenaf core particleboard for sound absorption test (Saad and Kamal, 2012)	29
Figure 2.13	Natural woven fibre sheets fabric (a) Jute, (b) Hemp, (c) cotton (Jirattanasomkul e al., 2019)	31
Figure 2.14	Compression test setup (Jirawattanasomkul et al., 2019)	32

Figure 2.15 Flexural Testing Setup for concrete samples (C.Zhou et al., 2020)	33
Figure 2.16 : Impedance tube setup (a) measurement (b) BC-MPP sample setup (Chin et al., 2018)	33
Figure 2.17 Absorption coefficient (a) Ijuk absorption coefficient (b) Kenaf absorption coefficient (Yahya et al., 2017)	35
Figure 2.1 Figure 2.1 Natural fibre (a) kenaf ; (b) sisal ; (c) coir ; (d) wool ; (e) jute ; (f) hemp (Rajak et al., 2019)	41
Figure 2.2 Classification of Natural Fibres (Noryani et al. 2018)	43
Figure 3.1 Flowchart of methodology	46
Figure 3.2 Size of kenaf core, (a) 30 mm (b) 20 mm (c) 10 mm (d) 40 mesh (e) 20 mesh	48
Figure 3.3 Foam Beads	49
Figure 3.4 A bag of 50 kg cement	51
Figure 3.5 Dimension of mould size for the composite cylindrical samples	52
Figure 3.6 Dimension of mould size for the composite cube samples	52
Figure 3.7 UP PLUS 2 3D printer	53
Figure 3.8 The mixtures of sample in mould	55
Figure 3.9 Figure 3.10 Samples being soaked in water	55
Figure 3.10 Bosch GWS 060 Professional Angle Grinder	56
Figure 3.11 Standard of compression testing setup	57
Figure 3.12 Standard of flexural testing setup	58
Figure 3.13 Impedance Tube Testing	59
Figure 3.14 Scanning electron microscope (SEM)	60
Figure 4.1 Trial sample of mixing kenaf core and concrete	62

Figure 4.2 Sample condition (a) acceptable (b) reject	62
Figure 4.3 Fabricaton steps (a) cement add (b) manual mixing (c) final mix concrete	63
Figure 4.4 Concrete curing in mould	63
Figure 4.5 Selected sample after cured (a) cement with too much water (b) good samples that mix well	64
Figure 4.6 The examples rejected samples	64
Figure 4.7 The curing process (a) at initial state a (b) at 28 days of submerging	65
Figure 4.8 The examples of three-point flexural test	66
Figure 4.9 The condition of sample after the testing	66
Figure 4.10 Comparison of flexural strength of each size of ratio	67
Figure 4.11 The small crack propagation line after flexural test of 20 mesh	68
Figure 4.12 SEM analysis for 30 mm of kenaf core and concrete	68
Figure 4.13 SEM analysis for polystyrene foam reinforced concrete	69
Figure 4.14 SEM analysis for 10 mm KC	69
Figure 4.15 Setup for compression test	76
Figure 4.16 Condition of the samples after testing	76
Figure 4.17 Comparison of compression performance for the ratio size of kenaf core	77
Figure 4.18 Mechanical Performance Summary Graph.	85
Figure 4.19 The graph of sound absorption with no gap coefficient with the comparison of all samples	88
Figure 4.20 The graph of sound absorption with 10 mm air gap coefficient with the comparison of all samples	89
Figure 4.21 The graph of sound absorption with 10 mm air gap coefficient with the comparison of all samples	91

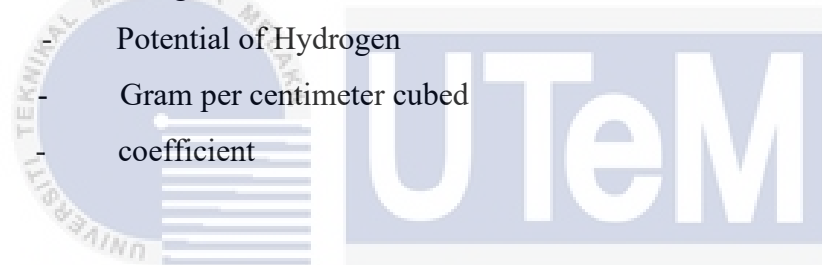
Figure 4.22 The graph of sound absorption with 30 mm air gap coefficient with the comparison of all samples	92
Figure 4.23 Graph of sound coefficient of C1 without air gap	94
Figure 4.24 Graph of sound coefficient of C1 with 10 mm air gap.	96
Figure 4.25 Graph of sound coefficient of C1 with 20 mm air gap.	97
Figure 4.26 Graph of sound coefficient of C1 with 30 mm air gap.	99
Figure 4.27 Graph of sound coefficient of C2 with no air gap.	100
Figure 4.28 Graph of sound coefficient of C2 with 10 mm air gap.	102
Figure 4.29 Graph of sound coefficient of C2 with 20 mm air gap.	103
Figure 4.30 Graph of sound coefficient of C2 with 30 mm air gap.	105
Figure 4.31 Graph of sound coefficient of C3 with no air gap	107
Figure 4.32 Graph of sound coefficient of C3 with 10 mm air gap	108
Figure 4.33 Graph of sound coefficient of C3 with 20 mm air gap	110
Figure 4.34 Graph of sound coefficient of C3 with 30 mm air gap	111
Figure 4.35 Graph of sound coefficient of C4 with no air gap	113
Figure 4.36 Graph of sound coefficient of C4 with 10 mm air gap	115
Figure 4.37 Graph of sound coefficient of C4 with 20 mm air gap	116
Figure 4.38 Graph of sound coefficient of C4 with 30 mm air gap	118
Figure 4.39 Graph of sound coefficient of C5 with no air gap	119
Figure 4.40 Figure 4.34 Graph of sound coefficient of C5 with 10 mm air gap	121
Figure 4.41 Graph of sound coefficient of C5 with 20 mm air gap	122
Figure 4.42 Graph of sound coefficient of C5 with 30 mm air gap	124
Figure 4.43 Graph of sound coefficient of F with no air gap	125
Figure 4.44 Graph of sound coefficient of F with 10 mm air gap	127

Figure 4.45 Graph of sound coefficient of F with 20 mm air gap	128
Figure 4.46 Graph of sound coefficient of F with 30 mm air gap	130
Figure 4.47 Graph of sound coefficient of C no air gap	131
Figure 4.48 Graph of sound coefficient of C 10 mm air gap	133
Figure 4.49 Graph of sound coefficient of C 20 mm air gap	135
Figure 4.50 Graph of sound coefficient of C 30 mm air gap	136
Figure 4.51 The best samples for sound absorption (a) 30 mm thickness of C5 (b) 30 mm thickness of C3	140
Figure 4.52 Illustration of sound absorption of the sample with a 30 mm thickness sample.	142
Figure 5.1 Memory of ITEX 2023	148



LIST OF SYMBOLS AND ABBREVIATIONS

D,d	-	Diameter
ASTM	-	American Society for Testing and Materials
SEM	-	Scanning Electron Microanalysis
UTeM	-	Universiti Teknikal Malaysia Melaka
°C	-	Celsius Degree
wt.%	-	Weight Percentage
GC	-	Geopolymer Concrete
Mm	-	Milimeter
Kg	-	Kilogram
pH	-	Potential of Hydrogen
g/cm^3	-	Gram per centimeter cubed
α	-	coefficient



اونيورسيتي تيكنيكل مليسيا ملاك

UNIVERSITI TEKNIKAL MALAYSIA MELAKA

LIST OF APPENDICES

APPENDIX	TITLE	PAGE
APPENDIX A		158
APPENDIX B		159



CHAPTER 1

INTRODUCTION

1.1 Background

Nowadays, composite is widely used for different application such as in the automotive industry aerospace, sports, transportation and infrastructure (Rizkalla et al., 2015). Jawaid and Thariq (2018) describes that composite as a combination of two or more materials to form a unique combination of properties. Jawaid and Thariq discovered that composite have high strength, high toughness, corrosion resistant and durable. Due to the cos of composites is higher and they are not biologically friendly, natural fibre composites is used to replace the composite materials.

Several studies have revealed that natural fibre has huge potential to replace the synthetic fibre in acoustical application. Since natural fibre comes from plant material, it becomes the main focus due to its cost, availability, low density, good mechanical properties, eco-friendliness and biodegradability characteristic as mentioned by Siakeng et al., (2019) and it offers remarkable advantages over synthetic fibre. Besides that, it can also be used as a replacement for conventional fibres, such as carbon glass, aramid and others. Zhu et al., (2013) concluded that natural fibre should have the same mechanism for acoustic absorption as other conventional synthetic fibrous materials such as glass fibre and mineral wool (Muthukumar et al., 2019). These fibres are often light and they are not harmful to human health and therefore can be used in room acoustic products and noise barrier as sound absorber.

Mohanty and Fatima (2015) have reported that so many studies have been discovered on the eco-friendly and biodegradable materials such as jute (Mohanty and Fatima 2015), hemp (Kinnane et al., 2016), cotton, coir (Fadzlita et al., 2014), banana leaf (Satyanarayana et al., 1990) and kenaf (Lim et al., 2018) for noise control applications. There are some of natural fibre such as jute, sisal, banana and coir that can be made into composite panels with a suitable resin for sound absorber application as they have low density and cost application that is similar to synthetic reinforced composites. It can be concluded that natural fibres have huge potential to replace synthetic noise materials according to their similar acoustic mechanical properties. Therefore, in this study, it focuses on kenaf plant to fabricate the acoustical panel in order to improve the existing acoustic products.

According to Sadrmanesh and Chen (2019), kenaf (*Hibiscus Cannabinus L.*), which can be developed under various climatic conditions, is an individual from the Malvaceae family. Kenaf plants can develop to a height of 2.5 m to 4.0 m under ideal temperature ranging from 22°C to 30°C and soil pH from 6.0 – 6.8 conditions. The kenaf stems's widths range from 10 to 20 mm. Harmaen et al., (2018) stated that kenaf is characterized by low density, non-abrasivity during processing, high mechanical properties and biodegradability. In the production of pulp and paper industry, kenaf utilized as an alternative to avoid damaged forests, textiles, fibreboards and non-oven mats in automotive.

Kamal (2014) stated that there are many encouragements given by Malaysian government efforts to improve the utilization of kenaf products and Malaysian Government has identified kenaf plants as the seventh commodity crops. The studies on kenaf for bio-composite are still in the early stages, although researchers from around the world have been successfully setting goals to include kenaf as one of the important resources for bio-composite researches for so many years before which is mentioned by Kamal. Furthermore, Kamal compared to the market price of kenaf fibre and synthetic fibre most used in the

current industry. Kenaf fibre has good mechanical properties and relatively cheaper which is RM 4.00 per kg compared to glass fibres are RM 18.00 per kg and it was a good choice for composite products for automotive applications. In 2010, Summerscales et al., reported that the extraction of bast fibre from the outer bark of kenaf has equivalent strength compared to other natural fibres such as jute, hemp and flax. High α -cellulose components, especially kenaf basts, which has high strength in kenaf-based products, are the main role in providing the good mechanical properties.

In addition, Abdullah et al., (2016) discovered that the kenaf core has a density of 0.10 to 0.20 g/cm^3 which is more porous compared to the bast and lighter which is also supported by Yahya et al., (2017) and Saad and Kamal (2012). Kenaf has a high hemicellulose content and lignin content is low making it becomes an ecological lignocellulosic raw material. Okuda and Sato (2004) has studied the properties of the binderless boards made from kenaf core with different type of manufacturing condition. Xu et al., (2014) reviewed the development of a low-density board compaction ratio is 1.0 with a low-density board of 0.4 g/cm^3 having the same raw material value using heat and steam processes. While, Miller et al., (1993) investigated the low-density board phenol-formaldehyde (PF) kenaf core as reinforced 0.256 g/cm^3 board density. Xu et al.,(2014) reported that the kenaf core binderless particleboards were successfully established using $0.40 - 0.65 \text{ g/cm}^3$ steam injection presses. The result from their experiment partially recognized the lightweight characteristic of the kenaf core when the board's density is low, the board's sound performance is high. It can be concluded that the kenaf core has a high potential for sound absorption and thermal insulation products. In order to generate high pressure drive, it is necessary to increase the sound efficient and conservative ways of producing sound absorption materials in automobiles, manufacturing environments and equipment. Basically, the most commercial material for production of porous sound absorber is made from synthetic fibre such as glass

wool and rock wool by Chin et al., (2018). Arenas and Crocker (2010) stated that the main elements of sound absorbing materials from asbestos based materials to synthetic fibres is due to the public health concerns. There are a lot of studies have shown that synthetic fibres such as fibre glass and rock wool cause damage to our lung tissues and leads to the risk of lung cancer after prolonged experience as these materials could scatter the dangerous floating dust particles that can easily enters our lungs and it is supported by Zhu et al., (2015). Non-biodegradable materials can contribute to the increasing of carbon dioxide and global waring (Chin et al., 2018), as well as causing pollution to our environment.

Due to these health risks, the needs of finding an alternative way such as using the natural fibre to replace synthetic fibres for sound absorption materials can be necessary. It can solve this problem in order to reserve our surrounding environment without abandoning our health concern and it has been proven experimentally and retains good sound absorption qualities. Kenaf core has a huge potential; to solve this problem because they have very low toxicity which is good for protecting the environment.

1.2 Problem Statement

There are many researches for sound absorber on the basis of natural fibre composite based and synthetic fibre. However, the research focuses on natural fibres of kenaf core is still lacking and limited as mentioned by Saad and Kamal (2012). Therefore, this research is carried out to analyse the sound absorption properties of kenaf core and kenaf fibre in acoustic applications. Moreover, the materials and equipment used to manufacture the acoustic panels based on kenaf core must be affordable and suitable in Malaysia.

Abdollah et al.,(2015) argued that the natural fibres are non-uniformity, dimensions variation and their mechanical propertird compared to synthetic fibres. Besides that, these green materials cause mechanical properties instability, loss of dimensional stability and swelling due to their high moisture absorption which indicates changes in composite weights

and dimensions. The finding is consistent with findings from past studies by Abdollah et al., which Sapuam et al., (2018) stated that moisture absorption is the major objectionable features of natural fibres causing it to swell and accelerate the loss of mechanical properties, cracks and breeds decaying fungi. Previous studies have reported that the high moisture absorption in treated composites and natural fibres for commercial fire retardants can be hygroscopic by Mokhothu et al., (2017). Polyurethane (PU) can reduce the water intake of laminate PU coated because of their good moisture resistance properties associated with its crosslinking density. Thus, in this research, noise control needs to be improved in our lives because noise can be defined as undesirable sound that disturbs our surroundings. There are so many ways to improve the noise control and one of them is by developing a sound absorber material from natural fibre composites. Tinianov (2018) found that the lack of proper treatment in offices, apartments and lecture rooms may interfere with people's unpleasant feelings in those rooms. The noise is undesirable in the person is unable to communicate or hear the conversation effectively, even though the noises not dangerous. Sound absorber is very important in order to absorb the sound vibration from outside. Consideration of the techniques used is important in order to reduce the noise from the existing components and the design of quieter product.

Due to the high demand of cement and concrete production around the world, the cement and concrete industries becoming more interested in finding alternative materials to replace the use of synthetic fibre resources with natural fibres (Jiang et al., 2018). There are many research primarily studied the properties of natural fibres that can be used to replace or mix with cement thus can lower the content of cement due to environmental issues. Since there are only few past studies related to kenaf core and concrete for sound absorption panel such as door or walls. Therefore, this research will further focus on the study about the development of acoustical panel from kenaf core and concrete.

1.3 Objectives

The objectives of this research are as the followings:

- a) To fabricate the acoustical panel made from different size of kenaf core with cement using 3d printing mould.
- b) To investigate the composite composition for acoustic and mechanical performance
- c) To propose the best composite size for optimum performance that best for acoustical panel.

1.4 Scope of Research

The scope of this research are as follows:

- a) To study the potential of kenaf core and concrete used to produce acoustical panel.
- b) This study involves five types of kenaf core which are 30 mm, 20 mm, 10 mm, 40 mesh and 20 mesh.
- c) This study will involve process of moulding and curing on kenaf core reinforced concrete before proceeding with testing.
- d) This study will determine the best size of kenaf core reinforced concrete to produce acoustical panel.
- e) To identify the mechanical strength and acoustical properties depending on the various size of kenaf core reinforced concrete.
- f) This research will included testings such as compressive test and impedance tube testing according to ASTM standard.
- g) The kenaf core reinforced concrete will be test at low, medium and high frequency range

CHAPTER 2

LITERATURE REVIEW

2.1 Introduction of Composite

According to Clyne et al. (2019), composites have become one of the most significant and versatile classes of engineering materials, alongside steels, in terms of industrial importance and range of applications. This finding is consistent with previous studies by Rajak et al. (2019), which also highlighted the widespread use of composite materials in modern technologies since the mid-20th century. Aerospace, military applications (Ngo Tri-Dung, 2020), transportation (Rubino et al., 2020), and infrastructure (Li F et al., 2019) are some of the industries where composites are extensively employed. The development of composites involves blending different materials or components to modify their properties and enhance their capabilities, as commonly practiced in the engineering industry.

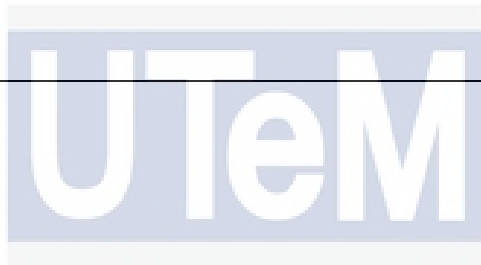
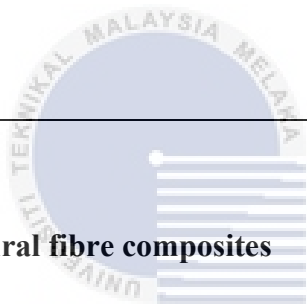
As mentioned by Ngo Tri-Dung (2020), a composite consists of three main components: the matrix, which acts as the continuous phase; the reinforcements, such as fibers, serving as the discontinuous or dispersed phase; and the interface, known as the fine interphase region. David et al. (2020) pointed out that composites possess characteristic performance traits that their individual components cannot achieve on their own. This enables the creation of lightweight designs with high stiffness and strength. Based on this rationale, the present research focuses on developing biodegradable composite materials as alternatives to non-biodegradable synthetic composites, supported by the works of Malviya et al. (2020) and Sanjay et al. (2018).

In another study, Raju et al. (2021) identified several factors influencing the development of composites, including the availability of matrix types, variety of fibers, selection of reinforcing fibers, fiber processing methods, cost of processing fibers, mechanical properties of the fibers, and procurement costs. Various surface treatments for natural fibers have been employed to enhance interfacial adhesion with the matrices and improve their mechanical properties. Rajak et al. (2019) categorized composite materials primarily into natural fibers and synthetic fibers, and the combination of these fibers with a matrix material yields hybrid composites with enhanced mechanical properties. Table 2.1 provides an overview of manufacturing techniques and applications of specific fibers with their respective matrix materials.

Table 2.1 Manufacturing techniques and applications of some fibres with their matrix materials (Rajak et al., 2019)

Material Used		Applications	Manufacturing Technique
Fiber Reinforcement	Matrix/ Binder Material		
Carbon	Polypropylene(PP), metals, ceramics, epoxy resin, Polyether ether ketone (PEEK).	Lightweight automotive products, fuel cells, satellite components, armour, sports.	Injection moulding, filament winding, resin transfer moulding (RTM).
Graphene	Polystyrene (PS), epoxy, Polyaniline (PANI).	Wind turbines, Gas tanks, aircraft/automotive parts.	Chemical vapor deposition (CVD), pultrusion, hand/spray up method.
Sisal	PP, PS, epoxy resin.	Automobile body parts, roofing sheets.	Hand lay-up, compression moulding.
Hemp	Polyethylene (PE), PP, Polyurethane(PU).	Furniture, automotive.	RTM, compression moulding.
Kenaf	Polylactic acid(PLA), PP, epoxy resin.	Tooling, bearings, automotive parts.	Compression moulding, pultrusion.

Flax	PP, polyester, epoxy.	Structural, textile.	Compression moulding, RTM, spray/ hand lay-up, vacuum infusion.
Ramie	PP, Polyolefin, PLA	Bulletproof vests, socket, prosthesis, civil.	Extrusion with injection moulding.
Rice Husk	PU, PE	Window/door frames, automotive structure.	Compression/ injection moulding
Jute	Polyester, PP	Ropes, roofing, door panels.	Hand-lay-up, compression/ injection moulding.
Coir	PP, epoxy resin, PE	Automobile structural components, building boards, roofing sheets, insulation boards.	Extrusion, injection moulding.



2.1.1 Natural fibre composites

The recent advancements in composites have amplified the demand for natural fibers and their role in mitigating acoustic disruptions. Dong (2018) research findings further highlight the favorable properties of natural fibers, such as their lightweight nature, affordability, and abundance in terms of raw materials. In 2020, Malviya et al. emphasized that reducing the reliance on fossil-based resources, particularly petroleum, can address environmental concerns. The utilization of green composites also offers substantial benefits, including a significant reduction in non-renewable energy consumption and the emission of carbon dioxide (CO₂), sulphur dioxide (SO₂), nitrogen oxide (NO_x), and carbon monoxide (CO).

Natural fibers can generally be categorized into three groups: plant fibers, mineral fibers, and animal fibers. Kurinjimalar et al. (2021) noted that plant fibers, also known as cellulose-based fibers, encompass important varieties such as cotton, flax, and hemp. Animal fibers, which are protein-based, include wool, mohair, and silk. Figure 2.1 provides a visual representation of several natural fibers.

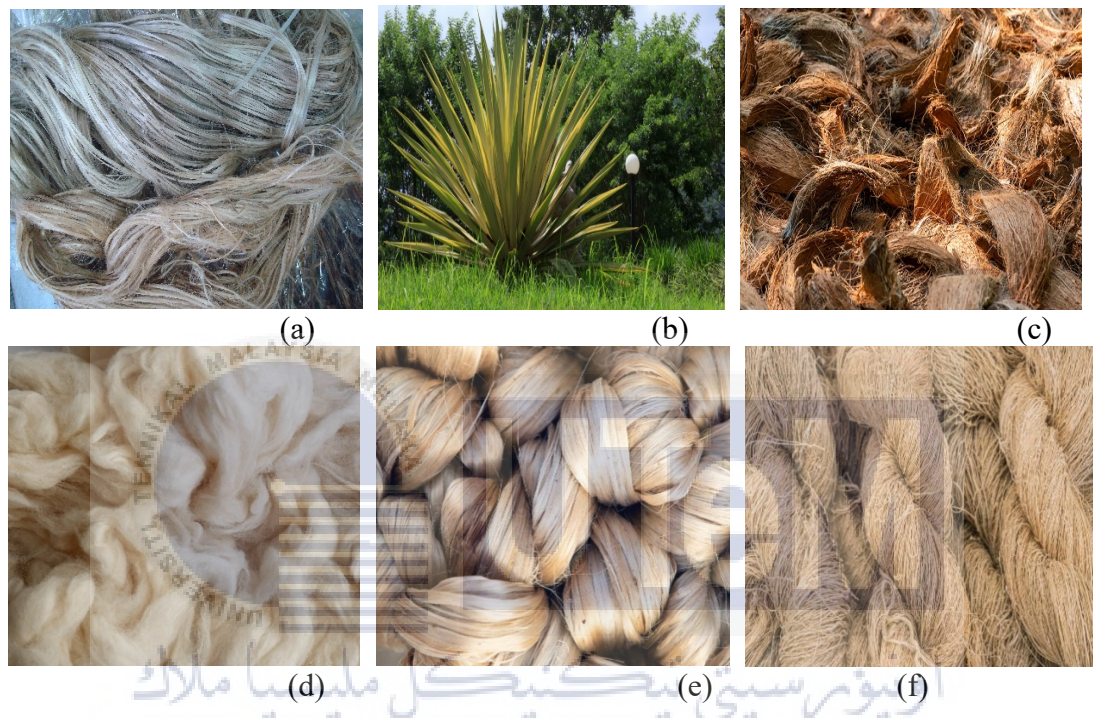


Figure 2.1 Figure 2.1 Natural fibre (a) kenaf, (b) sisal, (c) coir, (d) wool, (e) jute, (f) hemp (Rajak et al., 2019)

In a study by Sahu et al. (2020), it was demonstrated that natural fibers offer significant advantages in terms of the development of cost-effective and environmentally friendly sustainable products. Researchers are actively exploring ways to minimize the consumption of synthetic fibers, also known as man-made fibers. However, according to de Azevedo et al. (2021), the usage of natural fibers also presents certain drawbacks, such as the lack of uniform properties. This variability in properties is primarily attributed to the composition of their constituents, including cellulose, hemicellulose, and lignin. Table 2.2 shows the advantages and disadvantages of natural fibres.

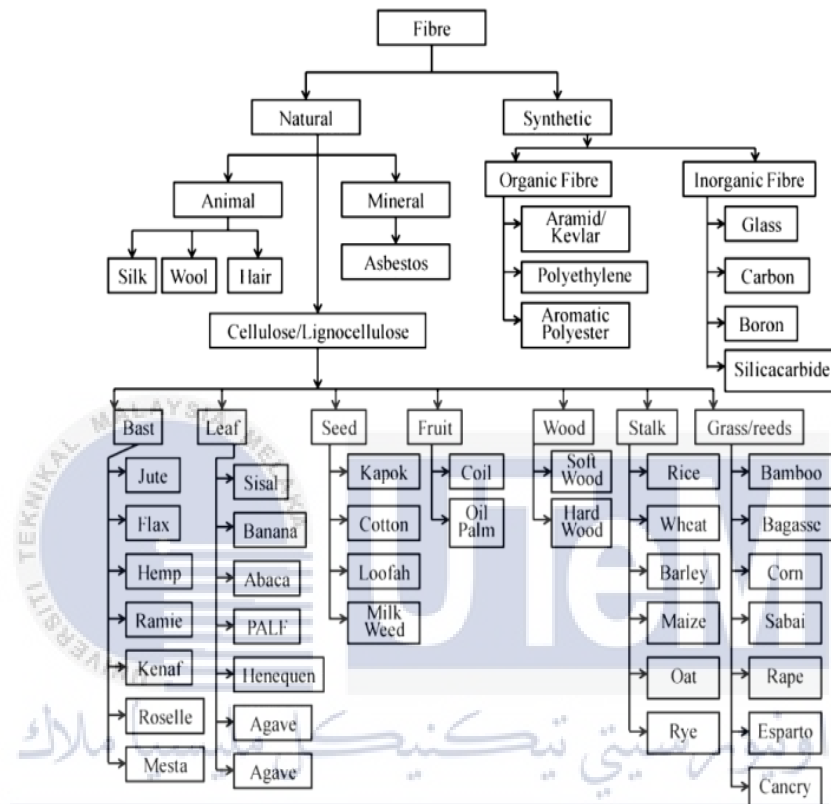
Table 2.2 Advantages and disadvantages of natural fibres (Asyraf et al., 2022)

	Advantages	Disadvantages
Natural fibres	Lightweight	Flammable
	Recyclable	Dimensional instability
	Improved specific mechanical properties	High moisture absorption
	Eco-friendly, carbon dioxide neutrality	Anisotropic behaviour
	Doesn't generate any harmful gasses during processing and low energy requirements during the production	Limited processing temperature (-200 – 230 °C)
	Good thermal properties	Sensitive to ultraviolet (UV)
	Good acoustic properties	Fungal attack and microbial attack
	Low cost, availability, renewable resources, disposal by composting	Low strength than synthetic fibres especially impact strength
	Non-abrasive and great formability	Variable quality, influenced by weather
	No dermal issue for handling	Low durability
	Safer crash behaviour in test	Poor fibre/ matrix adhesion

2.1.2 Classification of natural fibre composite

Generally, this study highlighted on plant fibres. Non-wood fibres for example like hemp, kenaf, flax and sisal have gained a mass production in the design of bio-composites

in engineering materials and it is supported by Noryani et al. (2018). Figure 2.2 demonstrated the classification of natural fibres which can be categorized to animal based, plant based and mineral based.



UNIVERSITI TEKNIKAL MALAYSIA MELAKA
 Figure 2.2 Classification of Natural Fibres (Noryani et al., 2018)

In recent years, Natural Fibers Reinforced Composites (NFRCs) referred to the component that is made from natural fibres composites and they have been applied in various sectors. While NFRCs are gaining a lot of attention in terms of business and also academia, Dhakal et al. (2021) indicated that the manufacture and use of NFRCs will improve the long-term viability of material manufacturing.

2.2 Kenaf

As noted by Lim (2018), Kenaf, scientifically known as *Hibiscus Cannabinus L.*, belongs to the Malvaceae family and shares similarities with cotton. Its stem comprises 65% inner core fiber and 35% outer bast fiber, which can be used to produce both low and high-quality pulp. Karim et al. (2020) have reported that Kenaf cultivation is widespread across more than 20 countries, with significant growth seen in China, India, and Thailand. According to Shahar et al. (2019), Kenaf can reach heights of up to 6 meters within 6 to 8 months of planting, and it has the potential to yield around six to ten tonnes of dry fiber annually. This makes Kenaf a viable substitute for other composite materials available in the market. The life cycle of a polymer composite is depicted in Figure 2.3.

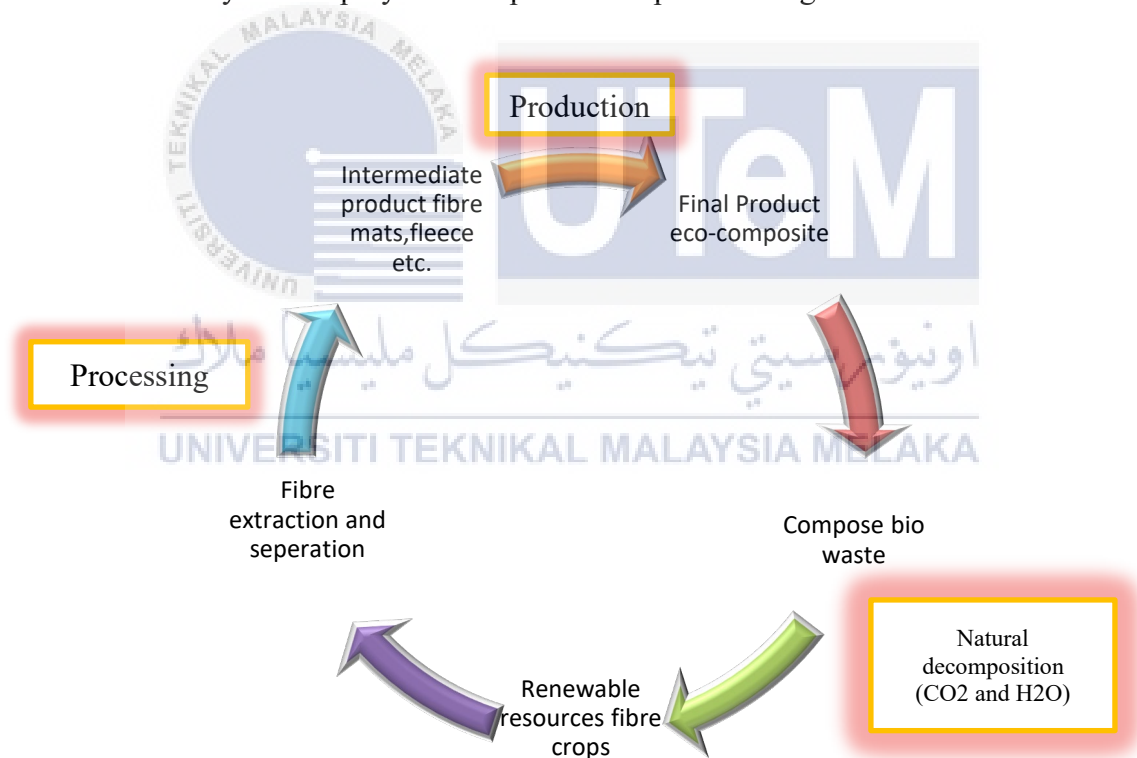


Figure 2.3 Life Cycle of Polymer Composite (Arjmandi et al., 2021)

According to Arjmandi et al. (2021), Kenaf processing is very environmental friendly which leads to a better working condition at the same time reducing the risk of dermal and

respiratory problem comparing to synthetic fibres. Figure 2.4 is a depiction of Kenaf plant itself.



Figure 2.4 Kenaf plant (Afzal et al., 2022)

A few studies has been carried on and they found out that Kenaf itself composed of diverse types of useful component for example like stalk, leaves and seeds with a variety kind of useful portions like fibres, fibre strands, proteins, oils, and allelopathic chemicals Giwa et al. (2019). The research study by Al-Mamun et al. (2023) stated that Kenaf can grow in areas with a relative humidity ratio of 68 to 82% along with the temperature that has a range in between 22.6 to 30.3 °C. In Malaysia, kenaf is still new and is still in development when it comes to the cultivation and processing the kenaf's plant itself. That is a government initiative to make a diversity from tobacco production about 10 years ago by establishing the National Kenaf and Tobacco Board. However, it was greatly inspired by the Malaysians.

2.2.1 Introduction to Kenaf Fibre and Kenaf Core

Many researches have been characterising kenaf fibre and its composite in recent years. Radzuan et al. (2020) claim that the extruded, moulded, and non-woven products

made from kenaf bast fibre have good flexural strength and good tensile strength. According to Arjmandi et al. (2021), cellulose, hemicellulose, lignin, waxes, and a few water-soluble chemicals make up the majority of plant fibres, with cellulose, hemicellulose, and lignin serving as the main elements. According to Lim et al.,s (2018) findings, the coefficient of variation of the kenaf fibre sample rose with increasing thickness. Table 2.3 shows the thickness and mass of the kenaf fibre.

Table 2.3 Thickness and mass of the kenaf fibre, (Lim et al., 2018)

Thickness, t (mm)	75	60	50	40	25
Mass, m (g)	6.0	4.8	4.0	3.2	2.0

Figure 2.5 shows the results of the normal incidence absorption coefficient of 75 mm, 60 mm, 50 mm, 40 mm and 25 mm thickness. Based on the results obtained, the fibre thickness of more than 40 mm fluctuates at high frequency from 0.8 to unity. The sound absorption performance of kenaf fibre is similar to the sound performance coefficient of synthetic rock wool.

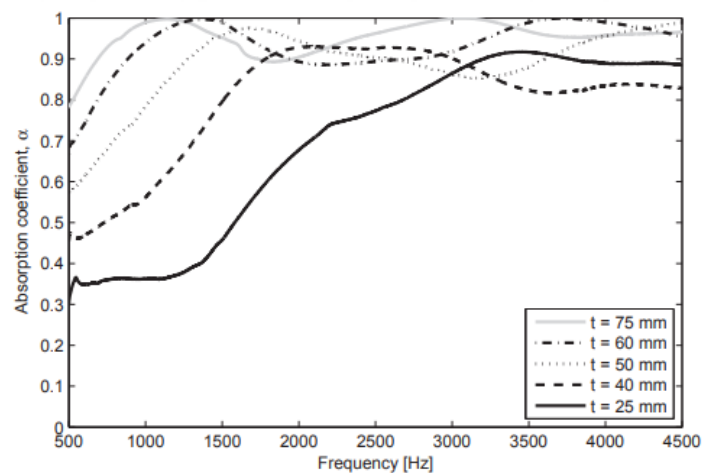


Figure 2.5 : Absorption coefficient of kenaf fibre of varied thickness with constant bulk density of 93.5 kg/m^3 (Lim et al. 2018)

In 2022, Awoyera et al. published a paper in which they described kenaf core is almost similar to fine aggregate and has a potential to replace sand. Besides, it is useful in production of insulation board low, density particle boards, fire retardant-treated particle boards polymer composites, thermos-acoustic applications and sound barriers Yuhazri et al, (2020). Figure 2.6 shows a few examples of kenaf core size which are 20 mesh and 40 mesh.

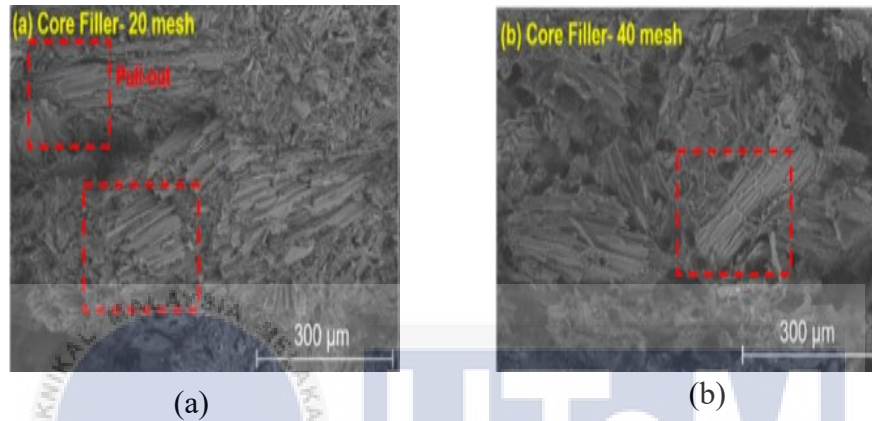


Figure 2.6 Kenaf core size (a) 20 mesh, (b) 40 mesh (Radzuan et al., 2019)

According to earlier research by Shahar et al. (2019), kenaf fibres and cores are more affordable and stronger than other natural fibres. Three distinct techniques, including hand harvesting and retting, decorticator machines, and whole stalk harvesters, can be used to obtain kenaf fibres. They added that the core fibre would be totally ground into powder in order to produce kenaf powder. According to Taban et al. (2020), because it is mostly made of carbon, hydrogen, and oxygen, kenaf can function as a porous material. We can therefore draw the conclusion that kenaf fibre and kenaf core have the potential to absorb more noise due to their better porosity behaviour.

2.2.2 Kenaf Fibre Structural Application

Kenaf fibre has been one of the most attractive research subjects in recent decades due to its good qualities under tension stress conditions, as well as other exceptional

attributes Yusuff et al. (2021). Kenaf is used as an alternative to wood in the pulp and paper industries. This helps to prevent forest destruction, and kenaf can also be used as non-woven mats in the automotive, textile, and fibre sectors. According to Taban et al. (2020), excessive noise pollution has increased globally as a result of fast urbanisation and transportation growth. As a result, effective engineering noise control methods including a wide range of measures and techniques are essential, and employing kenaf fibres and kenaf cores in structural applications could be beneficial.

2.2.3 Application of Kenaf in Cementitious Composite

According to Baghban and Reza (2020), researchers are continuously striving to enhance concrete mixtures not only to improve various properties but also to minimize their environmental impact. In line with these objectives, the utilization of additional cementitious materials (SCMs) and fiber-reinforced concrete (FRC) has gained traction. The use of natural fibers presents an intriguing option from a sustainability perspective, especially as fibers are increasingly replacing steel reinforcing bars in concrete applications. Kenaf fiber, a widely available non-wood plant fiber, exhibits a relatively high tensile strength (930 MPa), a high Young's modulus (53 GPa), and is cost-effective, making it a favorable choice for reinforcement in cement composites, as supported by Zhou et al. (2020). Abdalla et al. (2022) conducted an investigation revealing that the kenaf fiber concrete exhibited a hardness index approximately three times higher than that of the control concrete. The microstructural analysis also demonstrated strong bonding between the concrete matrix and kenaf fibers. Figure 2.7 showcases kenaf fiber-reinforced concrete with varying fiber content.

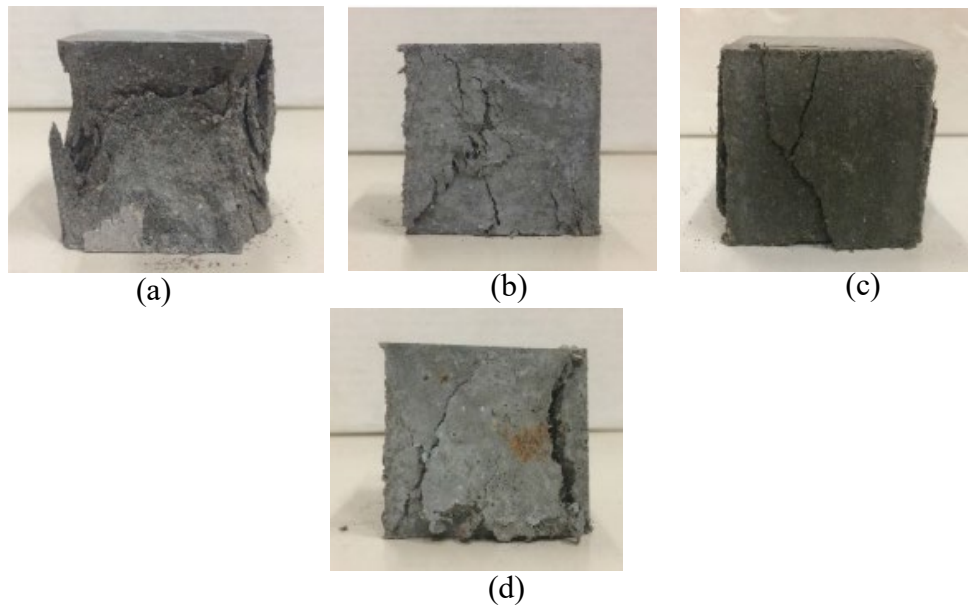


Figure 2.7 : Kenaf fibre-reinforced concrete (a) 0%, (b) 1%, (c) 1.5%, (d) 2% (Zhou et al., 2020)

2.3 Concrete

Concrete structures are constructed using concrete, which is a mixture of cement, water, and aggregates such as sand and gravel that hardens over time to form a strong, durable material. Concrete is one of the most widely used building materials in the world, thanks to its strength, durability, and versatility. Van (2018) stated that around 35 billion tonnes of concrete and mortar are used in construction, which is twice as much as all other industrial building materials combined, such as wood, steel, plastic, and aluminium. Similar to the foundations of our buildings, if not the complete structures themselves, concrete is used extensively in the construction of roads, bridges, tunnels, dams, power plants, ports, airports, dikes and seawalls, waste- and fresh water facilities, and networks. As mentioned by Wangler et al. (2019), when normalised by volume, concrete has a relatively low carbon footprint compared to competing building materials; however, the enormous volume requirements of concrete, 10 km³ annually in 2011, are what have an excessively negative impact on the environment. Therefore, one of the major potential benefits of natural fibre concrete is the potential to lower CO² emissions through improved material efficiency and

increased shape efficiency. Previous research has found that concrete is a relatively robust building material on its own. However, due to exposure to harsh environmental conditions, loading, effects of aggressive actions, corrosion of embedded metal, frost, overload, concrete's resistance to volume changes, abrasion/erosion, and chemical actions, concrete infrastructure may deteriorate by Taheri (2019).

2.3.1 Structure

Concrete structures exhibit a wide range of shapes, encompassing simple slabs and walls to intricate multi-story buildings and bridges. Common forms of concrete construction include foundations, walls and columns, beams and slabs, and bridges. In their 2019 publication, Alexander and Beushausen discussed the durability of reinforced concrete structures, defining it as the ability to withstand the design environment over the design life without significant loss of serviceability or the need for major repairs. Concrete structures, under the assumption of a service life of approximately 50 years, generally exhibit resilience and satisfactory performance. However, according to Dasgupta (2018), regular concrete structures may require retrofitting due to various issues such as corrosion, inadequate detailing, bond failure, and others. Fiber-reinforced polymers (FRP) have emerged as a relatively recent technology for retrofitting and repairing structural damage. This research aims to examine the effectiveness of using FRP in concrete structures to enhance structural performance in terms of strength and ductility. Structural elements including slabs, beams, columns, and bridge culverts have been subjected to testing thus far. Preliminary findings suggest that employing FRP for retrofitting provides a favorable alternative to conventional methods and often presents the most cost-effective and optimal solution for structural rehabilitation challenges.

Ultra-high-performance concrete (UHPC) combines a novel composite construction material with a distinct type of concrete. By carefully optimizing the packing of fine and ultrafine particles and incorporating steel fibers, UHPC achieves a high compressive strength and ductility. Bajaber et al. (2021) explain that this optimization results in a unique distribution of particles at the micro size, where smaller particles fill the spaces between larger particles. Figure 2.8 showcases examples of structures constructed using UHPC concrete.

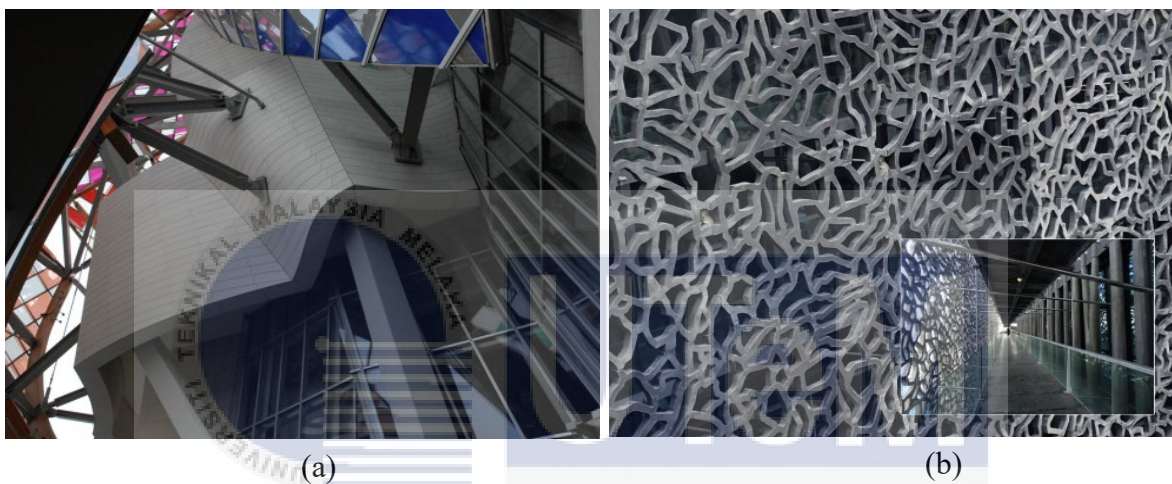


Figure 2.8 Structures that are made of UHPC concrete (a) Curved panels of the Louis Vuitton Foundation Building in Paris (b) The “fishnet” façade of the Mucem museum in Marseille (Van, 2018)

2.3.2 Properties

As mentioned by Qasim (2018), when reinforced concrete constructions are planned, concrete crucial properties are the physical material property. Due to changes in the types and nature of the materials used to improve concrete technology, the proportions of the materials and mix, test method, mixing strategy, and testing environment have a significant impact on the concrete strength's key characteristics, especially since control specimen sizes and shapes may vary from State to State.

Previous research has found that the use of construction and demolition (C&D) waste as recycled concrete aggregates (RCA) in fresh concrete (RCA concrete systems) was first investigated as a result of the enormous volumes of structural debris that accumulated during World War II by Jayasuriya et al. (2021). Because of its comparatively poor thermal conductivity, concrete is an effective insulator. However, elements like the density, porosity, and moisture content of the concrete can have an impact on its thermal properties. It also generally weak in tension compared to compression, so reinforcement is often added to increase its tensile strength.

2.3.3 Natural Fibre-Reinforced Concrete

According to Jirawattanasomkul et al. (2019), one way that concrete structures are now being strengthened to enhance structural performance is by improving the strength and stiffness of structural components. Fiber-reinforced polymers (FRPs), which are lightweight, extremely corrosion-resistant, and simple to install, are one of the potential approaches. Using standard FRPs like carbon, aluminium, and glass can significantly increase a structure's strength and ductility. The use of natural fibres to restrict concrete, such as flax and coir fibres in reinforced concrete (CFRC) tubes, has lately been studied by a number of researchers. They successfully show how FFRP and CFRC tubes can boost concrete's compressive strength.

Based on Saravanan and Buvaneshwari (2018), fibre reinforced concrete is composed of cement, water, fine and coarse aggregate, and discontinuous discrete fibres. The natural isolated fibre known as sisal is frequently used. The leaves of the sisal plant are used to make it. A form of concrete that uses sisal fibres is known as sisal fibre reinforced concrete (SFRC). Sisal fibre reinforced concrete is a material that can be used to enhance

the engineering attributes of many fundamental materials, including fracture toughness, flexural strength, and resistance to fatigue, impact, thermal shock, and spalling.

Banana fibre reinforced concrete is a high-performance fibre reinforced concrete with substantial tensile behaviour, according to Chandramouli et al. (2019). When compared to unreinforced concrete, banana fibre reinforced concrete has a 34.62% higher compressive strength after 56 days of cure. In addition, when concrete is reinforced with banana fibre, its tensile strength progressively increases to 4% and then gradually declines when it reaches that level. The results of the experimental tests showed that adding banana fibres to the concrete increased its strength potential. The compressive strength of concrete is assessed following the curing process. The results for compressive strength at 28, 56, and 90 days are given. The strength characteristics of concrete, particularly compressive and tensile strength, were greatly improved by the inclusion of banana fibres.

Table 2.4 Compressive strength of Banana-reinforced concrete (Chandramouli et al.,2019)

% of banana fibre	Compressive strength (N/mm ³)		
	28 days	56 days	90 days
0	40.8	43.75	47.81
1	43.49	47.07	54.95
2	49.47	53.70	62.41
3	55.10	58.90	67.33
4	55.92	56.96	65.05
5	49.29	52.90	60.53
6	47.17	50.77	57.99

2.4 Acoustic Panel

There are many researchers try to find some alternative materials and have been comprehensively applied in the making of acoustical panel to minimize the noise level. The

common acoustical panels are made from synthetic fibre which commonly of glass fibre, glass foam and other materials that can possibly be very harmful to the environment at the same times towards the human society too by Saad and Kamal, (2012). Taban et al. (2020) stated that passive noise reduction techniques are commonly used using sound-absorbing materials. These porous or fibrous acoustic absorbers typically have pores, canals, cracks, or cavities where acoustic energy is lost due to friction between air molecules and the walls and viscous effects and converted into heat, resulting in acoustic absorption over a broad frequency range. These acoustic panels are the ideal material for noise suppression in the construction, building, and transportation industries since they are lightweight, affordable, and have excellent formability.

Acoustic panels have different variety of sizes, types and colors depending on the design requirement. These panels should be suitable for both indoor and outdoor applications especially for area with acoustical isolation. Usually, the use of acoustic panel are mostly found in apartments, condominiums, hotels, schools and hospitals which is required to have a proper design in term of walls, ceilings and floors to minimise or possibly eliminate the disruption of the sound's transmission as stated by Tinianov (2018). Figure 2.9 shows some of the acoustic baffle examples.

According to Kishore et al. (2021), natural fibres have a porous structure that provides excellent acoustic performance. When porous material is exposed to accidental sound waves, the air within the pores vibrates and transforms into different energy types. Because natural fibres are environmentally friendly, biodegradable, cost-effective, and have no negative effects, they are referred to as green materials. Fibre geometry, such as diameter, length, cross-section shape, and regularity, has a considerable impact on acoustic characteristics. The impedance tube approach was used to characterise the sound absorption measurement. Without the use of a binder, the acoustic properties of natural fibres such as

kenaf, wood, hemp, coconut, cork, cane, mineralized wood, and cardboard are investigated . The mineralized wood and dense kenaf have the highest airflow resistivity.

2.4.1 Synthetic Sound Absorber

According to Taiwo et al. (2019), artificial fibres like rock wool and glass wool are frequently used as sound absorbers in the building sector. It is used in many different types of building and construction projects, including wall and roof tiles, flooring, and partition boards. Natural and sustainable acoustic materials are presently of attention because it was shown that they had considerable negative environmental effects. As a result, agro-waste, plant waste, and industrial waste were used to create natural fibres. Research is currently being done on natural fibres such coir, pineapple, sugarcane bagasse, jute, ramie, kapok, and others. Natural and synthetic fibres are compared in terms of several qualities in Table 2.5.

Yang et al. (2020) studied that glass fibre and mineral wool dominated the European insulator materials industry in 2005, accounting for 60% of the market. While organic foamy materials such as polystyrene and polyurethane, as well as other materials, account for 27% and 13% of the market, respectively. Although glass fiber and mineral wool outperform in terms of acoustic and thermal insulation, it cannot be overlooked that some potential human health issues arise as a result of skin irritation and particle lay-down in the lung alveoli caused by inhaling fibres and particles. Figure 2.9 shows some examples of synthetic sound absorber that is use for acoustic panel that will be applied in various kind of building



Figure 2.9 Synthetic sound absorber (a) Glass wool (b) Rock wool (Yap et al., 2021)

According to Samaei et al. (2021), porous composite materials have gained significant traction in the building and automotive industries in recent years due to their numerous advantages, such as favorable physio-mechanical properties, noncombustibility, and promising thermal and acoustical properties. Sustainable composite materials are preferred for their lightweight nature, cost-effectiveness, biodegradability, and minimal environmental impact. Additionally, the study by Yang et al. (2020) examined the interaction between sound waves and porous structures, highlighting the loss of energy through thermal and viscous effects within the pores. This conversion of acoustic energy to heat energy contributes to the overall sound attenuation. Judawisastra (2022) emphasized the current trend in green technology, which focuses on substituting synthetic materials with natural alternatives that offer comparable performance. For instance, corn fiber, coconut fiber, and sugarcane fiber are now being utilized as replacements for synthetic fibers.

A comprehensive review of available literature on arenga pinnata fiber was conducted by Yahya et al. (2017), and sound absorption coefficient data was obtained using the impedance tube method, as conducted by Corredor et al. (2021) following the ASTM E1050-98 standard. The findings revealed that as the sample thickness increases, the sound absorption coefficient of arenga pinnata also increases. Figure 2.10 showcases an image of the arenga pinnata tree.



Figure 2.10 *Arenga pinnata* tree (Yahya et al., 2017)

Yang et al. (2020) highlighted that in order to prepare natural fiber sound absorbers for commercial use, several pretreatment steps are necessary, including fiber bundle extraction, alkaline treatment, and the fabrication of panels or nonwoven fabrics. However, it is worth noting that natural fibers can also function as sound absorbers in their raw or minimally processed states. Table 2.5 provides a compilation of studies examining the acoustic properties of raw natural sound absorbers.

Table 2.5 5 A summary of raw material fibre sound absorbers (Yang et al., 2020)

Researcher	Raw Material	Key Findings
Glé et al. (2012)	Hemp particle	The acoustical qualities of hemp particles can be anticipated depending on particle parameters and configuration. The particle size distribution has a positive influence on low-frequency sound absorption.
Arenas et al. (2020)	Esparto grass	Raw esparto grass has comparable sound absorption to typical glass fibre materials of equivalent thickness.

Iannace et al. (2020)	Broom branch	Smaller diameter broom branches absorb less sound than larger diameter broom branches.
Putra et al. (2015)	Bamboo	Bamboo that was organised transversely had greater sound absorption than axially oriented samples.
Tang et al. (2018)	Corn husk	Because of its grooved structure, maize husk effectively absorbs sound.
Tang et al. (2020)	Green tea residues	The leftover green tea dregs can be used as filler materials to absorb sound.
Zunaidi et al. (2017)	Rice Straw	Sound can be successfully absorbed by rice straw fibre. The sound absorption coefficient is significantly influenced by the fibre mass and diameter.
Horoshenkov et al. (2013)	Growing plants	The leaf area density and the predominant leaf orientation angle are two essential morphological traits for the acoustical properties.
Wong et al. (2010)	Vertical greenery systems	When compared to other building materials and furniture, the vertical greenery system is one of the best sound absorbers.

2.4.2 Acoustic Properties of Kenaf Fibre

Researches about the sound absorption of kenaf fibre has a high potential to become the material to produce acoustic panel has been done by Lim et al. (2015). Based on the result gained by Lim et al the larger the thickness of the kenaf fibre sample, the larger the sound absorption coefficient will be at lower frequencies. Lim et al. applied the impedance tube method in finding the sound absorption coefficient of the kenaf fibre samples. Figure 2.11 shows the image of a non-woven kenaf fibre.



Figure 2.11 Non-woven kenaf fibre (Yuhazri et al., 2018)

The sound absorption coefficient of kenaf fibre is shown in Table 2.6. Lim et al. (2018) prepared the sample thickness in four distinct thicknesses, namely 10mm, 20mm, and 30mm. The sound absorption coefficient is larger than 0.5 when the frequency of sound is greater than 1000 Hz, and it is greater than 0.5 when the frequency is around 2000 Hz. The larger the thickness of the kenaf fibre sample, the higher the sound absorption coefficient at low frequencies. Table 2.6 shows the sound absorption coefficient of kenaf fibre.

Table 2.6 Sound absorption coefficient of kenaf fibre (Lim et al., 2018)

Thickness (mm)	Acoustic Range (α)		
	Low	Medium	High
10	0.2	0.5	0.62
20	0.28	0.68	0.86
30	0.4	0.98	0.96

2.4.3 Acoustic Properties of Kenaf Core Particleboard

In 2012, Saad and Kamal demonstrated that kenaf core as a particleboard in their research. Saad and Kamal prepared particleboard to study the effect of resin loading with

three different densities board of 350 kg/m^3 , 450 kg/m^3 and 550 kg/m^3 of urea formaldehyde resin loadings of 8%, 10% and 12 % respectively;

This particular study found that particleboards with high kenaf fibre and UF loading showed less sound absorption coefficient. The sample diameter were prepared in two different diameter which is 100 mm to measure frequency range 125 Hz to 1600 Hz and 28 mm for frequency range of 1200 Hz to 6000 Hz. The result obtained from the sound absorption coefficient with 8% and 10% UF loading show that they can become a good sound absorber compared to a UF loading of 12%. It was found in low, medium and high sound frequency. Saad and Kamal revealed that the lower the value of sound absorption coefficient, the higher the frequency range depends on their specific characteristic of the sound absorber in lower range but the sound is reflected in medium and high frequency range. Figure 2.12 shows the kenaf core particleboard sample for sound absorption test.



Figure 2.12 Kenaf core particleboard for sound absorption test (Saad and Kamal, 2012)

2.4.4 Acoustic Characterization

Based on Tinianov (2018) the present development, a new laminar structure and it is related to the manufacturing process revealed that it is significant to develop both material's installation effectiveness and the capability of a wall, ceiling, floor or door to reduce the sound in the spaces. Furthermore, Prędką et al. (2020) stated that the acoustic

characterization is based on the sound absorption coefficient. Prędko et al., also added that the sound absorbing material is influenced by material thickness, binder percentage, size and nature of the reinforcement material and air gap between samples and rigid wall. If the absorption coefficient value is close to 1, it is considered that the material has a good sound absorption properties.

2.5 Mechanical Properties and Sound Absorbing Testing

The testing were carried out to ensure the quality control, quality assurance and prediction of the sound performance and also the mechanical properties supported by the result data and stimulation. The frequency test is to measure the sound absorption coefficient of the acoustic panel by using impedance tube testing. The acoustical testing involves measuring the sound absorption of the acoustic panel is frequency testing. Basically, there are two basic vibration and acoustic testing can be carried out in order to establish the sound absorption of the materials which are impedance tube testing and reverberation room testing. The different between these two testing methods is the size of the sample. The sample size for impedance tube testing is smaller compare to the sample size for reverberation room testing.

There will be three testing that are going to be carried out to test the samples' mechanical properties. They are compressive strength test, flexural strength test and splitting tensile strength. For the compressive strength test, if the material does not have a lot of mechanical response in tensional load, the compression test will be more appropriate. For the flexural strength test, the test will use three-point flexural test to determine the flexural properties of a material under a bending strain or deflection. For splitting tensile strength test, it is important for a measure of a concrete's resistance to splitting or cracking under tension. It is commonly used to evaluate the tensile strength of concrete.

2.5.1 Compressive Strength Test

Jirawattanasomkul et al. (2019) investigated the impact of natural fibre reinforced polymers on the restricted compressive strength of concrete. Natural Fibre Reinforced Polymers (NFRP) composed of jute, hemp, and cotton were employed. A natural woven fabric with densities of 1.46, 1.48, and 1.51 g/cm³ for jute, hemp, and cotton, respectively. The thickness is computed by dividing the natural fabric's density by its weight per unit area. The weight per unit area of natural cloth is estimated using a weight scale with a precision of 10 mg. In the meantime, a gas pyrometer is used in a laboratory to determine density, which is defined as weight per volume. The specimens were created with epoxy resin, which has a tensile strength of 19 MPa and an elastic modulus of 1060 MPa. The natural woven fibre sheets are depicted in Figure 2.13.

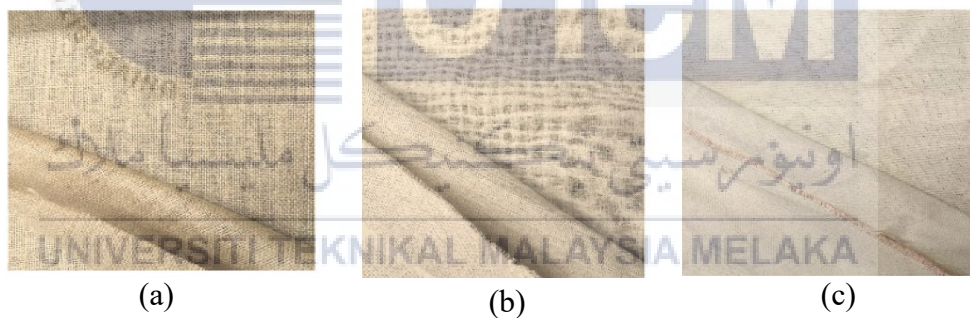


Figure 2.13 Natural woven fibre sheets fabric (a) Jute, (b) Hemp, (c) cotton (Jirattanasomkul e al., 2019)

For the compressive test, 63 cylinder concretes were used. comprised of nine control concrete cylinders (CC1-CC3), each 100 mm in diameter and 200 mm in height. All concrete cylinders were tested by Universal Testing Machine using a loading control and a loading rate of 0.30 MPa/s until they failed, in accordance with JIS A 1108-2006. The compression test setup is depicted in Figure 2.14.



Figure 2.14 Compression test setup (Jirawattanasomkul et al., 2019)

The outcome shows that the confinement effect of NFRPs has a significant influence on the ductility and compressive strength of concrete. Increasing the number of NFRP plies leads to improved strength and ductility. Specifically, the use of Jute-, Hemp-, and Cotton-NFRP results in a significant increase in the compressive strength of confined concrete by approximately 42%, 25%, and 28%, respectively.

2.5.2 Three Point Flexural Testing

According to C.Zhou et al. (2020), The enhancement in flexural strength and toughness of the high-strength cement composite due to kenaf fiber was more better compared to the low-strength grade. For optimal flexural strength and deflection in Kenaf Fiber-Reinforced High-Strength Cement (KFRHC), a fiber content of 1% was found to be suitable. As the strength grade increased, the improvement in deformability of KFRHC also escalated. Flexural testing involves subjecting a material to a bending force to assess its resistance to deformation and breaking under such conditions. The statement about the effectiveness of kenaf fiber reinforcement being more pronounced in high-strength cement composites compared to low-strength grades suggests that the performance of kenaf core may vary with the overall strength of the composite material. Flexural testing helps to understand this relationship and its implications. Figure 2.15 shows the setup of flexural testing upon samples.

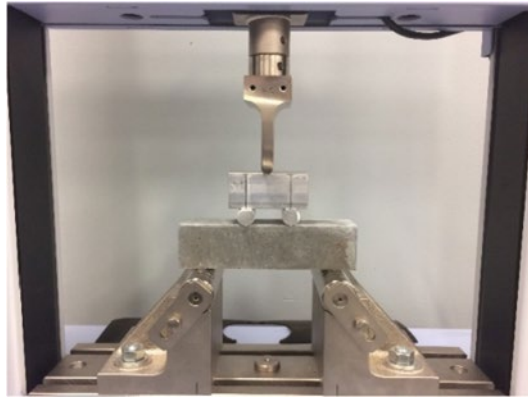


Figure 2.15 Flexural Testing Setup for concrete samples (C.Zhou et al., 2020)

2.5.3 Impedance Tube Testing

Impedance tube testing is performed to determine the coefficient of the kenaf core, specifically assessing its capacity to absorb sound waves at normal incidence. The test involved positioning a loudspeaker at one end of the impedance tube, while the testing sample was placed at the other end. The setup of the impedance tube is illustrated in Figure 2.15. This method serves the purpose of evaluating the material's sound absorption properties.



Figure 2.16 : Impedance tube setup (a) measurement (b) BC-MPP sample setup (Chin et al., 2018)

The frequency range utilized in the impedance tube testing spans from 1 Hz to 5000 Hz. The equipment employed includes an audio generator, microphone, impedance tube, loudspeaker, and oscilloscope to measure the sound absorption coefficient. The loudspeaker generates various types of sound waves such as broadband, stationary random, and sound

waves. Within the tube, sound waves propagate and interact between the sample and the sound source, resulting in patterns of standing waves displayed on the computer screen. The acoustic absorption coefficient, which depends on the frequency range, represents the ratio of absorbed acoustic energy to incident acoustic energy.

Yahya et al. (2017) conducted a study on the sound absorption properties of several widely available natural fibers in ASEAN nations, including kenaf, ijuk, palm oil frond, and coconut coir. Test samples for the sound absorption coefficient were constructed using natural latex rubber as a binder and a 60:40 ratio of latex rubber to the mentioned natural fibers as raw materials. Previous studies acknowledged the use of polypropylene and urea formaldehyde as reinforcing agents, which possess chemical properties. The sample sizes were determined based on the diameter of the impedance tube according to ASTM E1050-09, while their thickness was standardized at 50 mm, aligning with the industry standard for acoustic synthetic panels. The frequency band between 1000 and 5000 Hz exhibited optimal acoustic performance, with an average absorption value of 0.8.

The sound absorption coefficient is frequency-dependent, as depicted in Figure 2.16. The absorption coefficient value for the kenaf sample with 0% NR (natural rubber) increased in the low-frequency range, reaching approximately 0.84, decreased slightly in the mid-range frequencies, and gradually increased again at high frequencies, peaking at an absorption coefficient of 0.91 at 3750 Hz. The 0% NR kenaf sample, which solely consisted of fibers, exhibited a significant presence of porous material, making it ideal for absorber panels. Similar findings were observed for the Ijuk 0% NR sample in Figure 2.22. On the other hand, samples with 20%, 30%, and 40% NR content displayed consistent patterns. These samples exhibited a substantial increase in absorption coefficient values at low frequencies, surpassing 0.9, followed by a sharp decrease in the mid-range frequencies to values between 0.7 and 0.6, and a subsequent progressive increase at high frequencies.

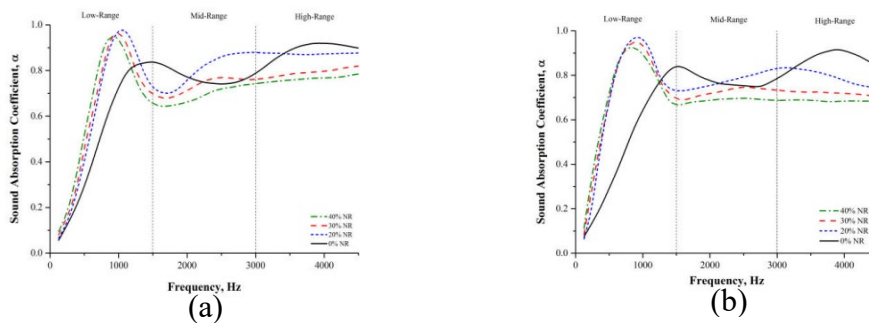


Figure 2.17 Absorption coefficient (a) Ijuk absorption coefficient (b) Kenaf absorption coefficient (Yahya et al., 2017)

2.6 Summary

As for the summary, many interesting information was found from previous research related to the kenaf core and kenaf fibre. The findings from this literature review include theoretical aspect had been done in the knowledge of kenaf core, kenaf fibre, natural fibres, concrete composites, acoustic properties of natural fibres and its mechanical properties of the kenaf fibre. All the related information and knowledge gathered in this chapter which is related to this research have been summarized including theory aspect as the guidelines and references.

In recent times, various materials have been employed in manufacturing for their acoustic properties. However, in light of environmental concerns, researchers have undertaken studies to explore natural materials as alternatives for acoustic panels. Kumar et al. (2022) highlighted several advantages of these natural materials, including their lower cost, sustainability, ease of production, favorable mechanical properties, and, notably, their eco-friendliness. The primary objective of utilizing natural fiber reinforced composites in industries is to achieve weight reduction and cost reduction. Multiple studies have demonstrated that the adoption of natural fiber composites can lead to approximately a 20% decrease in costs and a 30% reduction in weight.

Furthermore, natural fibres come from either plants, animals, or other natural resources. The highest demand natural fibres nowadays are from kenaf plant that consist of kenaf fibres and kenaf cores. According to previous journals, kenaf core have been a great potential of mechanical and chemical properties to replace other materials in the future in the application of new technologies. Table 2.7 summarized of previous research finding in the reported work on the application of kenaf core. Also, Harmaen et al. (2020) stated that density of kenaf core is higher and the absorption of the particles performed well than other materials thus kenaf core is one of the materials that have the potential to be used as the acoustical materials.

In addition, concrete has been studied by many researchers as a matrix component of kenaf core as a reinforcement in composites. When mixed with water, sand and cement, often known, as concrete, plays a critical role in the construction industry, particularly in structural engineering and mortars. It was also discovered that building structures made of cement or concrete have a lifespan of up to 100 years. Despite the fact that numerous studies on the acoustical properties of natural fibres have been conducted, it was discovered that few research on acoustical properties employing kenaf core reinforcement and concrete composite had been conducted. As a result, the focus of this research will be on the development and analysis of an acoustic panel made of kenaf core and concrete.

Table 2.7 Reported work on the application of kenaf

Matrix	Reinforce	Findings	References
Concrete	Steel fibre	A used of suitable length are crucial because short fibre tends to produce poor result of strength.	(Zhou, 2021)
Cement	Kenaf fibre	Kenaf fibre yielded improved mechanical strength of the cement- based composites	(Onuwe et al., 2018)

Clay soil	Carbon fibre	Carbon fibre does not produce a great result in strength because the contact area between the fibre and the clay is not enough	(Bao et al., 2021)
Cement	Kenaf fibre	The use of the appropriate length and content of KF improves the tensile and flexural strengths of cementitious composites	(Abbas et al., 2022)
Clay	Kenaf fibre	The more fibre is used, the material ductility will more likely to be increase and in this study the inclusion of reinforce	(Esmaeilpourshirvani et al., 2019)
HDPE	Kenaf core	The mechanical properties of 60/40 kenaf/HDPE mixture was improved with the pre-treatments of core particles.	(Li et al., 2020)
Bast fibre	Kenaf core	The improvement of mechanical properties will increase the life services of the boards as the kenaf core and bast fibre have great potential.	(Anyanywu et al., 2019)
Kenaf core	-	Fibre can be used as a dispersing phase for brake pad composites.	(Anyanywu et al., 2019)
Polythelene	Kenaf core	Addition of kenaf core, the tensile strength and modulus of the low density improved.	(Sarifuiddin et al., 2013)
Polypropylane	Wool fibre	PP/KF/APP/WF system had stable residual char at elevated temeperatures, significantly improving fire protection.	(Subasinghe et al., 2018)
Carbon	Kenaf fibre	Resistance of carbon fibre to high temperature and better fibre-matrix compatibility.	(Aisyah et al., 2019)
Pulverised fuel ash	Kenaf fibre	PFA cement that improves concrete to dense compared to normal concrete	(Azzmi et al., 2021)
Kenaf core	Glycerol	Kenaf core fibre able to absorb more oil molecules compared to cassava starch	(Mustaffa et al., 2018)

Kenaf core	Polylactide	Dry-distillation surface modification appears to be successful for improving the interfacial interaction and compatibility.	(Kawahara et al., 2017)
Polyurethane foams	Kenaf core	Freely expanding foams lead to poor reinforcement when mixed.	(Nar et al., 2015)
Polyurethane foams	Kenaf fibre	Kenaf core particles occupying the space in the PU that was previously occupied by air.	(Batouli et al., 2014)

According to Clyne et al. (2019), composites have become one of the most significant and versatile classes of engineering materials, alongside steels, in terms of industrial importance and range of applications. This finding is consistent with previous studies by Rajak et al. (2019), which also highlighted the widespread use of composite materials in modern technologies since the mid-20th century. Aerospace (et al., 2019), military applications (Ngo Tri-Dung, 2020), transportation (Rubino et al., 2020), and infrastructure (Li, 2019) are some of the industries where composites are extensively employed. The development of composites involves blending different materials or components to modify their properties and enhance their capabilities, as commonly practiced in the engineering industry.

As mentioned by Ngo Tri-Dung (2020), a composite consists of three main components: the matrix, which acts as the continuous phase; the reinforcements, such as fibers, serving as the discontinuous or dispersed phase; and the interface, known as the fine interphase region. David et al. (2020) pointed out that composites possess characteristic performance traits that their individual components cannot achieve on their own. This enables the creation of lightweight designs with high stiffness and strength. Based on this rationale, the present

research focuses on developing biodegradable composite materials as alternatives to non-biodegradable synthetic composites, supported by the works of Malviya et al. (2020) and Sanjay et al. (2018).

In another study, Raju et al. (2021) identified several factors influencing the development of composites, including the availability of matrix types, variety of fibers, selection of reinforcing fibers, fiber processing methods, cost of processing fibers, mechanical properties of the fibers, and procurement costs. Various surface treatments for natural fibers have been employed to enhance interfacial adhesion with the matrices and improve their mechanical properties. Rajak et al. (2019) categorized composite materials primarily into natural fibers and synthetic fibers, and the combination of these fibers with a matrix material yields hybrid composites with enhanced mechanical properties. Table 2.1 provides an overview of manufacturing techniques and applications of specific fibers with their respective matrix materials.

Table 2.8 Manufacturing techniques and applications of some fibres with their matrix materials (Rajak et al. 2019)

Material Used		Applications	Manufacturing Technique
Fiber Reinforcement	Matrix/ Binder Material		
Carbon	Polypropylene(PP), metals, ceramics, epoxy resin, Polyether ether ketone (PEEK).	Lightweight automotive products, fuel cells, satellite components, armour, sports.	Injection moulding, filament winding, resin transfer moulding (RTM).
Graphene	Polystyrene (PS), epoxy, Polyaniline (PANI).	Wind turbines, Gas tanks, aircraft/automotive parts.	Chemical vapor deposition (CVD), pultrusion, hand/spray up method.

Sisal	PP, PS, epoxy resin.	Automobile body parts, roofing sheets.	Hand lay-up, compression moulding.
Hemp	Polyethylene (PE), PP, Polyurethane(PU).	Furniture, automotive.	RTM, compression moulding.
Kenaf	Polylactic acid(PLA), PP, epoxy resin.	Tooling, bearings, automotive parts.	Compression moulding, pultrusion.
Flax	PP, polyester, epoxy.	Structural, textile.	Compression moulding, RTM, spray/ hand lay-up, vacuum infusion.
Ramie	PP, Polyolefin, PLA	Bulletproof vests, socket, prosthesis, civil.	Extrusion with injection moulding.
Rice Husk	PU, PE	Window/door frames, automotive structure.	Compression/ injection moulding
Jute	Polyester, PP	Ropes, roofing, door panels.	Hand-lay-up, compression/ injection moulding.
Coir	PP, epoxy resin, PE	Automobile structural components, building boards, roofing sheets, insulation boards.	Extrusion, injection moulding.

2.6.1 Natural fibre composites

The recent advancements in composites have amplified the demand for natural fibers and their role in mitigating acoustic disruptions. Dong's (2018) research findings further highlight the favorable properties of natural fibers, such as their lightweight nature, affordability, and abundance in terms of raw materials. In 2020, Malviya et al. emphasized that reducing the reliance on fossil-based resources, particularly petroleum, can address environmental concerns. The utilization of green composites also offers substantial benefits, including a significant reduction in non-renewable energy consumption and the emission of

carbon dioxide (CO₂), sulphur dioxide (SO₂), nitrogen oxide (NO_x), and carbon monoxide (CO).

Natural fibers can generally be categorized into three groups: plant fibers, mineral fibers, and animal fibers. Kurinijimalar et al. (2021) noted that plant fibers, also known as cellulose-based fibers, encompass important varieties such as cotton, flax, and hemp. Animal fibers, which are protein-based, include wool, mohair, and silk. Figure 2.1 provides a visual representation of several natural fibers.

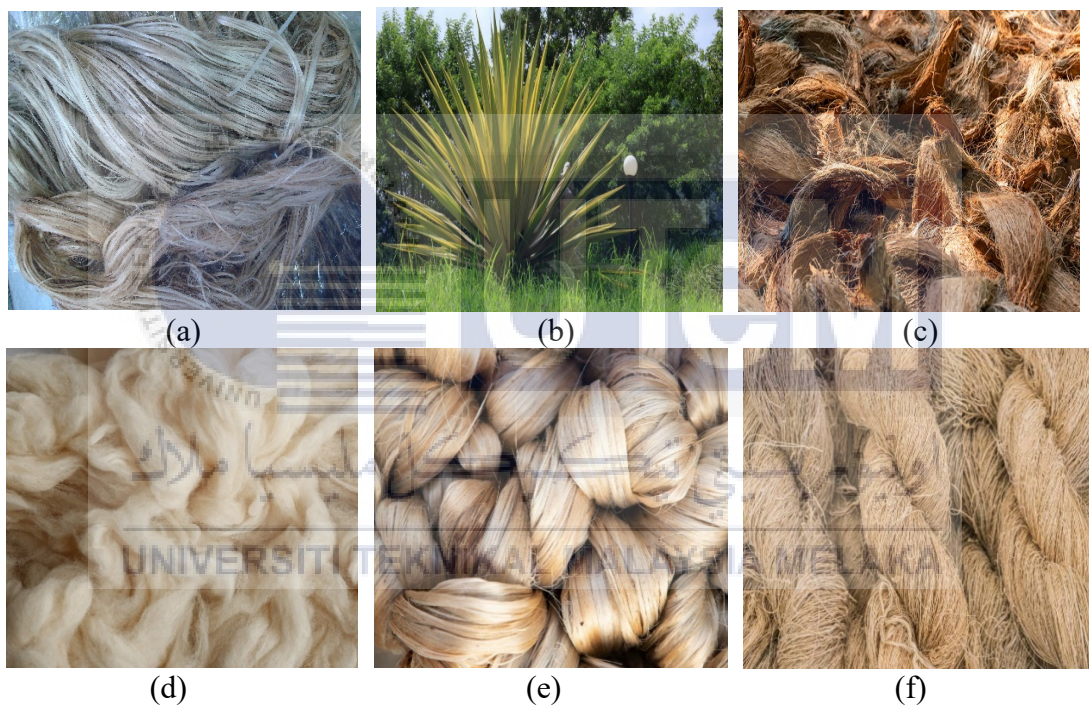


Figure 2.18 Figure 2.1 Natural fibre (a) kenaf ; (b) sisal ; (c) coir ; (d) wool ; (e) jute ; (f) hemp (Rajak et al., 2019)

In a study by Sahu et al. (2020), it was demonstrated that natural fibers offer significant advantages in terms of the development of cost-effective and environmentally friendly sustainable products. Researchers are actively exploring ways to minimize the consumption of synthetic fibers, also known as man-made fibers. However, according to de Azevedo et al. (2021), the usage of natural fibers also presents certain drawbacks, such as

the lack of uniform properties. This variability in properties is primarily attributed to the composition of their constituents, including cellulose, hemicellulose, and lignin. Table 2.2 depicts the advantages and disadvantages of natural fibres.

Table 2.9 Advantages and disadvantages of natural fibres (Asyraf et al. 2022)

	Advantages	Disadvantages
Natural fibres	Lightweight	Flammable
	Recyclable	Dimensional instability
	Improved specific mechanical properties	High moisture absorption
	Eco-friendly, carbon dioxide neutrality	Anisotropic behaviour
	Doesn't generate any harmful gasses during processing and low energy requirements during the production	Limited processing temperature (-200 – 230 °C)
	Good thermal properties	Sensitive to ultraviolet (UV)
	Good acoustic properties	Fungal attack and microbial attack
	Low cost, availability, renewable resources, disposal by composting	Low strength than synthetic fibres especially impact strength
	Non-abrasive and great formability	Variable quality, influenced by weather
	No dermal issue for handling	Low durability
	Safer crash behaviour in test	Poor fibre/ matrix adhesion

2.6.2 Classification of natural fibre composite

Generally, this study highlighted on plant fibres. Non-wood fibres for example like hemp, kenaf, flax and sisal have gained a mass production in the design of bio-composites in engineering materials and it is supported by Noryani et al. (2018). Figure 2.2 below demonstrated the classification of natural fibres which can be categorized to animal based, plant based and mineral based.

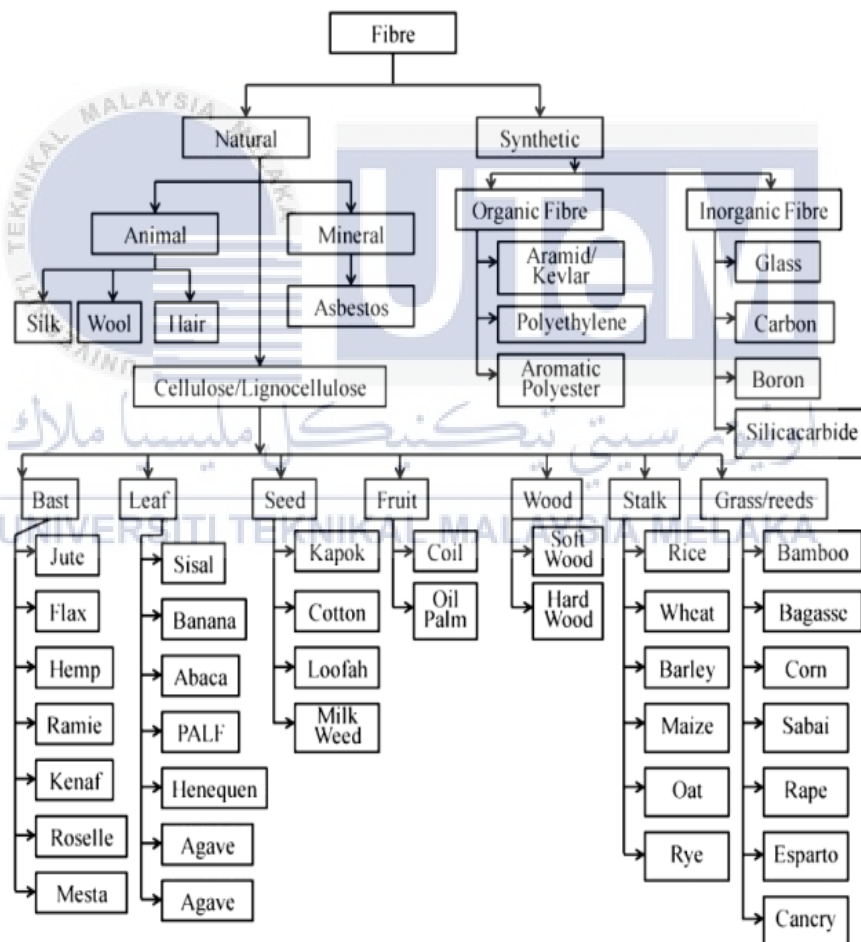


Figure 2.19 Classification of Natural Fibres (Noryani et al. 2018)

In recent years, Natural Fibers Reinforced Composites (NFRCs) referred to the component that is made from natural fibres composites and they have been applied in various sectors. While NFRCs are gaining a lot of attention in terms of business and also academia, Syduzzaman et al. (2020) indicated that the manufacture and use of NFRCs will improve the long-term viability of material manufacturing.



CHAPTER 3

METHODOLOGY

METHODOLOGY

3.1 Overview of Methodology

The flowchart of overall process in this research is depicted in Figure 3.1. This research began with the preparation of raw material which are kenaf core, kenaf fibre and concrete that will be mix with different size of composition for each sample. After the preparation, moulding and curing technique are carried out. Moulding is a technique to produce samples of acoustic panel with the dimension of 34.5 mm x 20 mm which allow the sample to be dried on ASTM standard. If the quality of the sample is good, it will proceed with the testing but if the quality is not good, new sample need to be prepared. When the samples are ready, the samples were tested to observe the new mechanical properties of the acoustic panel by compression test, flexural and of acoustical properties testing, the tests is impedance tube testing.

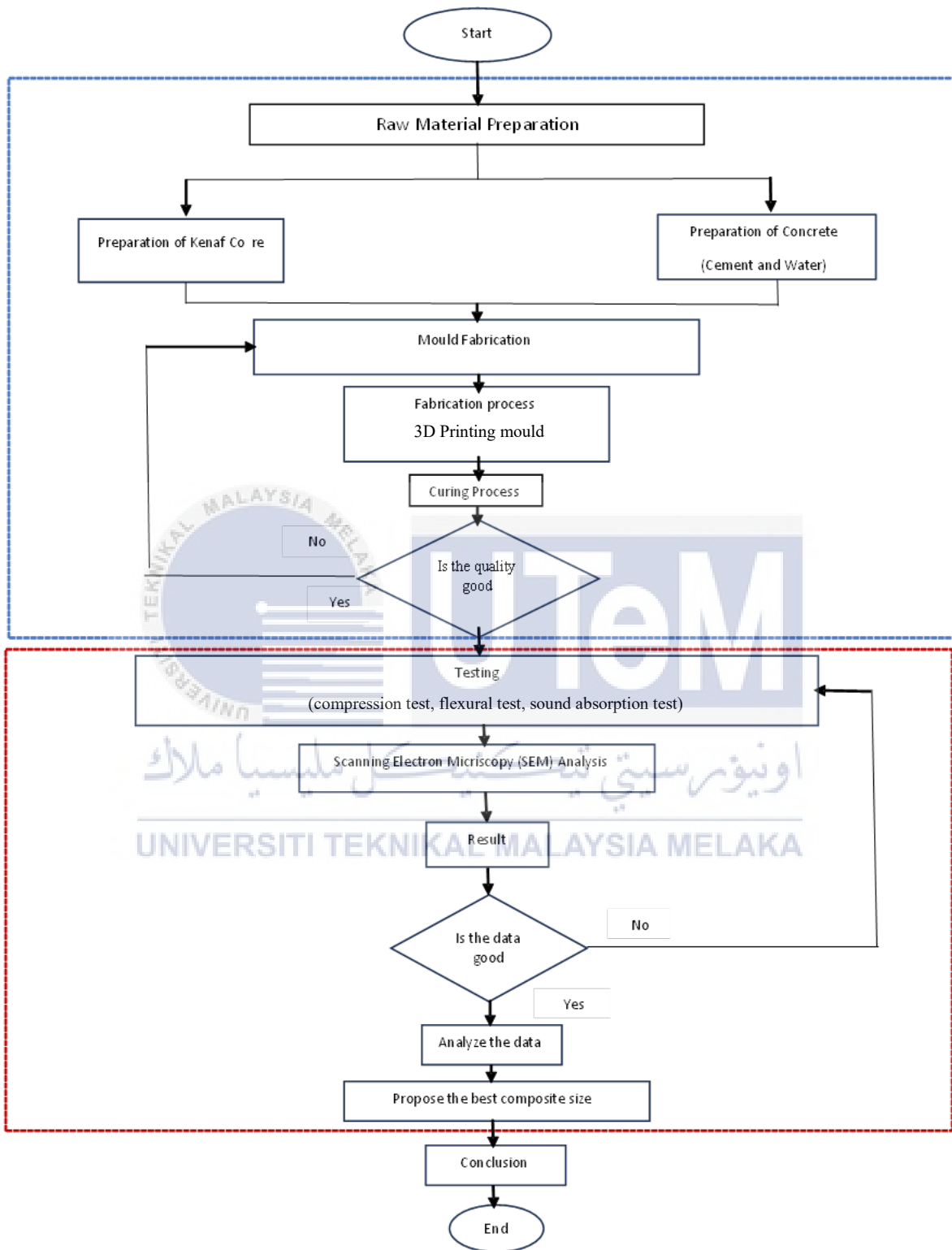


Figure 3.1 Flowchart of methodology

3.2 Raw Material Preparation

The preparation of raw materials is very important and crucial step to produce the best quality product. The aim of this research is to prepare the appropriate amount of various ratios of kenaf core, kenaf fibre, foam, cement and concrete. There are two types of material which are kenaf core, foam and pure cement used as reinforcement while concrete was used as the matrix material. The details specifications and characteristics of each raw material will be explained more further in this research. The dimension and quantity of the materials are measured accurately according to the requirements. The method of the fabrication process used is based on the previous study and it is suggested in this research

3.2.1 Kenaf core as reinforcement material

In this study, kenaf core (KC) is used as the reinforcing material. The properties of the KC are indicated in the Table 3.2. There are five types of KC will be used which are 10 mm, 20 mm, core chip 30 mm, 20 mesh and 40 mesh in size shown in Figure 3.3. Different size of KC being used to determine which size of KC will have the best acoustical properties and produces the best result when mixing with concrete in the production of the acoustical panel. This is because size of KC will influence the interfacial bonding of the composites when contact with the surface area to the concrete. The details price of each size of KC were provided in Table 3.3 and the KC was obtained from LTKN.

Table 3.1 The properties of kenaf core

Density, g/cm^3	Tensile Strength, MPa
0.09 – 0.11	20 - 230



Figure 3.2 Size of kenaf core, (a) 30 mm (b) 20 mm (c) 10 mm (d) 40 mesh (e) 20 mesh

Table 3.2 Price of kenaf core based on mesh size

Mesh size	Quantity (kg)	Price (RM)
40 mesh	10.0	12.00
20 mesh	10.0	9.00
30 mm – Core chip	10.0	3.50
20 mm	10.0	4.00
10 mm	10.0	4.50

3.2.2 Foam as reinforcement material

Foam can serve as a reinforcement material in concrete, contributing to the development of lightweight or foam concrete. This application offers several advantages, including a reduction in overall density, making the concrete lighter and suitable for situations where weight is a critical factor. Additionally, the incorporation of foam enhances thermal insulation properties, making it useful in construction scenarios where temperature control is crucial, such as in walls or roofs. The use of foam also improves workability, making the concrete mix more manageable, especially in projects with intricate shapes or molds. Foam can contribute to a decrease in shrinkage, reducing the likelihood of cracks and enhancing the overall durability of the structure. Furthermore, foam in concrete can improve sound insulation properties, making it beneficial in settings where noise reduction is a priority. It's essential to carefully consider the type of foam, its density, and the mixing proportions to achieve the desired properties in foam concrete, while acknowledging potential drawbacks such as reduced compressive strength compared to traditional concrete. Ultimately, the decision to use foam as a reinforcement material should align with the specific requirements and constraints of the project.



Figure 3.3 Foam beads

Table 3.3 The properties of foam beads

Density, g/cm^3	Tensile Strength, MPa
0.008 - 0.048 g/cm^3	1-2 MPa

3.2.3 Cement as matrix material

Cement is the matrix building used in this study as stated previously cement is the matrix material used in this study as stated before. Cement is a material that used in building structures and construction due to its high strength and have longer lifetime to damage. The production of cement is having higher demand in many applications as it easy to be produce. Cement is dense and a rigid material that tends to reflect sound rather than absorb it. When sound waves hit a cement surface, they bounce off and create echoes or reverberation. However, by installing acoustic panels, like kenaf core, it can reduce the echoes and improving the overall acoustic quality of the space. In this study, cement in Figure 3.4 was purchased from Apple Hardware Sdn. Bhd. with a cost of RM 19.00 per bag which have a mass of 50 kg per bag. Table 3.4 indicates the properties of the cement.

UNIVERSITI TEKNIKAL MALAYSIA MELAKA



Figure 3.4 A bag of 50 kg cement

Table 3.4 Properties of cement

Material	Portland cement
Density, ρ	2240 – 2400 kg/m ³
Compressive strength	20 – 40 Mpa
Tensile strength, σ	2 – 5 Mpa
Drying shrinkage	4 -8 X 10 ⁻⁴
Shear strength, τ	6-17 Mpa
Specific heat, c	0.75 kj/kg.K

3.3 Preparation of Mould

In this study, the mould for acoustical and mechanical panel had been fabricate using 3D printing machine and the filament that has been used is the Polylactic acid or polylactide (PLA) plastic. For the acoustical panel, the dimension for the mold is 50 mm x 50 mm and

the size is to ensure the sample for the testing is sufficient and to get the accurate results by 4 to 6 times testing by using impedance tube as shown in Figure 3.6.

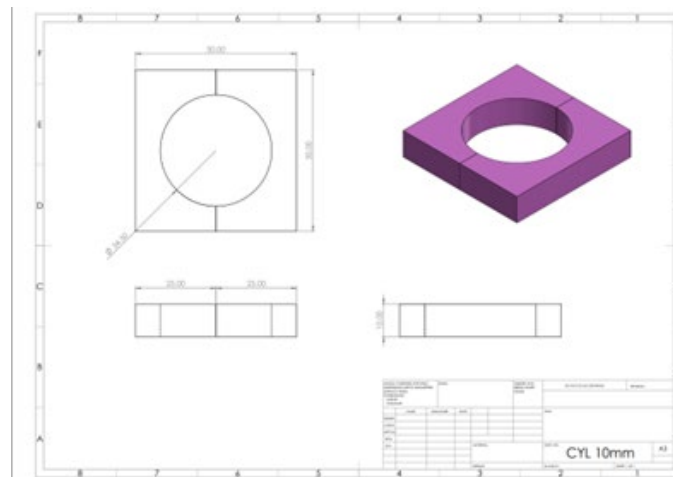


Figure 3.5 Dimension of mould size for the composite cylindrical samples

For the mechanical panels in flexural test, the dimension of the mould is 140 mm x 140 mm as shown in figure 3.7

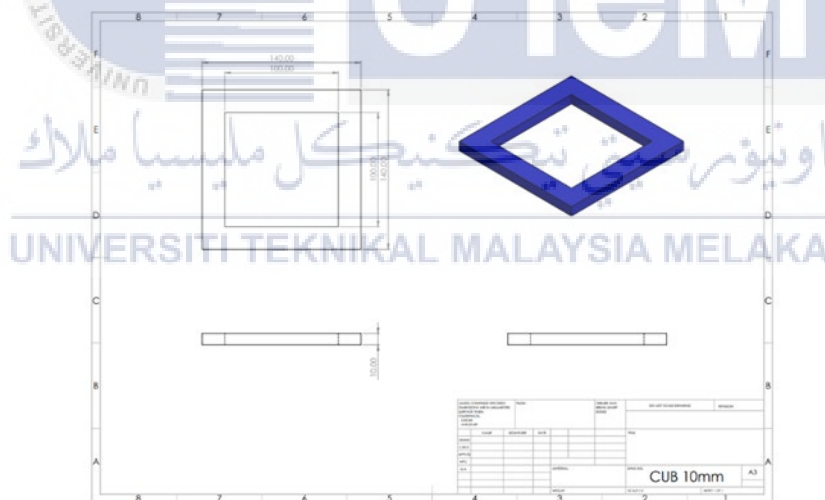


Figure 3.6 Dimension of mould size for the composite cube samples

3.4 Fabrication Process

In this fabrication process, there are three main processes had been involved which is 3D printing process, curing process and cutting process. The details of fabrication process of composite acoustic panel and mechanical panel will be mentioned in subsequent sections

3.4.1 3D printing machine

In order to prepare the acoustical panels and mechanical panels, we need to prepare the mould with a 3D printing machine. The material used to make the mould is PLA plastics. The 3D printing brand is UP PLUS 3D printer model with 110 – 220 VAC, 50 – 60 Hz, 220 W with a dimension of 245 mm width x 260 mm depth x 350 mm height at the Rapid Prototype Lab in UTeM. Figure 3.8 shows the 3D printing machine model and once the mould has been made.

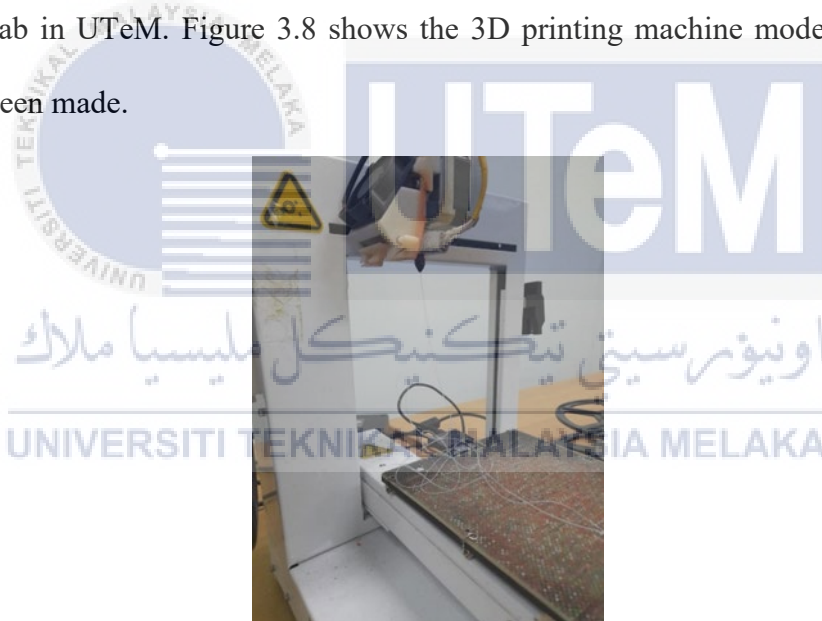


Figure 3.7 UP PLUS 2 3D printer

3.5 Preparation of the Composition

Before the fabrication process of the acoustic panel, the mould should be clean from the contaminant particles and dust. Then, the mould surface was covered by PVC plastic to easily remove from the mould. Next, silicone mould release was applied on PVC plastic surface to easily remove and good surface finishing in order to prevent the sample from sticking at the mould. The kenaf core and foam is weigh by 300g placed in a mixing plastic

container. As for the pure cement sample, 400g cement is needed. In this study, the concrete (C), will be prepared by mixing with water. Water is a major component of concrete and one of the most common types of water used in the manufacture of cement is tap water. The presence of water will cause the cement to hydrate. Also, the cement compound chemically combines with water to form new compound serves as the hardened cement's infrastructure by using standard grade of concrete M 25 that are 1:3. The mix proportion for C was 1: 3 (cement : kenaf/foam) a. The size of kenaf core will be different in each sample and it will be stated in Table 3.5.

Table 3.5 Samples of kenaf core and concrete

Sample	1		2		3		4		5		6		7	
Ratio	C	3 mm	C	20 mm	C	10 mm	C	20 mesh	C	40 mesh	C	Foam	C	C
wt. %	25	75	25	25	25	75	25	75	25	75	25	75	25	75

The kenaf core and cement were evenly using one hand so that the mixture is well mixed before it was poured into cylindrical and cube mould. The size of the kenaf core used in each sample is different for each sample because the purpose of this experiment is to determine the best size of kenaf core that can be used for the acoustic panel and the one which have best mechanical properties at the same time we would mix the cement with foam and the last sample is not mix with anything but purely cement. Therefore, the preparation of the composition started with the sample ratio of 1:3 (C: KC) of 3 mm core, 1:3 (C : KC) of 20 mm core, 1:3 (C : KC) of 10 mm core, 1:3 (C : KC) 20 mesh core, 1:3 (C : KC) 40 mesh core, 1:3 (C :F) foam and 1:3 (C : C) pure cement mixture. Figure 3.9 shows the mixture of samples being poured into the mould.



Figure 3.8 The mixtures of sample in mould

3.6 Curing Process

Curing process for concrete is the process of maintaining the moisture and temperature conditions of concrete for the hydration reaction to continue and help concrete to develop hardened properties over time. This process helps concrete to harden and bond with reinforcement material which is kenaf core while helps to prevent damages of vibration and impact to the bond of concrete and kenaf core. Based on ASTM standard for maturity of the concrete, curing process is carried out by submerged the harden samples into the water for about 28 days until reach the maturity and stimulate optimum strength. The samples then will be examined to check the quality of the samples. Figure 3.10 shows the samples being soaked in the water during the process.



Figure 3.9 Figure 3.10 Samples being soaked in water

3.7 Cutting Process

For cube samples that will be used in flexural testing, the cement needs to be cut into 5 parts with a hand grinder. A Bosch hand grinder with 670 W input power is used to cut the concrete cube and to ensure a good surface finishing, sandpapers were used to smooth up the edge of the samples and Figure 3.11 will show the hand grinder that has been used.



Figure 3.10 Bosch GWS 060 Professional Angle Grinder

3.8 Testing

There is only two mechanical testing that will be used to carry out on the samples in this research which is the compression test and flexural test and for sound testing is the impedance tube testing. All the testing will be performed based on requirements of ASTM standard. The objective of these mechanical testing is to determine the mechanical and acoustic properties of the samples. Table 3.6 shows the ASTM standards for each type of test.

Table 3.6 ASTM standard for mechanical and sound testing

Testing	ASTM Standard
Compression Test	ASTM 109
Impedance Tube Testing	ASTM E1050-09

3.8.1 Compression Test

If the material does not have a lot of mechanical response in tensional load, compression test would be the accurate test since it will represent the material's properties better. Compression test is used to determine the behaviour of a material by crushing load and is typically performed by applying compressive pressure to a test specimen using a 1500 kN compression machine. The specimen will be subjected to compression load under the ASTM 109 standard test method to analyze the qualities such as compressive strength, yield strength and elastic limit as illustrated in Figure 3.10. Five samples will be tested and the average result will be recorded.

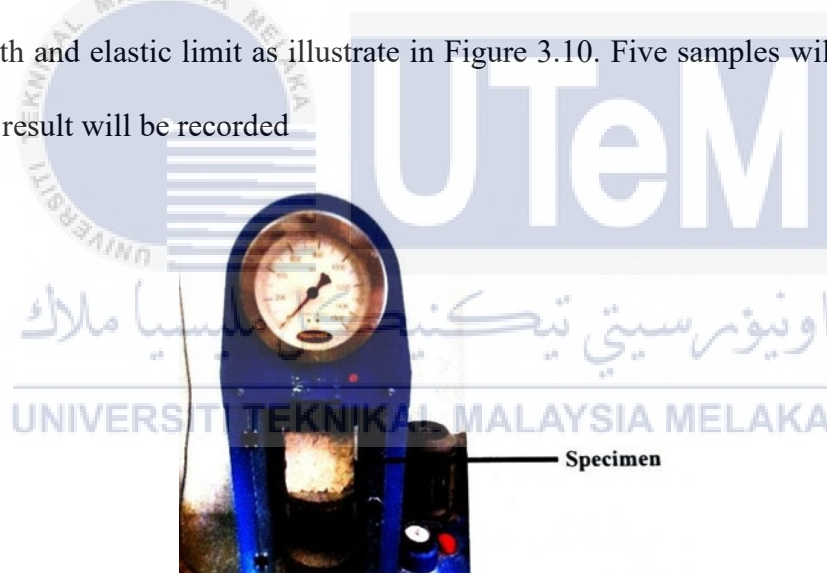


Figure 3.11 Standard of compression testing setup

3.8.2 Flexural test

Flexural testing, also known as bending or transverse testing, is a mechanical test method used to evaluate the behavior of a material subjected to bending loads. The test provides information about the material's flexural strength, modulus of elasticity, and other mechanical properties related to its ability to withstand bending stresses. This type of testing is particularly important for materials used in structural applications where they may

experience bending forces during use. In this study, the three bending flexural test has been used. The sample dimension is 100 mm x 20 mm x 10 /20/30/40/50mm. This test is based on standard ASTM D790 and this test will be carried ou in Material Testing Lab, UTeM Melaka as shown in Figure 3.13.

When experimenting, The load is applied gradually until the specimen deforms or fractures. The applied load and the corresponding deflection of the specimen are recorded. The recorded data is used to generate stress-strain curves, which provide insights into the material's behavior under bending. The results help assess the material's suitability for specific applications, especially in structural design where bending forces are common.



Figure 3.12 Standard of flexural testing setup

3.8.3 Impedence tube test

The impedance tube method is used to obtain a sound absorption coefficient (α) based on standard ASTM E1050-09. The sample thickness in the impedance tube is 10 mm, 20 mm, 30 mm 40 mm and 50 mm The frequency range used for impedance tube testing is from 1 Hz to 5000 Hz. The tesing will be carried out with no air gap, 10 mm air gap, 20 mm

air gap and 30 mm air gap. The impedance tube testing is available in Acoustic and Vibration Laboratory, UTeM, Melaka, shown in Figure 3.11.

When experimenting, the first step is to calibrate the impedance tube testing to ensure that the device works properly and prevents errors during the test. Besides, calibration is necessary to ensure that the results are accurate after the test is done and ensure that it is safe to use before testing. A total of five specimens for each sample with dimension of 34.5 mm in diameter and constant thickness of 10 mm. The specimens repeated at least five times to obtain accurate and reliable test data.



Figure 3.13 Impedance Tube Testing

3.9 Scanning Electron Microscope (SEM)

Scanning electron microscope (SEM) is a common instrument used only to examine the sample's morphological surface fracture of the kenaf core interface after sound testing. It uses a high beam of electrons to generate the signal to the surface of the sample to be observed. The sample fracture surface is cut out and fixed on the carbon tape-covered stub. During the observation, a gold coated vacuum (Auto Fined JEOL-JFC1600) is coated prevent the loading effect. Electrostatic charging during the test ad at the accelerating voltage of 10.0 kV shall be prevented for each sample. The surface failure will be observed and examined using SEM. Using SEM, the surface fracture of the kenaf core composite was

observed through the image of surface features. Figure 3.12 shows and electron scanning microscope.



Figure 3.14 Scanning electron microscope (SEM)

The flowchart of overall process in this research is depicted in Figure 3.1. This research began with the preparation of raw material which are kenaf core, kenaf fibre and concrete that will be mix with different size of composition for each sample. After the preparation, moulding and curing technique are carried out. Moulding is a technique to produce samples of acoustic panel with the dimension of 34.5mm x 20 mm which allow the sample to be dried on ASTM standard. If the quality of the sample is good, it will proceed with the testing but if the quality is not good, new sample need to be prepared. When the samples are ready, the samples were tested to observe the new mechanical properties of the acoustic panel by compression test and of acoustical properties testing, the tests are impedance tube testing.

CHAPTER 4

RESULTS AND DISCUSSION

4.1 Fabrication and Characteristics of Concrete with Different Composition

In this study, the reinforcement used was kenaf fibre, while pure cement were the matrix system for developing the concrete. The size of the kenaf core used in this research are 3 mm, 10 mm, 20 mm, 20 mesh and 40 mesh. There will be also a concrete samples that will be reinforced with foam and solely pure cement concrete. Firstly, the sample needed for this research is 150 samples for acoustic panels and 31 samples for the mechanical testing panels. There will be five different sizes of kenaf core that will be used and also the thickness of the concrete will be vary starting from 10 mm to 50 mm thickness. To fabricate the acoustic panels in time, 5 moulds with dimension of 50 mm x 50 mm x 10 / 20 / 30 / 40 / 50 mm were made using 3D printing machine with the measurement of each sample 34.5 mm x 10 / 20 / 30 / 40 / 50 mm and the shape for the acoustic panels are cylindrical. Then, for the second samples that will be used for mechanical testings used a mould with a dimension of 140 mm x 140 mm x 10 / 20 / 30 / 40 / 50 mm will be used and the samples for mechanical test panels will be in a cube shape for flexural and for compressive test, the samples for acoustic panels will be reused.. After drying the sample for 3 days, all the samples would submerge into the water to undergo the curing process for 28 days. Later on the samples will be cut into 5 parts with a dimension of 100 mm x 20 mm x 10 / 20 / 30 / 40 / 50mm.

To ensure the samples are qualified for testing, an experimental sample will be prepared to determine which method is convenient for mixing concrete and kenaf core to ensure that the mixture is well blended to be more robust and more stable. Figure 4.1 shows

the process of making the trial sample with different ratio. Then, all the trial samples were dried out under the sunlight for a few hours until thoroughly dried. The result of this trial sample showed in Figure 4.2, where the suitable ratio will give good strength and not easily crack when broken. Unfortunately, if wrong method is used and not thoroughly dried the sample, it will break easily and cannot be used for further process as illustrated in Figure 4.2.



Figure 4.1 Trial sample of mixing kenaf core and concrete



Figure 4.2 Sample condition (a) acceptable (b) reject

After confirming the suitable ratio for mixing the kenaf core and cement, the kenaf core will be thoroughly covered. Then water is added thus the mixture will have a good bonding with each other as shown in Figure 4.3. The mixture will be poured into the mould and compress using one thumb evenly to ensure the sample has the same density. Figure 4.4

illustrates the moulding process of the samples and will be dried out under the sunlight for 24 hours.

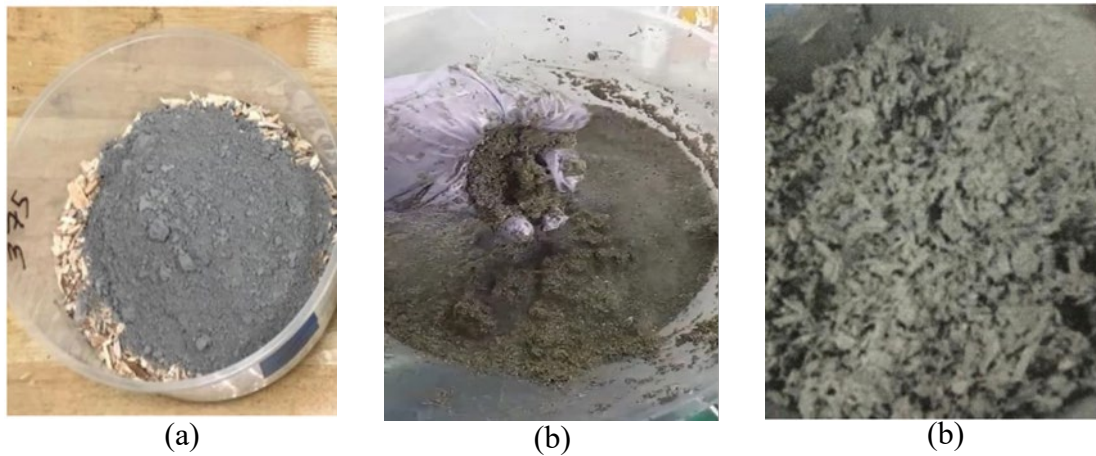


Figure 4.3 Fabrication steps (a) cement add (b) manual mixing (c) final mix concrete



Figure 4.4 Concrete curing in mould

After the drying process, the sample will be removed from the mould gently to avoid any vibration that will lead to the sample breaking or cracking easily. Figure 4.5 and Figure 4.6 show samples example after undergoing the drying process. While most samples have outcomes that are better with flat, smooth surfaces, some do not, and these samples cannot be utilised for the following process. Broken or fully cracked becomes rejected sample and needs to replace it with new samples because if it has been used, the crack will propagate

further during the cutting process because vibration occurs from the cutting tool. After that, the quality samples will be measure the mass before and after the curing process.



Figure 4.5 Selected sample after cured (a) cement with too much water (b) good samples that mix well

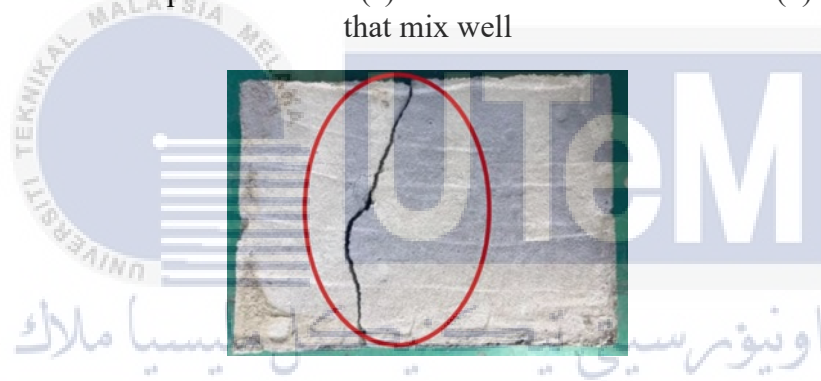


Figure 4.6 The examples rejected samples

The samples were submerged in the water for 28 days and the condition of the samples will be observed frequently to ensure water is enough throughout the process. Figure 4.7 shows the curing process of the samples before and after 28 days. After 28 days, the samples will be removed from the water and dried out for one day so that the samples are thoroughly dried. This drying method is vital for the samples because any trapped water inside the sample will negatively impact the next process. Although some samples happen to be cracked during the process, they still can be used for testing as it does not affect the condition of the samples.



Figure 4.7 The curing process (a) at initial state a (b) at 28 days of submerging

4.2 Mechanical Properties of Kenaf Core Concrete Sample

The performance of this experiment is determined by several testing which are threepoint flexural test and compression test according to ASTM standards. Each testing will determine the best performance of a sample of kenaf core reinforced concrete/ In this research, sample made of cement and polystyrene foam were used as the benchmark.

4.2.1 Flexural performance

In this section, flexural performance was conducted by testing samples using Universal Testing Machine (UTM) from Instron which has maximum capacity of 100 kN as shown in Figure 4.8. The size of sample for testing is 100 mm x 20 mm x 10 / 20 / 30 / 40 / 50 mm. The data is recorded thus the graphs were generated for analysis and comparison of flexural performance for each composition with different size of kenaf core. Figure 4.9 illustrates the mode of failure that occurs after the testing.

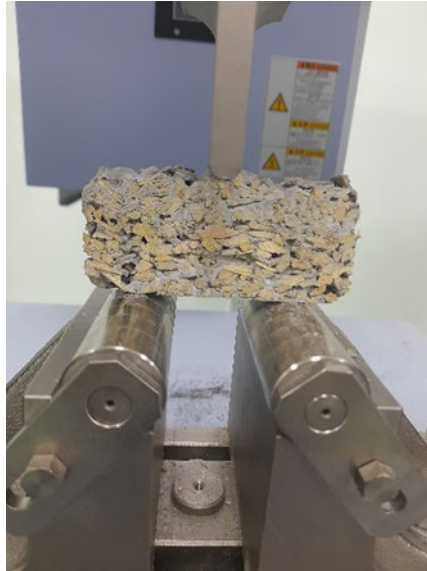


Figure 4.8 The examples of three-point flexural test

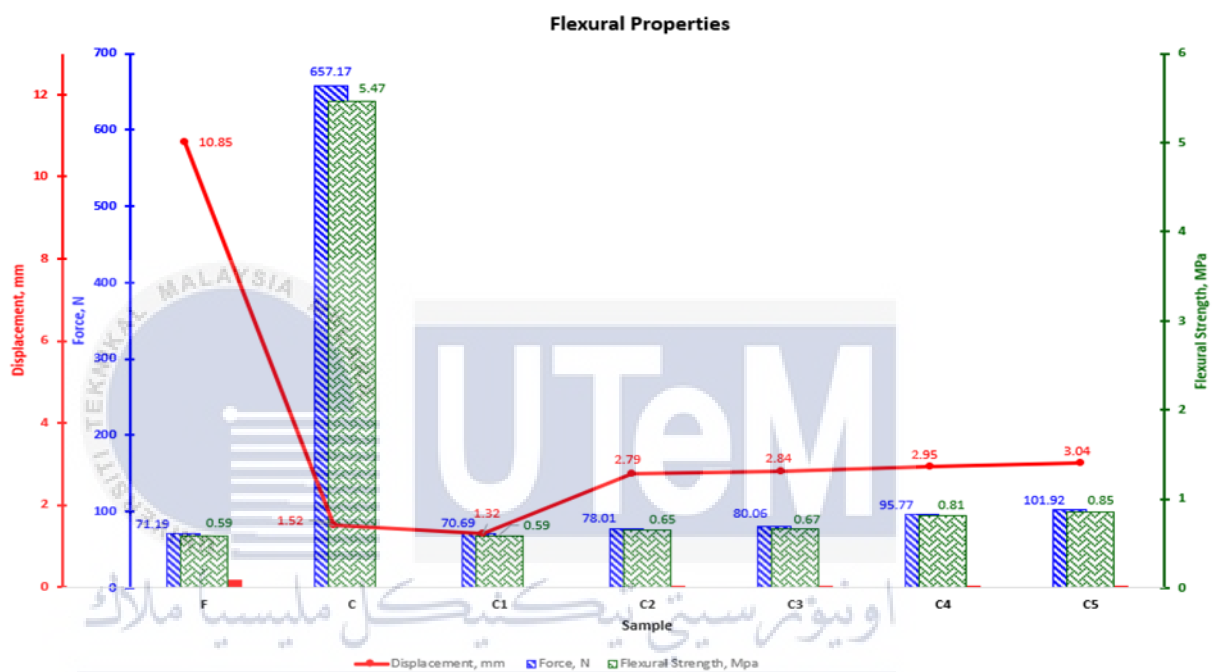


Figure 4.9 The condition of sample after the testing

4.2.1.1 Comparison flexural strength of kenaf core and concrete

Based on Figure 4.10, illustrates the 28-day flexural strength of each sample with different composition of kenaf. The flexural strength of 40 mesh, 20 mesh, 30 mm, 20 mm and 10 mm with 0.59 MPa, 0.65 MPa, 0.67 MPa, 0.81 MPa, and 0.85 MPa respectively. As for the control samples like foam and pure cement, the flexural strength is 0.59 MPa and 5.47 MPa. The trend of the chart shows that is linearly decreasing in strength when the smallest mesh is used in the sample. From the figure, it shows that core with the size of 40 mesh shows the lowest flexural performance of 0.59 MPa while the highest flexural performance was at 20 mm kenaf core with the value of 0.85 MPa. The calculated difference

between the lowest and highest has a significant value of 36.11%. The result is in lines of earlier study of Zhang et al. (2020) that found when the fibre content is higher than the concrete, the flexural strength rate growth slowly decreasing. It is shown that the smallest size of kenaf, the lower the flexural strength result. Cementitious materials are prone to crack and it affects the durability of the concrete structures. Because of their low tensile strength and brittleness, cementitious materials can be easily cracked.



UNIVERSITI TEKNIKAL MALAYSIA MELAKA
Figure 4.10 Comparison of flexural strength of each size of ratio

From Figure 4.10, there is a small crack line appears where it can be concluded that 20 mesh and 40 mesh is not strong enough to make it less susceptible to crack while in Figure 4.13, to shows there are large amount of porosity can be seen as the amount of ratio decreases. This is because bonding between the concrete and kenaf core is low. It can be said that reducing the reinforcement material in the sample will increase the flexural strength. Higher performance with smaller KC will gives good impact and better mechanical strength.

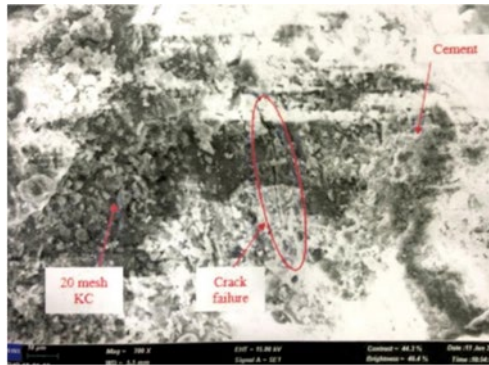


Figure 4.11 The small crack propagation line after flexural test of 20 mesh

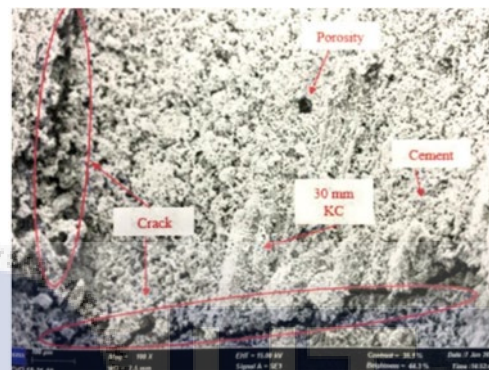


Figure 4.12 SEM analysis for 30 mm of kenaf core and concrete

According to Table 4.1, which depicts the cracking and failure pattern of the sample, the majority of the samples exhibit cracking propagation at the mid-span between the two points of force. During testing, the control sample which is pure cement failed in a brittle form, which happened abruptly without warning. Sample kenaf core with the size of 10 mm, 20 mm, 30 mm, 20 mesh, 40 mesh and foam on the other hand, failed in a ductile way, in which the cracking propagated and spread without splitting the beam in half. As stated by Zhou et al., (2020), adding kenaf fibres to concrete has the ability to delay crack propagation and change the mode of failure from brittle to ductile.

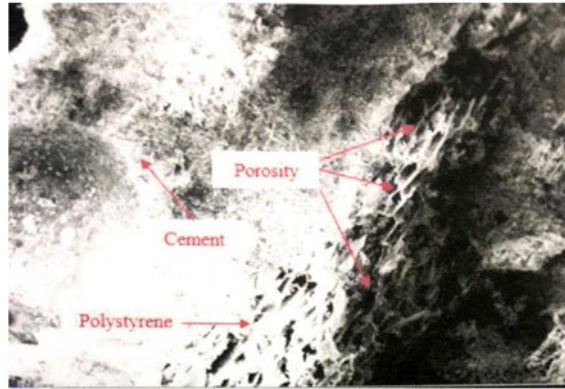


Figure 4.13 SEM analysis for polystyrene foam reinforced concrete

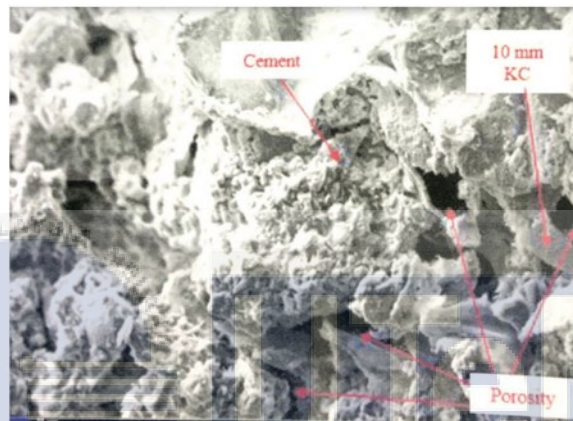



Figure 4.14 SEM analysis for 10 mm KC




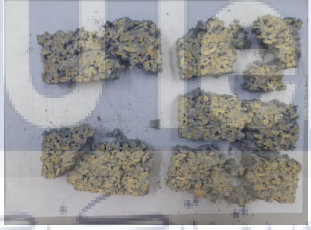
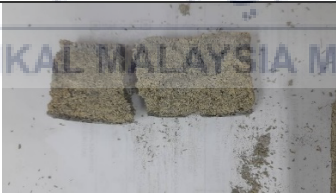

Table 4.1 Cracking pattern and failure mode sample

Thicknes s	Sampl e	Cracking Pattern	Failure mode
	10 mm (C5)		Ductil e



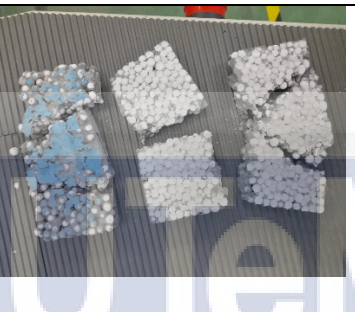
10 mm thickness	20 mm (C5)		Ductile
	3 mm (C4)		Ductile
	20 mesh (C2)		Ductile
	40 mesh (C1)		Ductile
	Pure cement (C)		Brittle
	Foam (F)		Ductile

20 mm thickness	10 mm (C3)		Ductile e
	20 mm (C5)		Ductile e
	3 mm (C4)		Ductile e
	20 mesh (C2)		Ductile e
	40 mesh (C1)		Ductile e
	Pure cement (C)		Brittle

	Foam (F)		Ductile
30 mm thickness	10 mm (C3)		Ductile
	20 mm (C5)		Ductile
	3 mm (C4)		Ductile
	20 mesh (C2)		Ductile
	40 mesh (C1)		Ductile
	Pure cement (C)		Brittle

	Foam (F)		Ductile
40 mm thickness	10 mm (C3)		Ductile
	20 mm (C5)		Ductile
	3 mm (C4)		Ductile
	20 mesh (C2)		Ductile
	40 mesh (C1)		Ductile

	Pure cement (C)		Brittle
	Foam (F)		Ductile
50 mm thickness	10 mm (C3)		Ductile
	20 mm (C5)		Ductile
	3 mm (C4)		Ductile
	20 mesh (C2)		Ductile

<p>40 mesh (C1)</p>		<p>Ductil e</p>
<p>Pure cement (C)</p>		<p>Brittle</p>
<p>Foam (F)</p>		<p>Ductil e</p>

4.2.2 Compression performance

In this part, compression test is according with ASTM 109 to determine the performance of the samples. Each test will measure the average of 6 samples for each ratio with measurement of 34.5 mm x 10 / 20/ 30 /40 /50 mm. Hence, these tests will determine the best performance of a sample of kenaf core reinforced concrete for compression test panel applications. In this research, sample of pure cement concrete and foam will be used as a benchmark. Figure 4.15 shows the setup for compression test and Figure 4.16 shows the condition after testing.



Figure 4.15 Setup for compression test

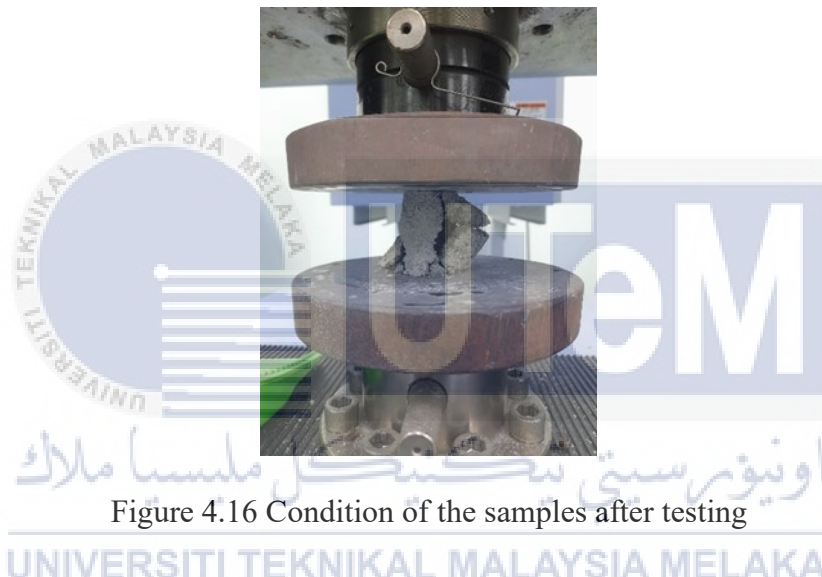


Figure 4.16 Condition of the samples after testing

4.2.2.1 Comparison of compression test kenaf core and concrete

Figure 4.17 demonstrated that the data of compression performance for had an upward trend when the size of te core is bigger. The discussion result begin with the lowest performance of kenaf concrete of 40 mesh is 0.15 MPa and the highest performance is 0.44 MPa and that is 20 mm kenaf core. The percentage difference between 0.15 MPa and 0.44 MPa is approximately 193.33% and it is a huge difference .From the data in Table 4.2, it is apparent that the crushing form of kenaf core concrete caused a gradual reduction in

specimen height. We can see that the smaller the ratio of kenaf core, the lower the performance of the compression. This is because a lower percentage of concrete was used that generally will lower percentage of concrete was used that generally will lower the ability for the samples to withstand higher force. However, interestingly, this is contrary to a study conducted by Solahuddin (2022). The author comes out with the finding that the additional of kenaf fibre will reduce the compressive strength of the concrete. This is because the concrete was not completely dry and hardened before and after the curing process. Compression testing on kenaf core concrete helps assess its suitability for structural applications and provides valuable insights into its mechanical properties. The results can be compared with established standards or used to optimize mix designs for specific applications. By understanding how variations in mix design affect the material's compressive strength and other mechanical properties, engineers can tailor kenaf core concrete for specific applications, optimizing its performance in different structural elements.

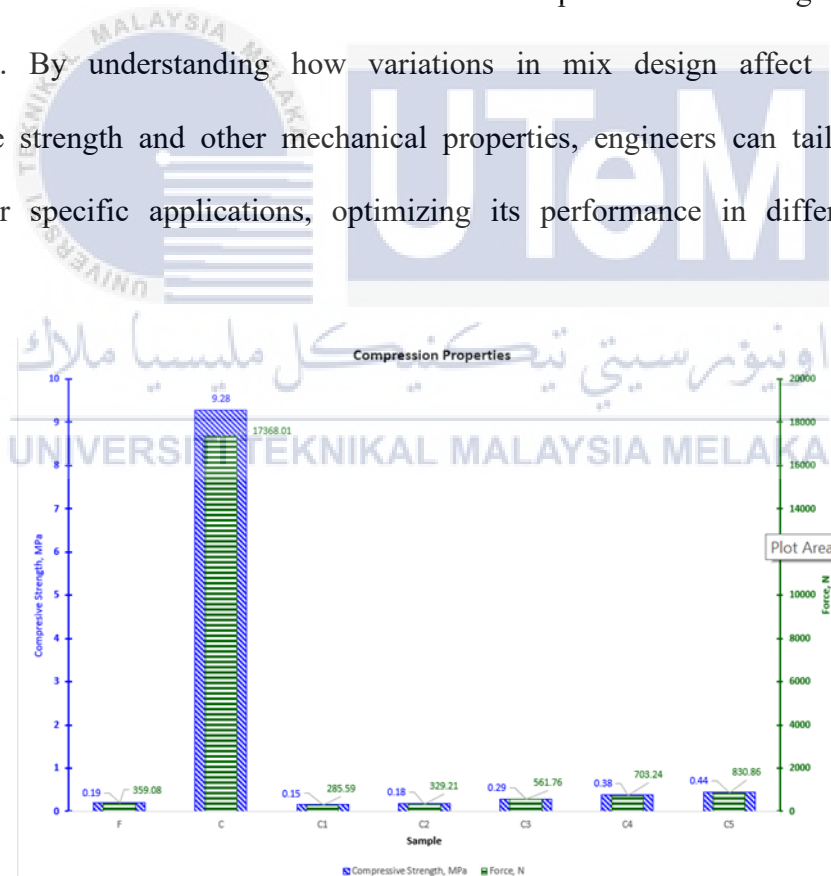



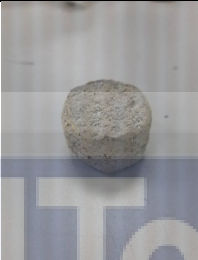

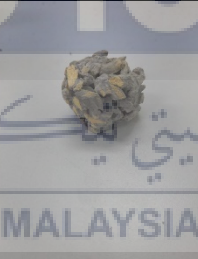





Figure 4.17 Comparison of compression performance for the ratio size of kenaf core

Table 4.2 Form of crack for kenaf core concrete

Thickness	Samples	Before	After
10 mm thickness	10 mm (C3)		
	20 mm (C5)		
	3 mm (C4)		
	20 mesh (C2)		
	40 mesh (C1)		

	Foam (F)		
	Pure Cement (C)		
20 mm thickness	10 mm (C3)		
	20 mm (C5)		
	3 mm (C4)		

	20 mesh (C2)		
	40 mesh (C1)		
	Foam (F)		
	Pure Cement (C)		
30 mm thickness	10 mm (C3)		

<p>20 mm (C5)</p>		
<p>3 mm (C4)</p>		
<p>20 mesh (C2)</p>		
<p>40 mesh (C1)</p>		
<p>Foam (F)</p>		

	Pure Cement (C)		
40 mm thickness	10 mm (C3)		
	20 mm (C5)		
	3 mm (C4)		
	20 mesh (C2)		

	40 mesh (C1)		
	Foam (F)		
	Pure cement (C)		
50 mm thickness	10 mm (C3)		
	20 mm (C5)		

<p>3 mm (C4)</p>		
<p>20 mesh (C2)</p>		
<p>40 mesh (C1)</p>		
<p>Foam (F)</p>		
<p>Pure Cement (C)</p>		

4.3 Summary of Mechanical Properties on Kenaf Core Reinforced Concrete

Figure 4.16 demonstrates the graph of mechanical performance summary on overall samples. There are 5 different kenaf core sizes used starting from F, C1, C2, C3, C4, C5 and C. It can be seen that the best in term of mechanical performance is C5, however C4 also in range of good performance. In the context of mix uniformity, the use of 20mm kenaf core appears advantageous compared to other sizes like 10mm, 40 mesh, 20 mesh, and 3mm. The longer length of the 20mm fibers, while potentially posing challenges in workability, offers benefits in terms of achieving a more uniform distribution throughout the concrete mix. Longer fibers tend to provide improved tensile and flexural strength, essential for reinforcing concrete structures. The 20mm Kenaf core's length may contribute to a more effective interlocking and dispersion within the matrix, promoting a homogeneous distribution of reinforcement. This can enhance the overall structural integrity and performance of the reinforced concrete. Cement was taken out due to nature of good performance and it was just used as a control sample, same goes to polystyrene foam.

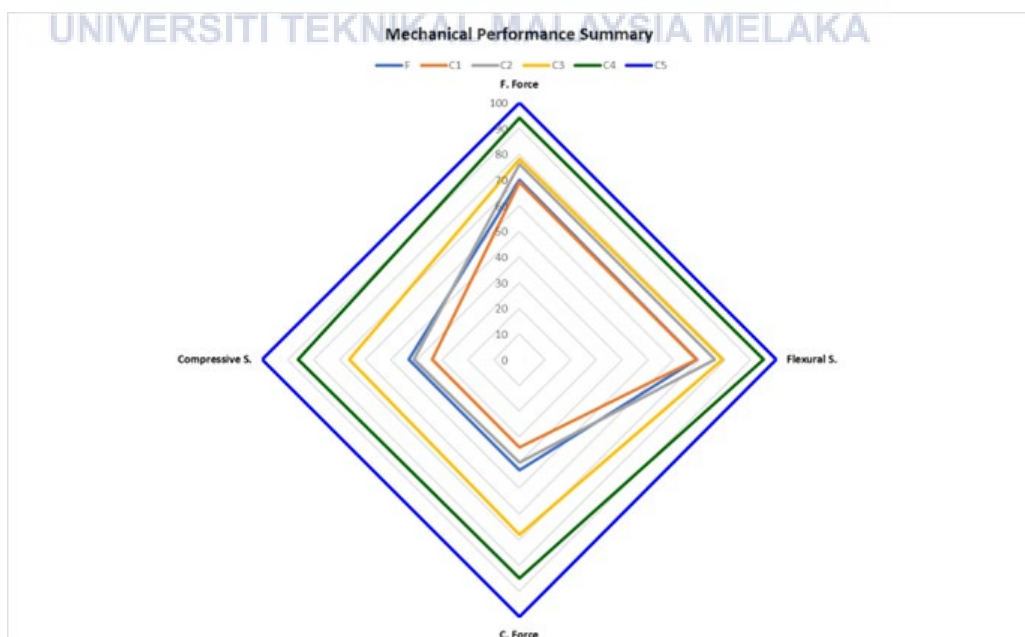


Figure 4.18 Mechanical Performance Summary Graph.

4.4 Sound Absorption Performance of Concrete With Different Air Gap.

The acoustic test is conducted using an impedance tube testing lab based on standard ASTM E1050-09 to analyse the sound absorption coefficient's performance. All the samples have different thickness starting from 10mm thickness to 50 mm thickness and the diameter of the sample is 34.5mm. This test will be carried out with no air gap, 10 mm air gap, 20 mm air gap and 30 mm air gap. The samples were measured at every peak of the frequency range from 500 Hz to 5000 Hz. The highest peak at every frequency is recorded, and the results will be compared. The average of different compositions of samples will be repeated for six times and three times for pure cement and polystyrene foam. The sound absorption coefficient showed a gradual increase in the range between <1000 Hz to >5000Hz

4.4.1 Sound absorption performance without air gap

From figure 4.19, F shows the lowest peak among all the samples, which is the value of 0.047572467 coefficient in 5000 Hz. The finding is consistent with the results of past studies obtained by Asdrubali (2006), in which polystyrene at 40 mm shows 0.5 coefficient at 500 Hz. Based on their research, polystyrene foam had the weakest sound absorption coefficient compare to the rest of the materials. Polystyrene foam is a stiff material that does not return to its original shape shape after impact has been made on the foam: this foam,s characteristics show low porosity (Coelho et al., 2013). From the results, it is clear that with no air gap, the C3 samples showed the best effect compared to other samples, which are reaching the highest peak at 500 Hz with a coefficient of 0.410138408 due to kenaf fibre itself has good sound absorption properties. Studies by Lim et al. (2018) investigates natural kenaf fibre's sound absorption such as pure kenaf fibre has an absorption coefficient starting from 500 Hz is above 0.5 and able to reach 0.85 on average above 1.5 kHz with a thickness of 25-30 mm.

Other than that, C4, C5 and F show a similar trend, reaching their highest peak at 500 Hz, which is the coefficient of 0.308959806, 0.388719108, 0.304315425 respectively. All samples had almost similar trends except for cement and 40 mesh starting at 3500 Hz until 4500 Hz with the difference value of 0.01 to 0.08 difference range of value approximately. For sample C1 at 1500 Hz, there's a notable increase to 0.290442, which might correspond to a peak in the graph. Sample F has a peak at 2500 Hz with a value of 0.250738, which would likely be one of the highest points for that sample on the graph. At 3500 Hz, sample C1 again has a significant value (0.210055), and at 4500 Hz, the sound coefficient for most samples drops to 0, indicating no absorption/effectiveness at that frequency. Finally, at 4000 Hz, sample C shows a sound coefficient of 0.231307, which might correspond to a peak or a higher value on the graph compared to the other frequencies for that sample. When comparing samples, C3 and C5 generally perform better at lower frequencies which is up to 1000 Hz, whereas samples C1 and F show better performance or peaks at mid to higher frequencies which is 1500 Hz and above. None of the samples show a sound coefficient close to 1, which would represent total absorption or maximum effectiveness. This implies that while there is some variation in performance, all samples have a relatively low sound absorption or effectiveness across the measured frequencies.

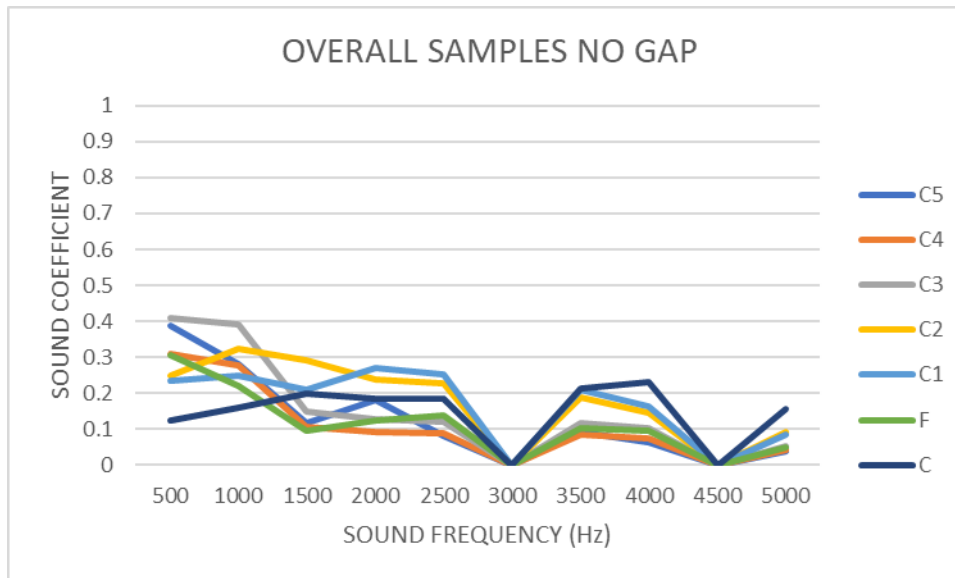


Figure 4.19 The graph of sound absorption with no gap coefficient with the comparison of all samples

4.4.2 Sound absorption performance with 10 mm air gap

Based on Figure 4.20, at 500 Hz, sample C4 has the highest sound coefficient which is at 0.426009, indicating it is most effective at this frequency with the air gap present. Meanwhile when the sound frequency is at 1000 Hz and 4000 Hz, all samples have significantly lower sound coefficients compared to other frequencies, suggesting they are less effective at these frequencies. At 1500 Hz, samples C and C1 have higher sound coefficients compared to the other samples, with C1 being the highest which is at 0.269885. When the frequency reached 2000 Hz, sample F has the highest sound coefficient of 0.343249, a marked increase compared to its performance at 1000 Hz. At 2500 Hz, sample C2 has a notable increase of 0.318043, whereas samples C1 and F also show relatively high values. At 3000 Hz and 4500 Hz, most samples' effectiveness drops to zero, indicating no absorption or effectiveness at these frequencies with the air gap present. The presence of a 10 mm air gap affects the sound absorption characteristics of the samples. The data indicates that the air gap generally reduces the effectiveness of the samples at certain frequencies, particularly at 1000 Hz, 3000 Hz, and 4500 Hz, where many samples show a sound

coefficient of zero. However, there are specific frequencies where certain samples demonstrate increased sound absorption even with the air gap, such as sample C4 at 500 Hz and sample F at 2000 Hz. Comparatively, the air gap seems to diminish the overall effectiveness across the frequency range, yet it allows for certain peaks at specific frequencies that were not as pronounced without the air gap. This information could be crucial for applications that require sound insulation or absorption at specific frequencies and suggests that the air gap can be a critical factor in the acoustic performance of these materials.

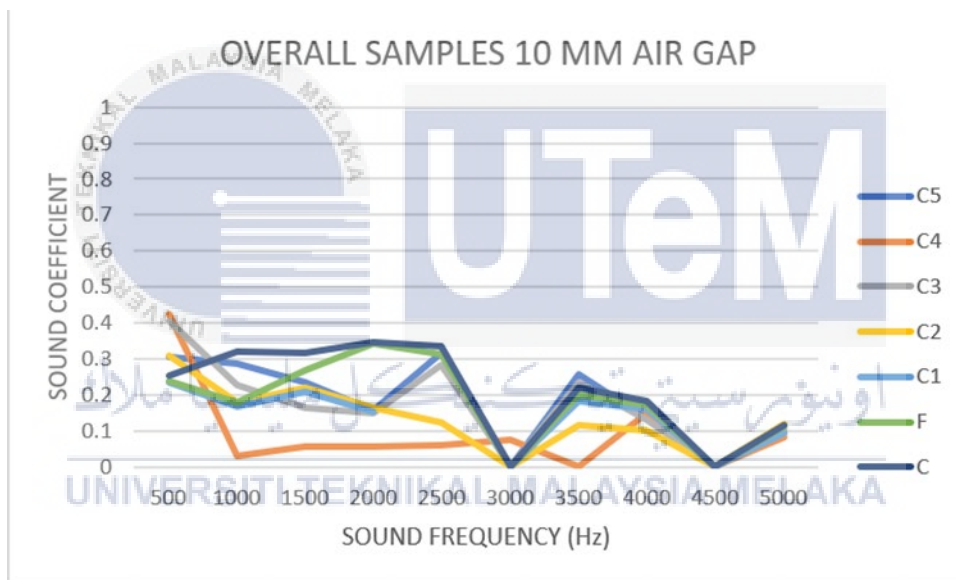


Figure 4.20 The graph of sound absorption with 10 mm air gap coefficient with the comparison of all samples

4.4.3 Sound absorption performance with 20 mm air gap

Figure 4.21 shows a graph of the sound coefficients of different samples with a 20 mm air gap at various sound frequencies. At 500 Hz, the sound coefficients are fairly high for most samples, with C3 and C4 having the highest values, indicating good absorption at

lower frequencies despite the larger air gap. 1000 Hz presents a significant drop in sound coefficient for all samples, particularly C4, which has reduced to 0.030885 from 0.402505 at 500 Hz. At 1500 Hz, the sound coefficients are somewhat uniform across the samples, with none standing out significantly. 2000 Hz frequency shows a slightly increased sound coefficient for sample F which is 0.384108, suggesting this sample interacts more effectively with sound at this frequency with a 20 mm air gap. At 2500 Hz, C5 has the highest sound coefficient which is 0.299897, with other samples like C1 and F also showing relatively good performance. At 3500 Hz, C4 has a notably high sound coefficient which is 0.079212, which is a significant recovery from the zero values at 3000 Hz. 4000 Hz presents a moderate increase for several samples, with C4 again having the highest coefficient which is 0.151337. Finally, at 5000 Hz, the coefficients are generally low but present, with C4 having the highest at 0.08094. The samples made of different kenaf core size generally show better sound absorption at lower frequencies at 500 Hz even with the larger air gap. However, the performance varies widely across different frequencies and samples. For instance, sample F stands out at 2000 Hz, suggesting that it might be particularly effective at damping sounds around this frequency when a 20 mm air gap is involved. Interestingly, the trend observed with the 10 mm air gap, where most samples' effectiveness diminished, is also seen with the 20 mm gap but with some differences in specific frequencies. This suggests that the size of the air gap is a critical factor in the acoustic performance of these materials and can have both negative and positive effects, potentially due to the phenomenon of standing wave formation within the gap or other complex acoustic interactions. The data from the 20 mm air gap can guide the design of acoustic materials where certain frequencies need to be targeted for absorption or enhancement.

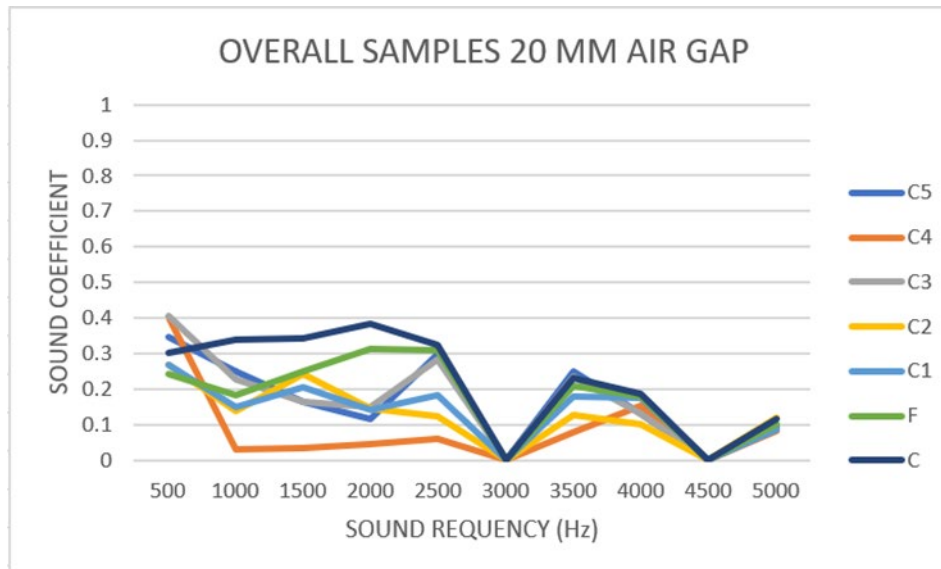


Figure 4.21 The graph of sound absorption with 10 mm air gap coefficient with the comparison of all samples

4.4.4 Sound absorption performance with 30 mm air gap

Figure 4.22 indicates a graph of the sound coefficients of different samples with a 30 mm air gap at various sound frequencies. All samples show moderate sound coefficients at 500 Hz frequency, with C3 having the highest sound coefficient at 0.464398. This indicates decent absorption effectiveness at this lower frequency despite the large air gap. At 1000 Hz, there is a general decline in sound coefficients for all samples, with C still maintaining a relatively higher value of sound coefficient of 0.349167 compared to others meanwhile at 1500 Hz frequency, the sound coefficients are lower, with F having the highest at this frequency which is the sound coefficient value of 0.249584. At 2000 Hz, the sound coefficient values slightly increase, with C showing a sound coefficient of 0.366579, indicating it's the most effective at this frequency point among all samples with a 30 mm air gap. C5 shows the highest coefficient 0.319522 suggesting a better performance at this mid-frequency at the value of 2500 Hz. At 3500 Hz, C4 and C5 exhibit increased coefficients, with C4 being the highest at 0.088102. At 4000 Hz, there is a moderate sound coefficient for several samples, with C4 again having a relatively high value of 0.132617. As for 5000 Hz,

there's a slight recovery with C3 showing the highest coefficient of 0.098345, although the values remain low. The 30 mm air gap significantly impacts the sound absorption characteristics of the materials, much like the 10 mm and 20 mm air gaps did, but with a different pattern. Notably, there is no absorption at 3000 Hz and 4500 Hz for any of the samples, which is consistent with the findings at 20 mm. However, the overall levels of sound coefficient are generally lower across all frequencies when compared to the 10 mm and 20 mm air gap data. This suggests that a larger air gap may not always enhance sound absorption, especially at certain critical frequencies where the air gap seems to cause the sound absorption to drop to zero. This could be due to the physical properties of sound waves and how they interact with the air gap and material, possibly creating destructive interference or standing wave effects at specific frequencies.

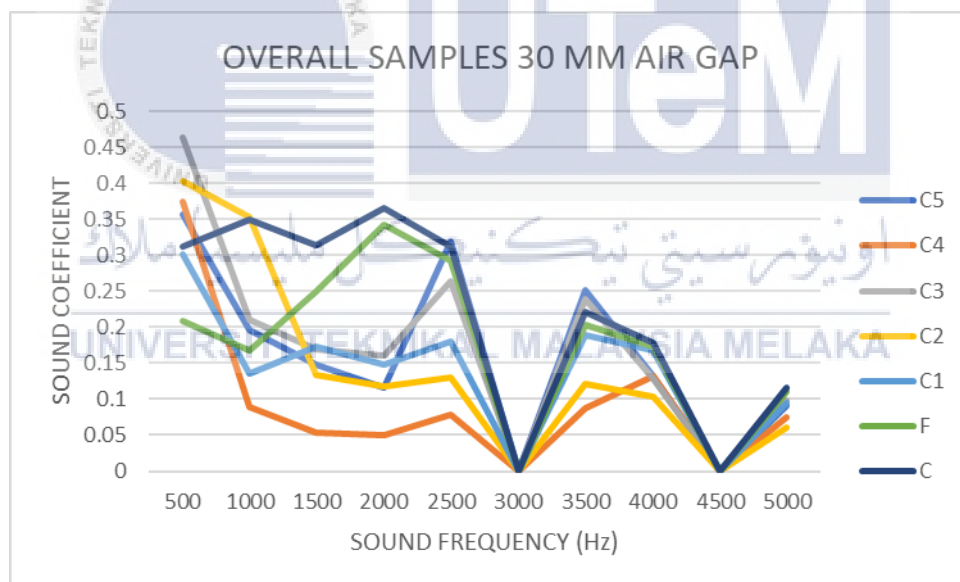


Figure 4.22 The graph of sound absorption with 30 mm air gap coefficient with the comparison of all samples

4.5 Sound Absorption Performance of Different Thickness of Samples

This research is to study the effect of five different sizes of thickness in order to evaluate the acoustical performance. The performance of acoustic panel was tested with a thickness of 10 mm, 20 mm, 30 mm, 40 mm and 50 mm in total. Before the sample is inserted into the tube, the sample were made sure free from dirt and dust contains. This is to avoid inaccurate data reading during the testing to get reliable results. The sample testing was repeated 6 times in order to get the accurate data for better performance result

4.5.1 Sample C1

First of all, this experiment will start with the concrete being reinforced with a 40 mesh size kenaf core and the samples were made with different thickness, starting from 10 mm to 50 mm and it will be carried out with no gap, 10 mm air gap, 20 mm air gap and 30 mm air gap.

4.5.1.1 Sample C1 sound Absorption performance without air gap

Figure 2.23 shows the sound absorption coefficients for sample C1 which stands for 40 mesh kenaf core size at varying material thicknesses from 10, 20, 30, 40, and 50 mm without an air gap, measured across a spectrum of sound frequencies. At 500 Hz frequency, the sound absorption coefficient increases from C1.10 to C1.20, decreases slightly for C1.30, and then further decreases for C1.40 and C1.50. At 1000 Hz, The highest coefficient is at C1.40 which is 40 mm thickness with 0.327855, showing a non-linear relationship with thickness meanwhile at 1500 Hz, the coefficients peak at C1.10 with 0.256436 and generally decrease with thickness. There's a notable increase for C1.20 with a coefficient of 0.346536, which then decreases for thicker materials. At 2500 Hz, coefficients are relatively high across all thicknesses, with C1.20 again having the highest value at 0.240434. The

coefficients are lower compared to 3500 Hz, with C1.40 and C1.50 showing similar values at 4000 Hz. For sample C1 without an air gap, the sound absorption performance shows variability with both frequency and material thickness. There is no consistent trend where an increase in material thickness leads to higher absorption across all frequencies. The complete absence of sound absorption at 3000 Hz and 4500 Hz for all thicknesses suggests these frequencies may be resonant frequencies where the material's intrinsic properties do not allow for effective sound damping. At lower frequencies (500 Hz and 1000 Hz), the relationship between thickness and absorption coefficient is not straightforward, indicating that the optimal thickness for sound absorption depends on the specific frequency. At mid-range frequencies (1500 Hz to 2500 Hz), thinner materials tend to have higher absorption coefficients, while at 3500 Hz and 4000 Hz, a material thickness of 40 mm appears to be more effective. These observations indicate that material thickness selection for sound absorption without an air gap must consider the specific frequencies of interest, as different thicknesses may perform better at certain frequencies.

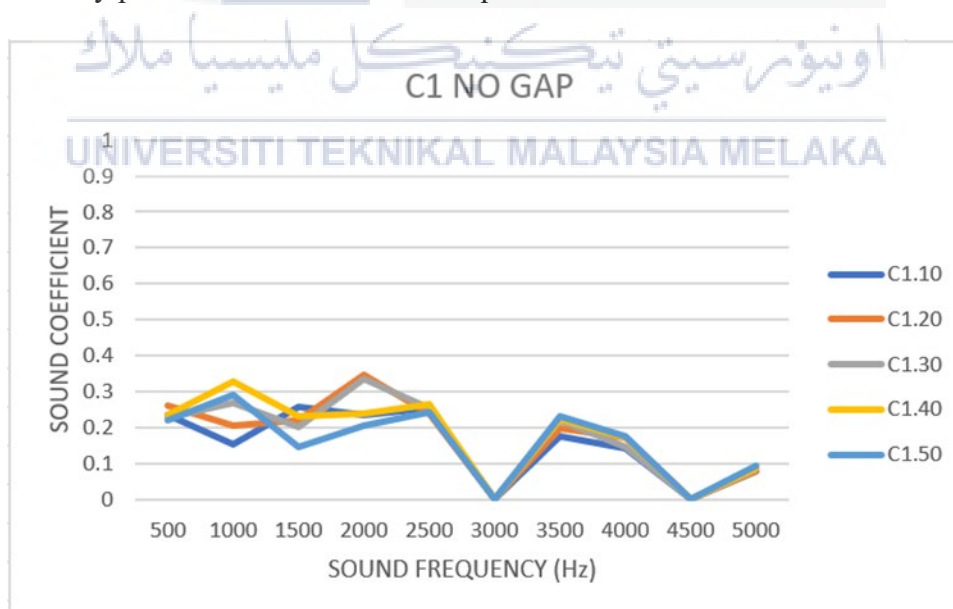


Figure 4.23 Graph of sound coefficient of C1 with no air gap.

4.5.1.2 Sample C1 sound absorption performance with 10 mm air gap

Next, the experiment will be carried out with 10 mm air gap as the graph illustrated in Figure 4.24 . At 500 Hz, the absorption coefficient generally increases with thickness, with C1.50 (50 mm) having the highest coefficient at 0.265708 but on the other hand, at 1000 Hz, there is a decrease in absorption for the thicker materials, with C1.50 showing a significant drop to 0.093596. C1.40 shows the highest absorption coefficient at 0.20185 at 2000 Hz but at 2500 Hz, coefficients for all thicknesses are lower than at 2000 Hz, with C1.30 having the highest value at 0.247207 and at 5000 Hz, sound absorption coefficients are low, with C1.40 showing the highest value at 0.098652. For sample C1 with a 10 mm air gap, sound absorption varies significantly with both frequency and material thickness. At lower frequencies from 500 Hz and 1500 Hz, thicker materials generally show higher absorption coefficients. However, at 1000 Hz, the thickest material C1.50 is not the most effective, indicating a non-linear relationship between thickness and absorption. The absence of sound absorption at 3000 Hz and 4500 Hz for all thicknesses suggests that these frequencies may correspond to resonant conditions created by the air gap where the material is ineffective at sound damping. At mid-range frequencies 2000 Hz and 2500 Hz, C1.30 and C1.40 tend to be more effective, while at the highest frequency tested 5000 Hz, C1.40 has the highest absorption coefficient. These findings suggest that for applications involving a 10 mm air gap, the selection of material thickness for sound insulation should be guided by the specific frequencies of interest. Different thicknesses may be more effective at absorbing different frequencies, and there is no single thickness that provides optimal absorption across the entire frequency range.

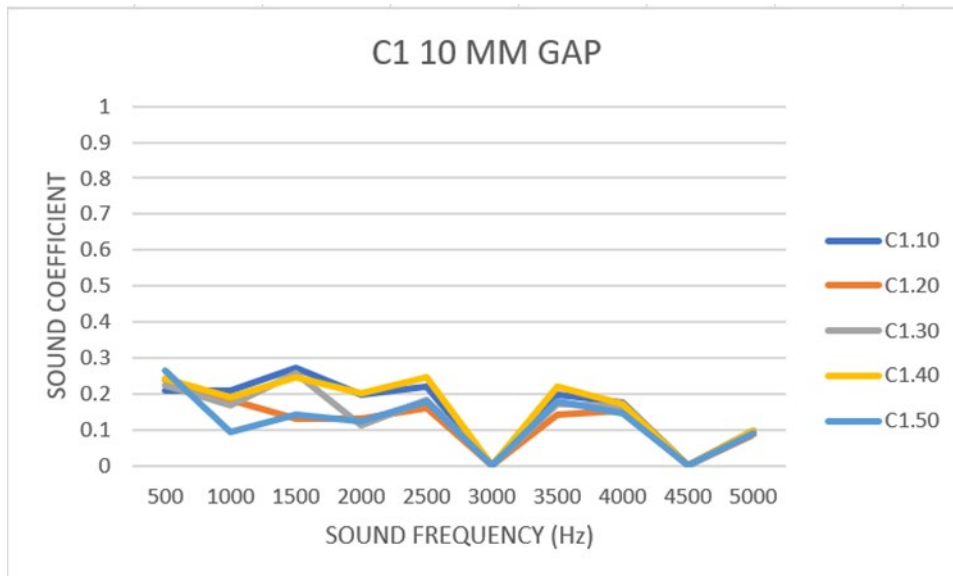


Figure 4.24 Graph of sound coefficient of C1 with 10 mm air gap.

4.5.1.3 Sample C1 sound absorption performance with 20 mm air gap

Figure 4.25 contains a graph of the sound absorption coefficients for sample C1 across various sample thicknesses with a 20 mm air gap at different sound frequencies. At 500 Hz, the absorption coefficient increases from C1.10 to C1.30, then levels off for C1.40 and C1.50. Moving to 1000 Hz, C1.10 exhibits the highest coefficient at 0.225186, decreasing as material thickness increases. For 1500 Hz, variability is observed, with C1.30 and C1.40 having the highest coefficients. At 2000 Hz, C1.40 displays the peak absorption coefficient at 0.183726. Transitioning to 2500 Hz, a decrease in absorption is noted for all thicknesses, with C1.40 having the highest coefficient at 0.238518. At 3000 Hz, all variations exhibit a coefficient of 0, indicating no sound absorption. Moving to 3500 Hz, absorption coefficients rebound, with C1.40 showing the highest at 0.230606. At 4000 Hz, coefficients are slightly lower, and C1.50 has the highest at 0.181622. For 4500 Hz, no sound absorption is recorded across all thicknesses. Finally, at 5000 Hz, sound absorption coefficients are low, with C1.10 having the highest value at 0.087313. For sample C1 with a 20 mm air gap, the absorption performance is influenced by both the frequency of the sound and the thickness of the material. The thickest materials do not consistently absorb more sound across all

frequencies. Instead, mid-range thicknesses (C1.30 and C1.40) often perform better, particularly at frequencies like 1500 Hz, 2000 Hz, and 3500 Hz. The complete lack of sound absorption at 3000 Hz and 4500 Hz across all thicknesses suggests these may be resonant frequencies where the air gap size impacts the material's ability to absorb sound. At higher frequencies (4000 Hz and 5000 Hz), there is no consistent trend showing that increased thickness improves absorption. In fact, at the highest frequency tested (5000 Hz), the thinnest material (C1.10) has the highest absorption coefficient. These findings indicate that material selection for sound absorption with a 20 mm air gap should be carefully considered based on the specific frequencies of interest. Different thicknesses may be more effective at different frequencies, and no single thickness optimizes absorption across the entire frequency range. This information is crucial for applications where precise acoustic control is needed.

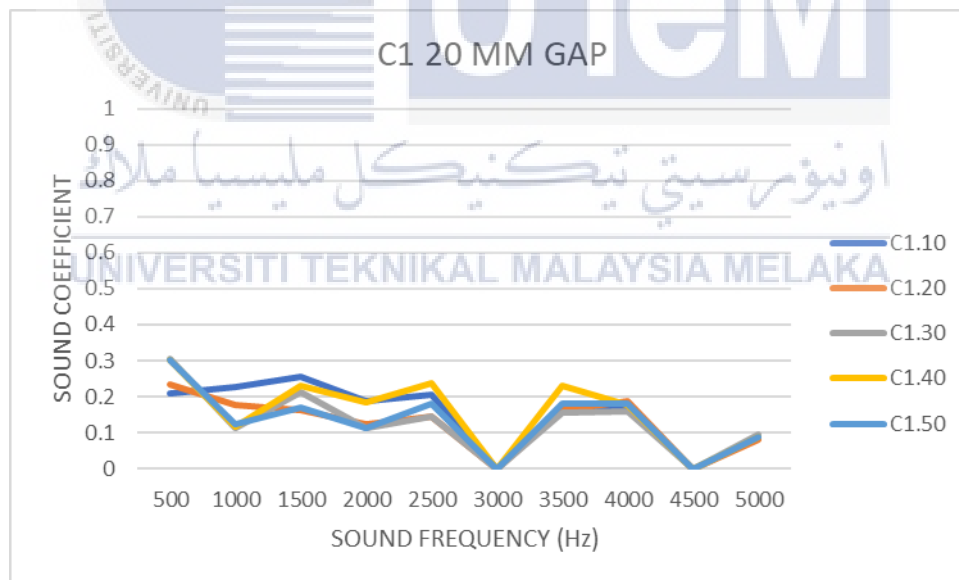


Figure 4.25 Graph of sound coefficient of C1 with 20 mm air gap.

4.5.1.4 Sample C1 sound absorption performance with 30 mm air gap

Figure 4.26 shows the graph of sound absorption coefficient against frequency of C1 with 30 mm air gap. Across various frequencies, the absorption coefficients exhibit distinct trends with material thickness. At 500 Hz, absorption increases with thickness, reaching its peak at C1.50 with a coefficient of 0.340099. However, at 1000 Hz, the trend reverses, and C1.50 displays the highest coefficient at 0.129581. Moving to 1500 Hz, there's a general increase in absorption with thickness, with the highest coefficient observed in C1.30 at 0.259188. At 2000 Hz, coefficients decline for thicker materials, with C1.20 20 mm showing the highest value at 0.137668. For 2500 Hz, absorption coefficients decrease compared to 2000 Hz, and C1.10 10 mm exhibits the highest coefficient at 0.197777. At 3000 Hz, all thickness variations show a coefficient of 0, indicating no sound absorption. The trend rebounds at 3500 Hz, with C1.40 40 mm displaying the highest coefficient at 0.228283. At 4000 Hz, coefficients are slightly lower than at 3500 Hz, with C1.10 and C1.50 showing the highest values. There is no sound absorption across all thicknesses at 4500 Hz, as indicated by coefficients of 0. Finally, at 5000 Hz, sound absorption coefficients are low, with C1.50 having the highest value at 0.100571. For sample C1 with a 30 mm air gap, the sound absorption performance is influenced by both the material thickness and the frequency of sound. Thicker materials do not always absorb more sound across the frequencies. Instead, different thicknesses are more effective at different frequencies, with no single thickness performing best consistently. The lack of sound absorption at 3000 Hz and 4500 Hz suggests these frequencies may be resonant frequencies where the 30 mm air gap prevents effective sound damping by the material. The data indicates that selecting a material thickness for sound insulation with a 30 mm air gap should be guided by the specific frequencies of interest. For

example, C1.30 is most effective at 1500 Hz, while C1.10 and C1.50 show better performance at higher frequencies like 4000 Hz and 5000 Hz.

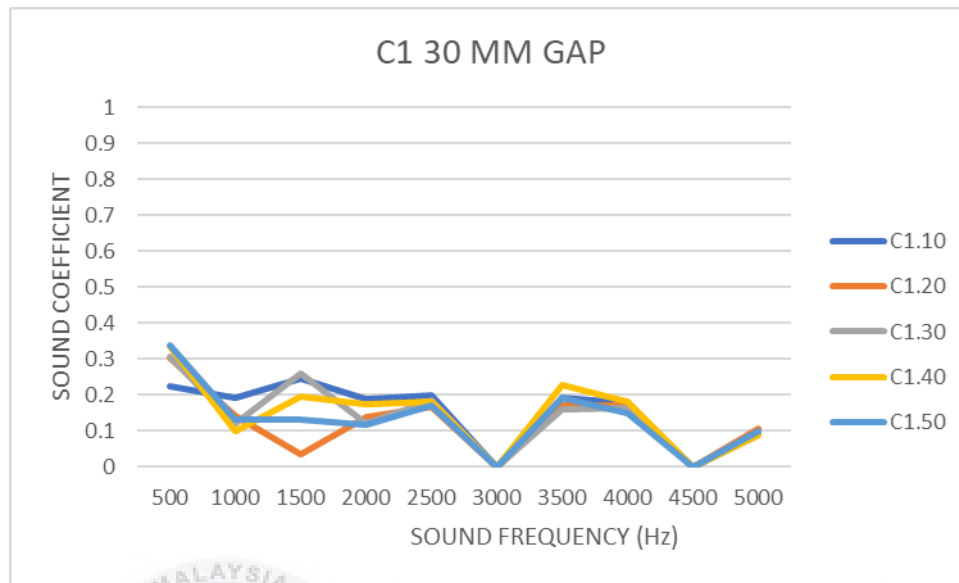


Figure 4.26 Graph of sound coefficient of C1 with 30 mm air gap.

4.5.2 Sample C2

This experiment will start with the concrete being reinforced with a 20 mesh size kenaf core and the samples were made with different thickness, starting from 10 mm to 50 mm and it will be carried out with no gap, 10 mm air gap, 20 mm air gap and 30 mm air gap.

4.5.2.1 Sample C2 sound absorption performance without air gap

Figure 4.27 shows the graph of sound coefficient of C2 with no air gap. At 500 Hz, the absorption coefficient increases with thickness, peaking at 50 mm. At 1000 Hz, thicker materials demonstrate higher absorption, with C2.50 reaching 0.409548. The trend continues at 1500 Hz, maintaining high absorption at C2.50. However, at 2000 Hz, a shift occurs with C2.10 (10 mm) having the highest coefficient. At 2500 Hz, absorption coefficients decrease, while at 3000 Hz, all thicknesses show no sound absorption. Recovery begins at 3500 Hz, with C2.40 (40 mm) having the highest coefficient. At 4000 Hz, coefficients are lower, and at 4500 Hz, there is no sound absorption. Finally, at 5000 Hz, absorption coefficients are

relatively low, with C2.20 (20 mm) having the highest value at 0.108199. This data illustrates the nuanced relationship between material thickness and sound absorption across different frequencies. For sample C2 without an air gap, the sound absorption characteristics significantly depend on both the frequency and material thickness. Thicker materials generally absorb more sound at lower frequencies (500 Hz to 1500 Hz), while at 2000 Hz, the thinnest material (C2.10) performs best. The complete absence of sound absorption at 3000 Hz and 4500 Hz across all thicknesses suggests these frequencies might correspond to resonant frequencies where the material's natural properties do not allow for sound damping. At higher frequencies (3500 Hz and 4000 Hz), there is no clear pattern that thicker materials absorb more sound; instead, C2.40 shows the highest coefficients, suggesting a complex interaction between material thickness, sound frequency, and the lack of an air gap.

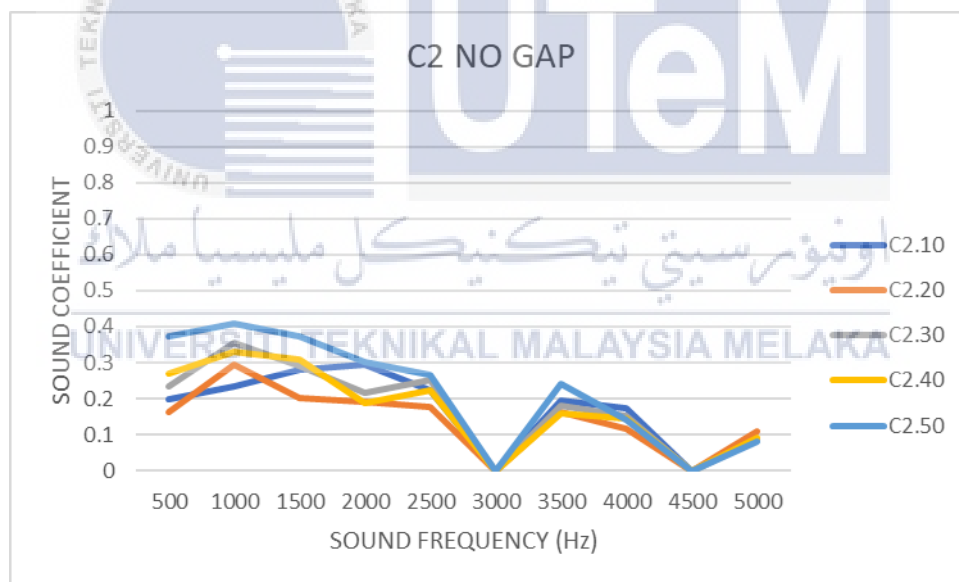


Figure 4.27 Graph of sound coefficient of C2 with no air gap.

4.5.2.2 Sample C2 sound absorption performance with 10 mm air gap

Figure 4.28 shows the graph of sound coefficient of C2 with 10 mm air gap. At 500 Hz, the absorption coefficient increases with thickness until C2.40, where it reaches 0.336957, followed by a slight decrease at C2.50 (50 mm). Moving to 1000 Hz, there's a notable decrease in absorption coefficients for all thicknesses compared to 500 Hz, with

C2.40 having the highest value at 0.228557. At 1500 Hz, coefficients increase, with C2.40 leading at 0.283353. The trend of increasing absorption with thickness persists at 2000 Hz, where C2.40 maintains the highest coefficient at 0.224766. At 2500 Hz, absorption coefficients decrease slightly, still led by C2.40. There's no sound absorption at 3000 Hz for all thickness variations. Absorption coefficients rebound at 3500 Hz, with C2.50 having the highest value at 0.118003. At 4000 Hz, coefficients are lower than at 3500 Hz, with C2.50 leading at 0.094842. At 4500 Hz, there's no sound absorption for all thicknesses, with coefficients at 0. Finally, at 5000 Hz, sound absorption coefficients are low, with C2.50 having the highest value at 0.109408. This comprehensive analysis reveals the nuanced relationship between material thickness and sound absorption across different frequencies.

For sample C2 with a 10 mm air gap, the sound absorption performance is influenced by both material thickness and frequency. Thicker materials generally have higher absorption coefficients, with C2.40 often showing the highest values across the frequency range except for the highest frequency measured, 5000 Hz, where C2.50 performs best. The absence of sound absorption at 3000 Hz and 4500 Hz across all thicknesses suggests that these frequencies are likely resonant frequencies where the 10 mm air gap prevents effective sound damping, a pattern consistent with other data sets for different air gaps and materials. At 5000 Hz, the coefficients are low for all thicknesses, but the highest coefficient is with the thickest material, suggesting that more material may help with absorbing higher frequency sounds when paired with a 10 mm air gap. Overall, the data suggests that a thicker material may be more effective for sound absorption across a range of frequencies when a 10 mm air gap is used, but this is not a uniform rule.

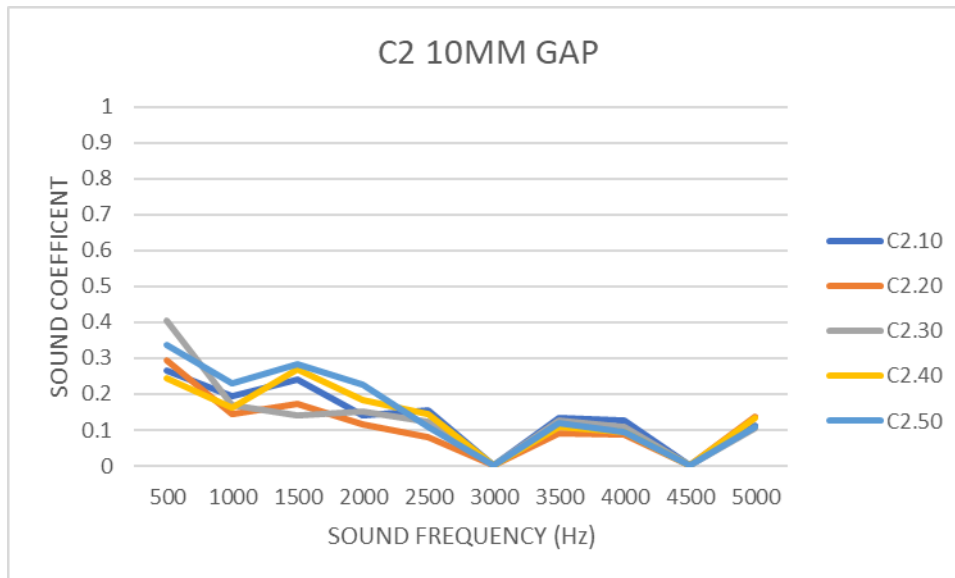


Figure 4.28 Graph of sound coefficient of C2 with 10 mm air gap.

4.5.2.3 Sample C2 sound absorption performance with 20 mm air gap

Figure 4.29 shows the graph of sound coefficient of C2 with 20 mm air gap. At 500 Hz, the absorption coefficient peaks at 20 mm thickness, with a value of 0.343212, and there is a slight increase for 50 mm thickness, revealing a non-linear relationship between thickness and absorption at this frequency. Moving to 1000 Hz, the trend is not consistent, as C2.40 with 40 mm thickness exhibits the highest coefficient at 0.155026. At 1500 Hz, C2.40 continues to lead with the highest absorption coefficient, while C2.30 with 30 mm thickness shows a significantly lower coefficient compared to C2.20 and C2.40. The pattern continues at 2000 Hz, where C2.40 maintains the highest coefficient. At 2500 Hz, coefficients are generally lower than at 2000 Hz, with C2.40 still having the highest value. At 3000 Hz, all thicknesses exhibit zero sound absorption. The coefficients rebound at 3500 Hz, with C2.40 showing the highest value. At 4000 Hz, coefficients are lower than at 3500 Hz, with C2.40 maintaining the highest value. There is no sound absorption at 4500 Hz for all thicknesses. Finally, at 5000 Hz, sound absorption coefficients are low, with C2.30 having the highest value. This analysis highlights the intricate relationship between material

thickness and sound absorption across different frequencies. For sample C2 with a 20 mm air gap, the sound absorption varies significantly with frequency and material thickness. The data does not display a consistent increase or decrease in absorption with material thickness. Instead, certain thicknesses, particularly C2.40, tend to perform better across multiple frequencies. The absence of sound absorption at 3000 Hz and 4500 Hz for all thicknesses suggests that these frequencies may be resonant frequencies where the air gap size hinders effective sound damping. At higher frequencies (3500 Hz and 4000 Hz), C2.40 consistently shows the highest absorption coefficients, while at 5000 Hz, C2.30 is the most effective, indicating that the optimal material thickness for sound absorption can vary greatly depending on the specific frequency.

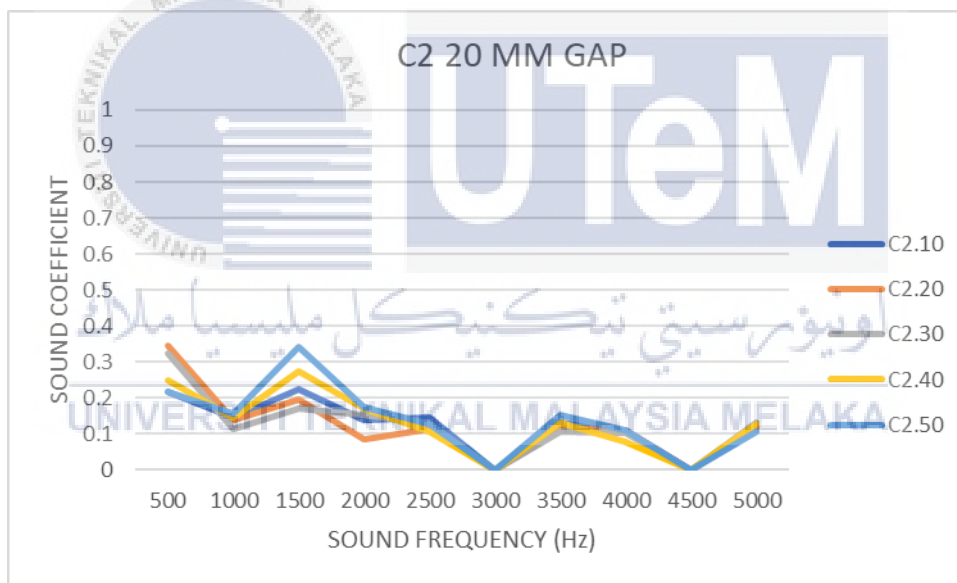


Figure 4.29 Graph of sound coefficient of C2 with 20 mm air gap.

4.5.2.4 Sample C2 sound absorption performance with 30 mm air gap

Figure 4.30 shows the graph of sound coefficient of C2 with 30 mm air gap. At 500 Hz, the absorption coefficient demonstrates an increase with material thickness, reaching its peak at C2.50 (50 mm) with a value of 0.447711. However, the trend shifts at 1000 Hz, where C2.40 (40 mm) exhibits the highest coefficient at 0.510631. Moving to 1500 Hz,

coefficients vary, with the thickest material, C2.50, displaying the highest value at 0.169015. At 2000 Hz, absorption coefficients remain relatively even, with C2.50 leading at 0.120676. Subsequently, at 2500 Hz, coefficients for all thicknesses decrease, and C2.50 maintains the highest coefficient at 0.128607. At 3000 Hz, all thickness variations show a coefficient of 0, indicating no sound absorption at this frequency. The recovery in sound absorption coefficients occurs at 3500 Hz, with C2.30 (30 mm) displaying the highest coefficient at 0.128464. Moving to 4000 Hz, coefficients are lower than at 3500 Hz, with C2.50 having the highest value at 0.111427. At 4500 Hz, there is no sound absorption across all thicknesses, as indicated by coefficients of 0. Finally, at 5000 Hz, sound absorption coefficients are low, with C2.30 showing the highest value at 0.069674. This analysis illustrates the dynamic relationship between material thickness and sound absorption across different frequencies. For sample C2 with a 30 mm air gap, sound absorption varies with frequency and material thickness. The data shows an initial increase in absorption with material thickness at lower frequencies (500 Hz). At higher frequencies (1000 Hz and above), the pattern becomes less clear, with no consistent relationship between thickness and higher absorption coefficients. The complete lack of absorption at 3000 Hz and 4500 Hz suggests these frequencies are likely resonant frequencies where the material's properties, in combination with the 30 mm air gap, are ineffective for sound damping. At the highest frequency tested (5000 Hz), C2.30 shows the highest absorption, indicating that neither the thinnest nor the thickest materials provide the best performance consistently across all frequencies.

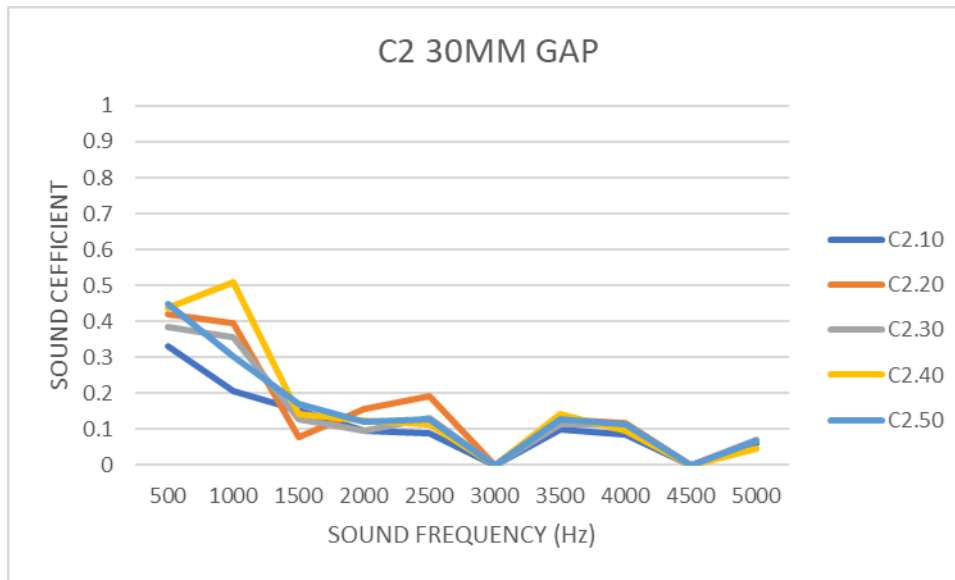


Figure 4.30 Graph of sound coefficient of C2 with 30 mm air gap.

4.5.3 Sample C3

This experiment will start with the concrete being reinforced with a 10 mm size kenaf core and the samples were made with different thickness, starting from 10 mm to 50 mm and it will be carried out with no gap, 10 mm air gap, 20 mm air gap and 30 mm air gap.

4.5.3.1 Sample C3 sound absorption performance without air gap

Figure 2.31 shows the graph of sound coefficient of C3 without air gap. At 500 Hz, the absorption coefficient generally increases with material thickness, peaking at C3.50 (50 mm) with a coefficient of 0.481023, indicating enhanced absorption at this frequency with greater material thickness. Contrary to this, at 1000 Hz, the trend reverses, with C3.40 (40 mm) exhibiting the highest coefficient at 0.510631, while the thickest material, C3.50, shows a lower coefficient. Moving to 1500 Hz, C3.50 has the highest coefficient at 0.199796, suggesting that thicker materials might be more effective at absorbing sound at this frequency. At 2000 Hz, coefficients remain relatively even, with C3.50 leading at 0.135997. As we progress to 2500 Hz, absorption coefficients decrease, yet C3.50 maintains the highest

coefficient at 0.12082. At 3000 Hz, all thickness variations display a coefficient of 0, indicating no sound absorption at this frequency. The recovery in sound absorption coefficients occurs at 3500 Hz, with C3.40 exhibiting the highest coefficient at 0.140069. Transitioning to 4000 Hz, coefficients are lower than at 3500 Hz, with C3.40 having the highest value at 0.093614. At 4500 Hz, there is no sound absorption across all thicknesses, as indicated by coefficients of 0. Finally, at 5000 Hz, sound absorption coefficients are relatively low, with C3.40 having the highest value at 0.043596. This analysis underscores the nuanced relationship between material thickness and sound absorption across different frequencies. For sample C3 without an air gap, the sound absorption characteristics exhibit significant variation with frequency and material thickness. Thicker materials tend to have higher absorption coefficients at lower frequencies (500 Hz and 1500 Hz), and this trend generally continues up to 2500 Hz. At mid-range frequencies, particularly 3500 Hz and 4000 Hz, C3.40 shows the highest coefficients, suggesting that slightly less than the maximum thickness tested may be more effective for these frequencies. The absence of absorption at 3000 Hz and 4500 Hz across all thicknesses suggests that these frequencies are not effectively damped by the material, potentially due to the resonance that occurs with the lack of an air gap.

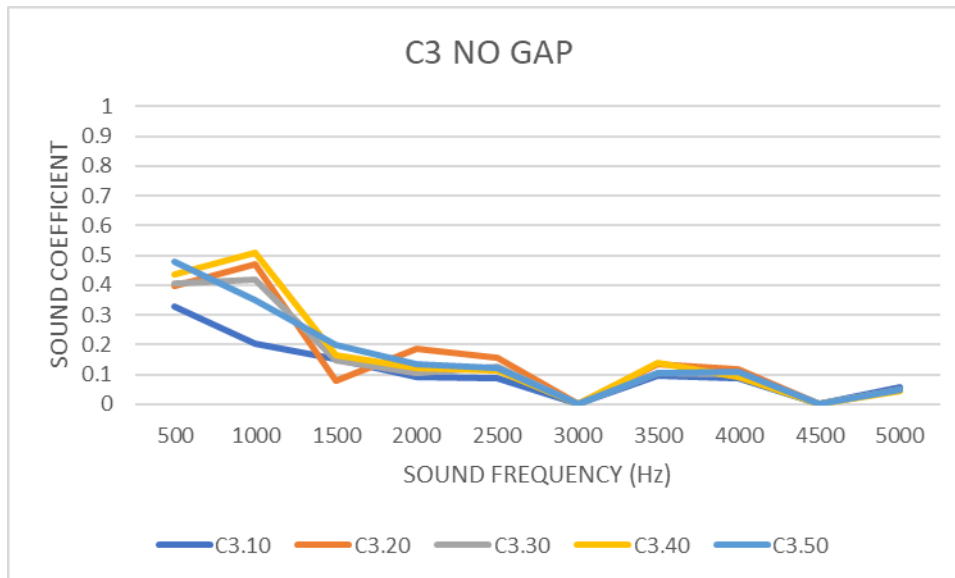


Figure 4.31 Graph of sound coefficient of C3 with no air gap

4.5.3.2 Sample C3 sound absorption performance with 10 mm air gap

Figure 2.32 shows the graph of sound coefficient of C3 with 10 mm air gap. At 500 Hz, the sound absorption coefficient reaches its peak at C3.50 (50 mm thickness) with a value of 0.541409. In general, there is an increase in the absorption coefficient with material thickness at this frequency. Transitioning to 1000 Hz, the coefficients for all thicknesses are lower than those at 500 Hz, with C3.10 (10 mm) exhibiting the highest coefficient at 0.20565. At 1500 Hz, coefficients show variation, with C3.30 (30 mm) displaying the highest value at 0.228762, suggesting better performance at this thickness for this frequency. Moving to 2000 Hz, the coefficients exhibit variation again, with C3.50 having the highest value at 0.152715. At 2500 Hz, there is a general increase in sound absorption, and C3.50 demonstrates the highest coefficient at 0.300408. However, at 3000 Hz, every thickness variation shows a coefficient of 0, indicating no sound absorption. The recovery in absorption coefficients occurs at 3500 Hz, with C3.30 showing the highest coefficient at 0.283271. Moving to 4000 Hz, the coefficients are lower than at 3500 Hz, with no clear trend regarding the impact of thickness. At 4500 Hz, there is no sound absorption across all

thicknesses, as indicated by coefficients of 0. Finally, at 5000 Hz, sound absorption coefficients are low, with C3.50 having the highest value at 0.094296. This analysis underscores the dynamic relationship between material thickness and sound absorption across different frequencies. For sample C3 with a 10 mm air gap, sound absorption characteristics display significant variability depending on both frequency and material thickness. Thicker materials tend to have higher absorption coefficients at lower frequencies (500 Hz) and mid-range frequencies (2500 Hz and 3500 Hz), while at 1000 Hz, the thinnest material (C3.10) performs best. The consistent absence of sound absorption at 3000 Hz and 4500 Hz across all thicknesses suggests these frequencies may be resonant frequencies where the air gap size negates effective damping by the material. At 4000 Hz and 5000 Hz, the absorption coefficients are generally low for all thicknesses, indicating limited effectiveness in these higher frequency ranges.

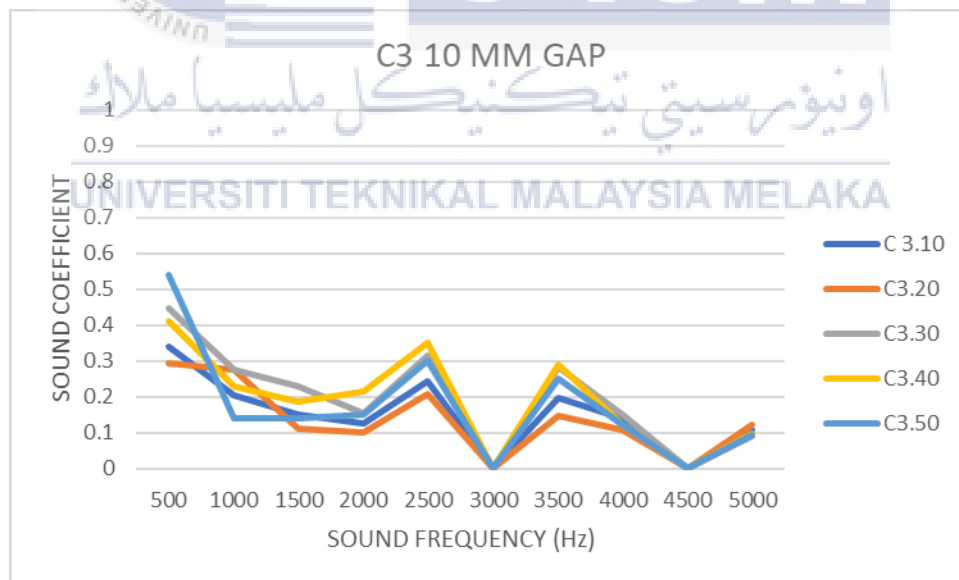


Figure 4.32 Graph of sound coefficient of C3 with 10 mm air gap

4.5.3.3 Sample C3 sound absorption performance with 20 mm air gap

Figure 4.33 shows the graph of sound coefficient of C3 with 20 mm air gap. At 500 Hz, the absorption coefficient shows an increase with thickness, reaching its peak at C3.50 (50 mm) with a value of 0.615545, suggesting improved absorption with greater material thickness at this low frequency. Transitioning to 1000 Hz, the absorption coefficients decrease across all thicknesses from their values at 500 Hz, and C3.10 (10 mm) displays the highest coefficient at 0.251407. Moving to 1500 Hz, the coefficients exhibit a mixed trend, with C3.50 having the highest value at 0.197123, indicating enhanced performance at this thickness for this frequency. At 2000 Hz, the coefficients remain relatively consistent across thicknesses, and C3.40 (40 mm) displays the highest value at 0.237001. As we progress to 2500 Hz, there's an increase in sound absorption, and C3.30 (30 mm) exhibits the highest coefficient at 0.340342. However, at 3000 Hz, all variations show a coefficient of 0, indicating no sound absorption. The recovery in absorption coefficients occurs at 3500 Hz, with C3.30 showing the highest coefficient at 0.29621. At 4000 Hz, coefficients are lower than at 3500 Hz, with C3.10 and C3.50 showing similar values. Moving to 4500 Hz, there is no sound absorption across all thicknesses, as indicated by coefficients of 0. Finally, at 5000 Hz, sound absorption coefficients are low, with C3.20 having the highest value at 0.124734. This analysis underscores the dynamic relationship between material thickness and sound absorption across different frequencies. For sample C3 with a 20 mm air gap, sound absorption varies with frequency and material thickness, displaying no uniform trend across all frequencies. At the lower frequency of 500 Hz, the thickest material (C3.50) exhibits the highest absorption, while at 1000 Hz, the thinnest material (C3.10) performs best. The consistent lack of absorption at 3000 Hz and 4500 Hz suggests these may be resonant frequencies where the air gap prevents effective sound damping, regardless of material thickness. At mid-range frequencies, particularly at 2500 Hz and 3500 Hz, medium

thicknesses (C3.30) show the highest absorption coefficients, while at the higher frequency of 5000 Hz, a less thick material (C3.20) has the highest coefficient.

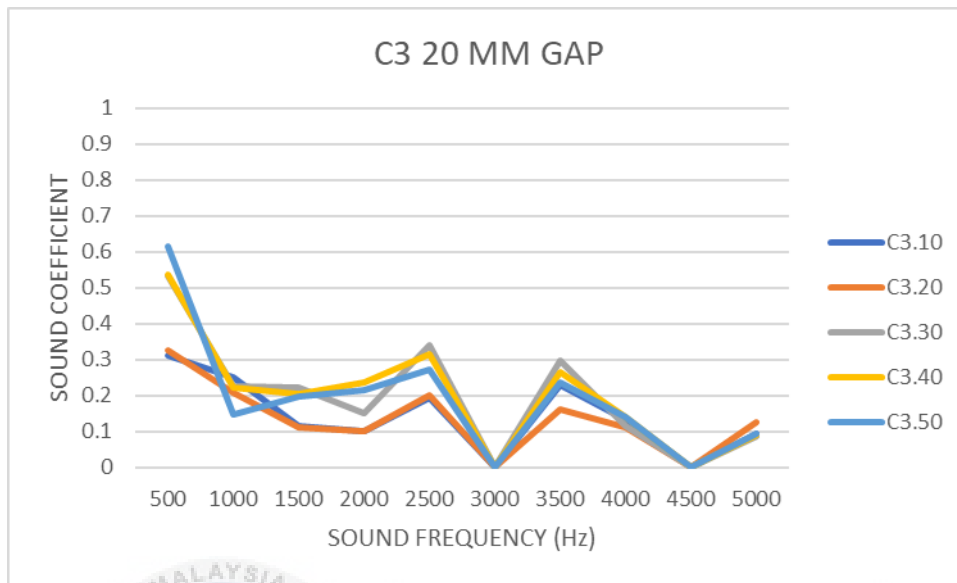


Figure 4.33 Graph of sound coefficient of C3 with 20 mm air gap

4.5.3.4 Sample C3 sound absorption performance with 30 mm air gap

Figure 4.34 shows the graph of sound coefficient of C3 with 30 mm air gap. At 500 Hz, the absorption coefficient generally increases with material thickness, peaking at C3.50 (50 mm) with a coefficient of 0.603663. Moving to 1000 Hz, the absorption coefficients are lower for all thicknesses compared to 500 Hz, with C3.20 (20 mm) having the lowest coefficient at 0.142514, and C3.40 (40 mm) having the highest at 0.184295. At 1500 Hz, the coefficients exhibit variation, with C3.50 (50 mm) showing the highest value at 0.200941, suggesting improved performance at this thickness for this frequency. Transitioning to 2000 Hz, absorption coefficients are relatively even, with C3.50 (50 mm) displaying the highest value at 0.164369. Progressing to 2500 Hz, there's an increase in sound absorption, and C3.50 exhibits the highest coefficient at 0.338729. However, at 3000 Hz, every thickness variation shows a coefficient of 0, indicating no sound absorption. The recovery in absorption coefficients occurs at 3500 Hz, with C3.30 (30 mm) displaying the highest coefficient at 0.245766. At 4000 Hz, coefficients are lower than at 3500 Hz, with C3.10 (10

mm) having the highest value at 0.143846. Moving to 4500 Hz, there is no sound absorption across all thicknesses, as indicated by coefficients of 0. Finally, at 5000 Hz, sound absorption coefficients are low, with C3.10 showing the highest value at 0.09861. This analysis highlights the dynamic interplay between material thickness and sound absorption across different frequencies. For sample C3 with a 30 mm air gap, the sound absorption characteristics show that material thickness affects the sound absorption significantly. Thicker materials (C3.50) tend to have higher absorption coefficients at lower frequencies (500 Hz and 2500 Hz), and this trend generally continues up to 2000 Hz. The complete lack of sound absorption at 3000 Hz and 4500 Hz suggests that these frequencies are resonant points where the air gap size negates effective damping by the material across all tested thicknesses. At higher frequencies, particularly at 3500 Hz and 4000 Hz, there is no consistent pattern that thicker materials absorb more sound; instead, C3.30 and C3.10 respectively show the highest coefficients. These findings suggest that when considering materials for sound insulation with a 30 mm air gap, specific thicknesses may be more effective at certain frequencies.

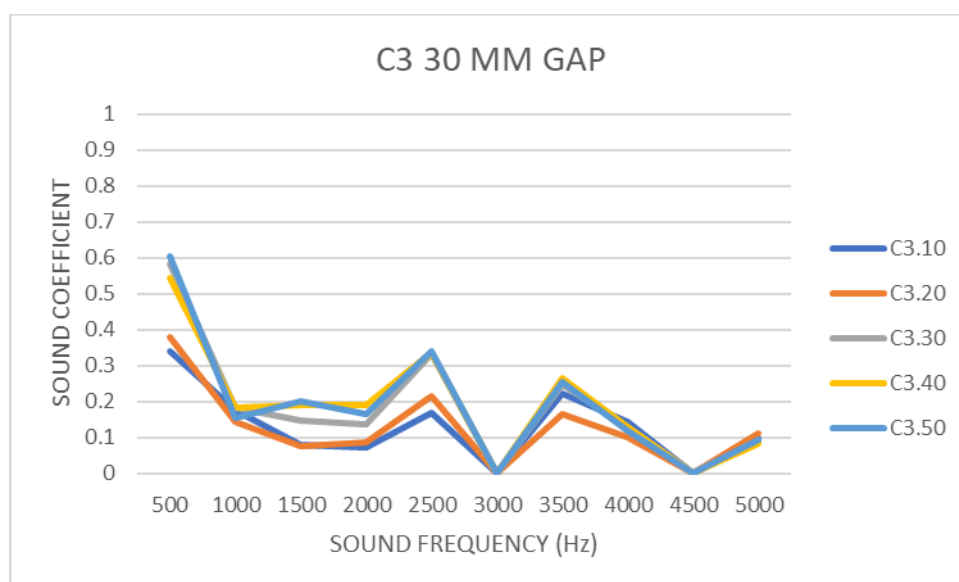


Figure 4.34 Graph of sound coefficient of C3 with 30 mm air gap

4.5.4 Sample C4

This experiment will start with the concrete being reinforced with 3 mm size kenaf core and the samples were made with different thickness, starting from 10 mm to 50 mm and it will be carried out with no gap, 10 mm air gap, 20 mm air gap and 30 mm air gap.

4.5.4.1 Sample C4 sound absorption performance without air gap

Figure 4.35 illustrates the graph of sound coefficient of C4 with no air gap. At 500 Hz, the sound absorption coefficient increases with material thickness, reaching its peak at C4.30 (30 mm) with a value of 0.356331, followed by a slight decrease for thicker materials. Shifting to 1000 Hz, the absorption coefficients are lower across all thicknesses compared to 500 Hz, and C4.50 (50 mm) has the highest coefficient at 0.34992. At 1500 Hz, the coefficients present a mixed trend, with the lowest for C4.20 (20 mm) and the highest for C4.50 at 0.092562. Moving to 2000 Hz, sound absorption is relatively low for all thicknesses, with C4.30 showing the highest value at 0.089569. At 2500 Hz, C4.50 has the highest coefficient at 0.081267, indicating a slight increase in absorption compared to thinner materials at this frequency. However, at 3000 Hz, all variations exhibit a coefficient of 0, indicating no sound absorption. The recovery in absorption coefficients occurs at 3500 Hz, with C4.40 showing the highest coefficient at 0.085398. At 4000 Hz, the coefficients are low, with C4.10 and C4.50 showing similar values (around 0.05). Moving to 4500 Hz, there is no sound absorption across all thicknesses, as indicated by coefficients of 0. Finally, at 5000 Hz, the sound absorption coefficients are relatively low, with C4.10 showing the highest coefficient at 0.07. This analysis underscores the intricate relationship between

material thickness and sound absorption across different frequencies. For sample C4 without an air gap, the sound absorption performance exhibits variability that is dependent on both the material thickness and the frequency. At lower frequencies, a medium thickness (C4.30) appears to be most effective, while at 1000 Hz and 2500 Hz, the thickest material (C4.50) provides slightly better absorption. The consistent lack of absorption at 3000 Hz and 4500 Hz suggests these frequencies may be resonant frequencies for the materials where the intrinsic properties do not allow for sound damping. At higher frequencies, specifically at 3500 Hz and 5000 Hz, the differences in sound absorption between the various thicknesses are not as pronounced, indicating a more uniform performance.

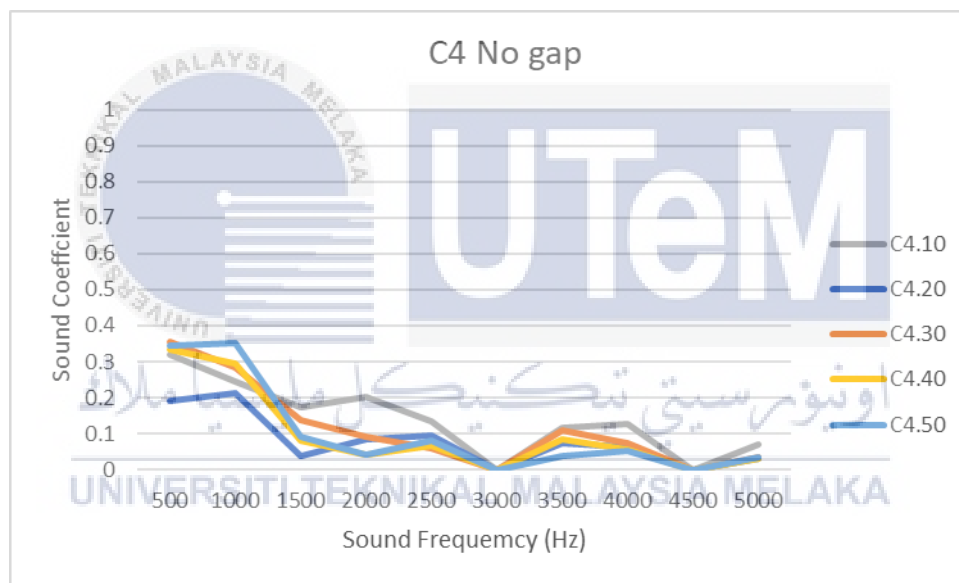


Figure 4.35 Graph of sound coefficient of C4 with no air gap

4.5.4.2 Sample C4 sound absorption performance with 10 mm air gap

Figure 4.36 shows the graph of sound coefficient of C4 with 10 mm air gap. At 500 Hz, the highest sound absorption coefficient is observed at C4.10 (10 mm) with a value of 0.48858. Generally, absorption decreases as material thickness increases. Transitioning to 1000 Hz, all thicknesses show a significant reduction in absorption coefficients compared to 500 Hz, with the least drop observed in C4.40 (40 mm). Moving to 1500 Hz, sound

absorption coefficients increase compared to 1000 Hz, and C4.10 (10 mm) has the highest value at 0.084471. At 2000 Hz, coefficients remain relatively consistent across thicknesses, with C4.30 (30 mm) showing a slightly higher coefficient. Progressing to 2500 Hz, there is a general decrease in the sound absorption coefficient, and C4.40 (40 mm) has the highest value at 0.058279. At 3000 Hz, all thicknesses exhibit a coefficient of 0, indicating no sound absorption. The recovery in sound absorption coefficients occurs at 3500 Hz, with C4.10 (10 mm) displaying the highest coefficient at 0.098173. At 4000 Hz, there's an increase in absorption coefficients, and both C4.10 and C4.50 show higher values than the other thicknesses. Moving to 4500 Hz, similar to 3000 Hz, there is no sound absorption across all thicknesses, as indicated by coefficients of 0. Finally, at 5000 Hz, the sound absorption coefficients are relatively low, with C4.10 showing the highest value at 0.096814. This analysis underscores the nuanced relationship between material thickness and sound absorption across different frequencies. For sample C4 with a 10 mm air gap, the sound absorption characteristics vary notably with frequency and material thickness. At lower frequencies (500 Hz), the thinnest material (C4.10) shows the highest absorption, suggesting that less material is more effective at absorbing sound at this frequency with the given air gap size. However, at higher frequencies (4000 Hz and 5000 Hz), the thinnest material continues to show higher absorption coefficients, which could indicate that the interaction between sound waves and the air gap size is more favorable for thinner materials at these frequencies. The consistent absence of sound absorption at 3000 Hz and 4500 Hz for all thicknesses suggests these are resonant frequencies where the 10 mm air gap prevents effective sound damping across all the tested material thicknesses.

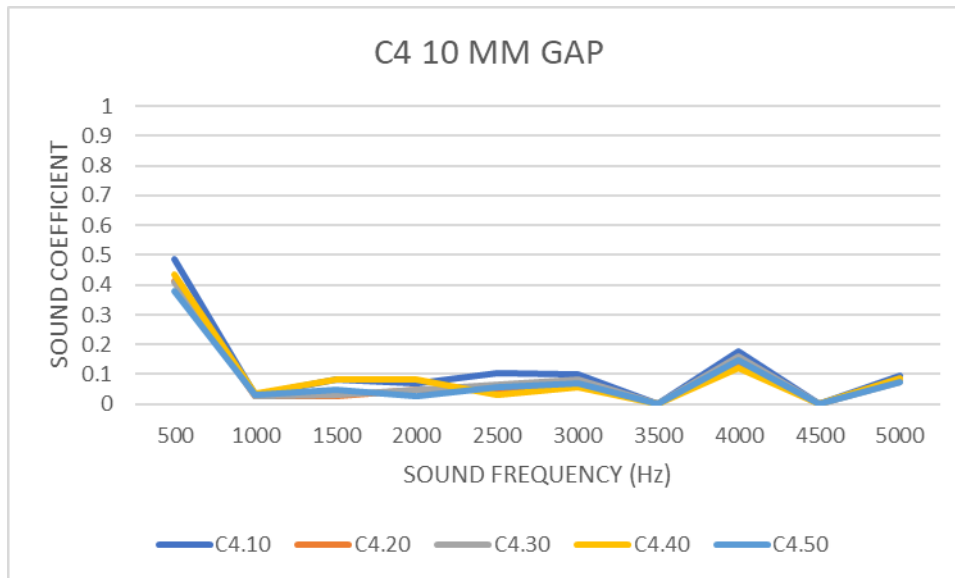


Figure 4.36 Graph of sound coefficient of C4 with 10 mm air gap

4.5.4.3 Sample C4 sound absorption performance with 20 mm air gap

Figure 4.37 shows the graph of sound coefficient of C4 with 20 mm air gap. At 500 Hz, the sound absorption coefficient reaches its peak for C4.10 (10 mm thickness) at 0.469183 and decreases for thicker materials, reaching the lowest value at C4.50 (50 mm thickness). Moving to 1000 Hz, there is a significant drop in absorption coefficients for all thicknesses compared to 500 Hz, with a slight increase observed for the thicker materials, specifically C4.40 and C4.50. At 1500 Hz, the sound absorption coefficients vary, and there is no clear trend in relation to thickness. C4.30 (30 mm) displays the highest value at 0.046697. Transitioning to 2000 Hz, absorption coefficients remain relatively even across thicknesses, with a small increase in C4.10 and C4.30 compared to C4.20 and C4.40. Progressing to 2500 Hz, the coefficients decrease compared to 2000 Hz, with C4.40 showing the highest value at 0.068121. At 3000 Hz, all variations exhibit a coefficient of 0, indicating no sound absorption. The recovery in sound absorption coefficients occurs at 3500 Hz, with C4.50 showing the highest value at 0.079635. At 4000 Hz, the absorption coefficients increase, and C4.40 (40 mm) has the highest coefficient at 0.14846. Moving to 4500 Hz,

there is no sound absorption across all thicknesses, indicated by coefficients of 0. Finally, at 5000 Hz, the coefficients are relatively low, with C4.10 having the highest value at 0.099615. This analysis highlights the nuanced changes in sound absorption across different frequencies and material thicknesses. For sample C4 with a 20 mm air gap, sound absorption varies with frequency and material thickness, but not in a uniform manner. At lower frequencies (500 Hz), the thinnest material (C4.10) shows the highest absorption, while at mid and higher frequencies (1500 Hz and 4000 Hz), medium thicknesses (C4.30 and C4.40) provide higher coefficients.

The consistent absence of sound absorption at 3000 Hz and 4500 Hz suggests these frequencies may be resonant points where the air gap size hinders effective sound damping across all tested material thicknesses. At higher frequencies, particularly at 4000 Hz, there's an increase in absorption for thicker materials, indicating a potential preference for thicker materials in absorbing higher frequency sounds when combined with a 20 mm air gap.

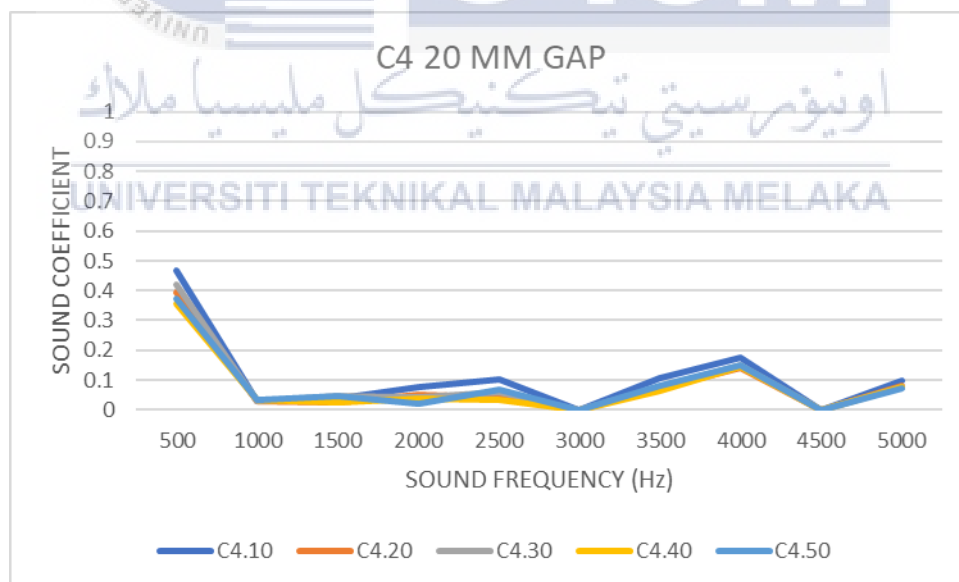


Figure 4.37 Graph of sound coefficient of C4 with 20 mm air gap

4.5.4.4 Sample C4 sound absorption performance with 30 mm air gap

Figure 4.38 shows the graph of sound coefficient of C4 with 30 mm air gap. At 500 Hz, the sound absorption coefficient reaches its peak for C4.10 (10 mm thickness) at 0.469183 and decreases for thicker materials, reaching the lowest value at C4.50 (50 mm thickness). Moving to 1000 Hz, there is a significant drop in absorption coefficients for all thicknesses compared to 500 Hz, with a slight increase observed for the thicker materials, specifically C4.40 and C4.50. At 1500 Hz, the sound absorption coefficients vary, and there is no clear trend in relation to thickness. C4.30 (30 mm) displays the highest value at 0.046697. Transitioning to 2000 Hz, absorption coefficients remain relatively even across thicknesses, with a small increase in C4.10 and C4.30 compared to C4.20 and C4.40. Progressing to 2500 Hz, the coefficients decrease compared to 2000 Hz, with C4.40 showing the highest value at 0.068121. At 3000 Hz, all variations exhibit a coefficient of 0, indicating no sound absorption. The recovery in sound absorption coefficients occurs at 3500 Hz, with C4.50 showing the highest value at 0.079635. At 4000 Hz, the absorption coefficients increase, and C4.40 (40 mm) has the highest coefficient at 0.14846. Moving to 4500 Hz, there is no sound absorption across all thicknesses, indicated by coefficients of 0. Finally, at 5000 Hz, the coefficients are relatively low, with C4.10 having the highest value at 0.099615. This analysis highlights the nuanced changes in sound absorption across different frequencies and material thicknesses. For sample C4 with a 30 mm air gap, the sound absorption characteristics show variability with frequency and material thickness. The thinnest material (C4.10) often has the highest absorption coefficients, particularly at the lower frequency of 500 Hz and the higher frequencies of 2500 Hz, 4000 Hz, and 5000 Hz. The complete lack of sound absorption at 3000 Hz and 4500 Hz for all thicknesses may suggest these are resonant frequencies where the air gap prevents sound damping, a

phenomenon consistent with the other data sets for different air gaps and materials. At mid-range frequencies, particularly 1500 Hz and 3500 Hz, there is no consistent pattern that thicker materials absorb more sound. Instead, the data shows fluctuations where certain thicknesses perform slightly better than others, but without a clear trend.

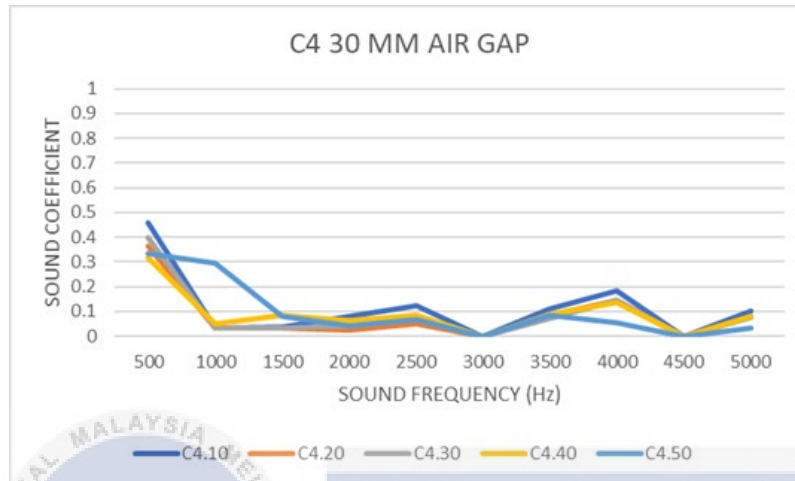


Figure 4.38 Graph of sound coefficient of C4 with 30 mm air gap

4.5.5 Sample C5

This experiment will start with the concrete being reinforced with 20 mm size kenaf core and the samples were made with different thickness, starting from 10 mm to 50 mm and it will be carried out with no gap, 10 mm air gap, 20 mm air gap and 30 mm air gap

4.5.5.1 Sample C5 sound absorption performance without air gap

Figure 4.39 shows the graph of sound coefficient of C5 with no air gap. At 500 Hz, the absorption coefficient peaks at 0.462855 for C5.50 (50 mm), increasing with material thickness. Transitioning to 1000 Hz, coefficients decrease, yet C5.50 maintains the highest value at 0.41803. At 1500 Hz, a varied pattern emerges, with C5.50 leading at 0.187518. Moving to 2000 Hz, C5.20 (20 mm) deviates with the highest coefficient of 0.409134. At 2500 Hz, coefficients decrease universally, but C5.50 retains the lead at 0.102167. For 3000

Hz, all thicknesses exhibit a coefficient of 0, indicating no sound absorption. At 3500 Hz, coefficients recover, with C5.50 leading at 0.114265. Progressing to 4000 Hz, coefficients dip, but C5.50 maintains the highest at 0.077662. At 4500 Hz, there's no sound absorption (coefficient = 0). Finally, at 5000 Hz, absorption coefficients are minimal, with C5.50 at the forefront with 0.036849. For sample C5 without an air gap, sound absorption characteristics demonstrate that material thickness plays a significant role in sound absorption at lower frequencies (500 Hz and 1000 Hz), with the thickest material generally showing the highest coefficients. However, this trend does not hold consistently across all frequencies. The absence of sound absorption at 3000 Hz and 4500 Hz for all thicknesses likely indicates these are resonant frequencies where the material properties are not conducive to sound damping. At mid-range frequencies (2000 Hz and 3500 Hz), the pattern becomes less predictable, with various thicknesses showing the highest absorption at different frequencies. At the highest frequency tested (5000 Hz), the absorption is minimal across all thicknesses.

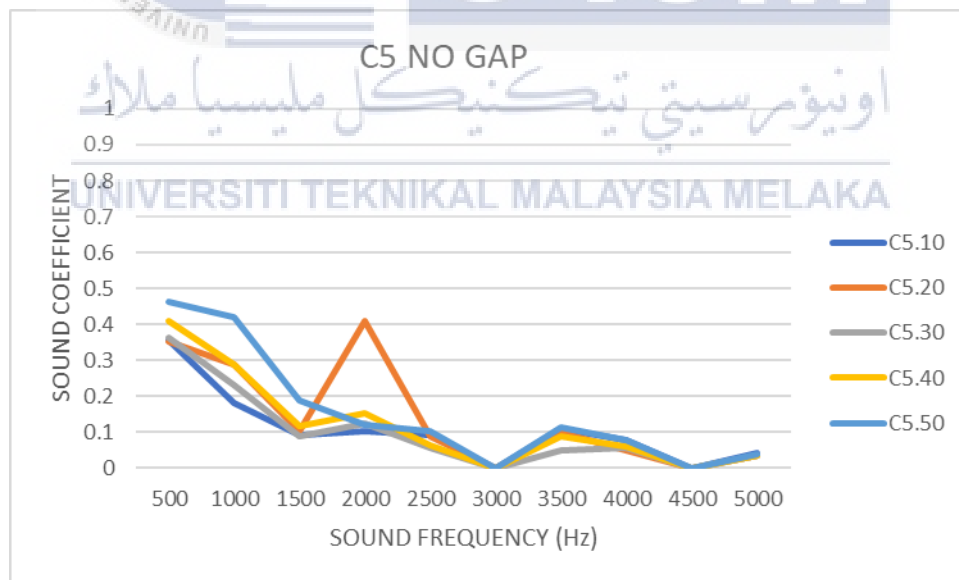


Figure 4.39 Graph of sound coefficient of C5 with no air gap

4.5.5.2 Sample C5 sound absorption performance with 10 mm air gap

Figure 4.40 shows the graph of sound coefficient of C5 with 10 mm air gap. At 500 Hz, thickness correlates with increased sound absorption, and C5.50 (50 mm) exhibits the highest coefficient at 0.359971. Progressing to 1000 Hz, the trend persists, with C5.50 leading at 0.243505. At 1500 Hz, absorption coefficients rise from C5.10 to C5.30, then slightly dip for C5.40 and C5.50. Moving to 2000 Hz, thicker materials have decreased coefficients, and C5.20 (20 mm) leads at 0.176198. At 2500 Hz, C5.40 (40 mm) takes the lead with the highest coefficient at 0.353338. No absorption occurs at 3000 Hz across all thicknesses (coefficient = 0). For 3500 Hz, absorption coefficients increase, with C5.40 having the highest at 0.274917. However, the trend breaks at 4000 Hz, where C5.40 has a lower coefficient than C5.10, C5.20, and C5.30. At 4500 Hz, there's no sound absorption (coefficient = 0) for all thicknesses. Finally, at 5000 Hz, absorption coefficients reach their lowest, with C5.50 showing a slight increase to 0.0988. For sample C5 with a 10 mm air gap, sound absorption varies depending on both the material thickness and the sound frequency. The absorption coefficients tend to increase with material thickness at lower frequencies (500 Hz and 1000 Hz). However, at mid-range frequencies (1500 Hz to 2500 Hz), the relationship is not as straightforward, with some intermediate thicknesses showing higher coefficients. The absence of sound absorption at 3000 Hz and 4500 Hz suggests these frequencies may be resonant frequencies where the air gap and material combination do not dampen the sound effectively. At higher frequencies (4000 Hz and 5000 Hz), the thickest material (C5.50) does not consistently offer the highest absorption, which indicates that the optimal material thickness for sound absorption can vary significantly with frequency when paired with a 10 mm air gap.

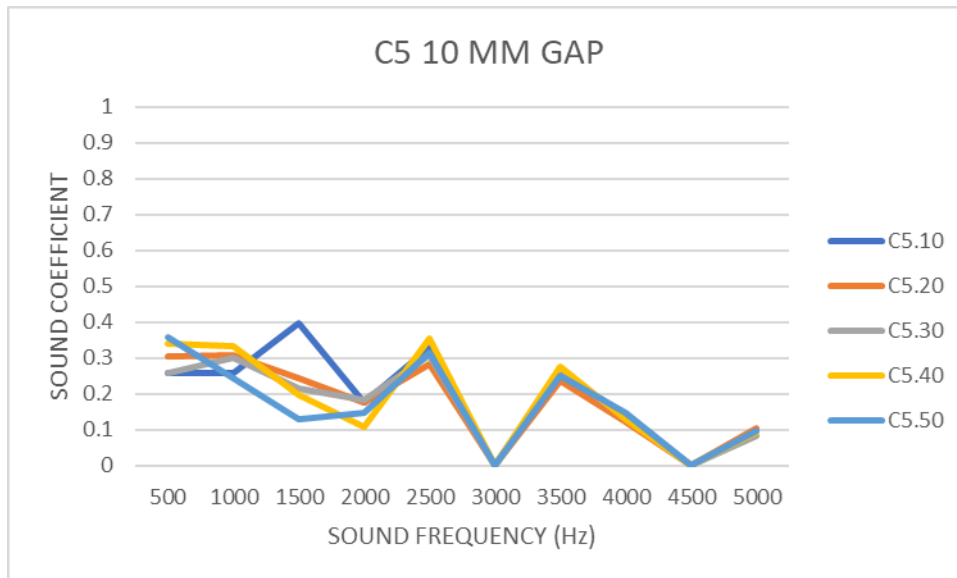


Figure 4.40 Figure 4.34 Graph of sound coefficient of C5 with 10 mm air gap

4.5.5.3 Sample C5 sound absorption performance with 20 mm air gap

Figure 4.41 shows the graph of sound coefficient of C5 with 20 mm air gap. At 500 Hz, the absorption coefficient rises with material thickness, reaching its peak at C5.50 (50 mm) with a value of 0.402563. Moving to 1000 Hz, absorption decreases with thicker materials, and C5.50 exhibits a lower coefficient of 0.173482 compared to thinner options. For 1500 Hz, C5.30 (30 mm) displays the highest coefficient at 0.168283, indicating superior absorption at this thickness for this frequency. At 2000 Hz, C5.20 (20 mm) leads with a coefficient of 0.124623, and the trend of increasing absorption with thickness is inconsistent. Transitioning to 2500 Hz, coefficients decrease compared to 2000 Hz, and C5.30 has the highest coefficient at 0.314996. At 3000 Hz, all thickness variations show a coefficient of 0, signifying no sound absorption. For 3500 Hz, sound absorption coefficients increase from zero at 3000 Hz, with C5.40 leading at 0.300108. At 4000 Hz, coefficients are generally lower than at 3500 Hz, and C5.50 has the highest coefficient at 0.116449. At 4500 Hz, there's no sound absorption for any thickness (coefficient = 0). Finally, at 5000 Hz, sound absorption coefficients are low, with C5.50 having the highest value at 0.098764. For sample

C5 with a 20 mm air gap, sound absorption is influenced by material thickness and sound frequency. At lower frequencies (500 Hz), thicker materials generally show higher absorption coefficients. However, this trend does not hold uniformly across all frequencies. For instance, at 1000 Hz and 2000 Hz, increased thickness does not always correspond to higher absorption. The absence of sound absorption at 3000 Hz and 4500 Hz for all thicknesses suggests these frequencies are resonant frequencies where the air gap size impacts the material's ability to absorb sound. At mid-range frequencies (1500 Hz and 2500 Hz), a medium thickness (C5.30) shows the highest absorption coefficients, while at 3500 Hz, a slightly thicker material (C5.40) is more effective. At the highest frequency tested (5000 Hz), the absorption is minimal across all thicknesses, although the thickest material (C5.50) performs slightly better.

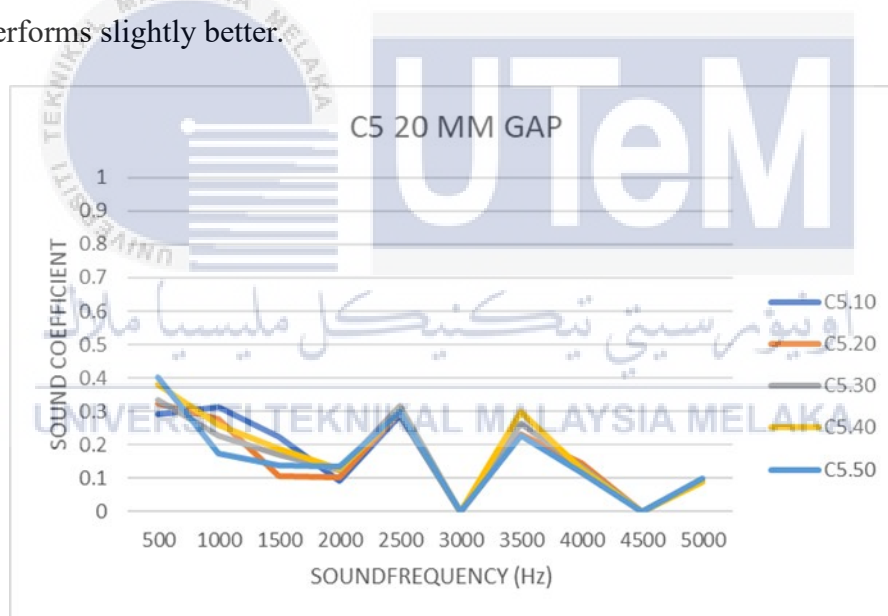


Figure 4.41 Graph of sound coefficient of C5 with 20 mm air gap

4.5.5.4 Sample C5 sound absorption performance with 30 mm air gap

Figure 4.42 shows the graph of sound coefficient of C5 with 30 mm air gap. At 500 Hz, the absorption coefficient rises with thickness, reaching its peak at C5.50 (50 mm) with a coefficient of 0.425566. Moving to 1000 Hz, the absorption coefficient is highest for C5.10

(10 mm) at 0.214831 and generally decreases as thickness increases. For 1500 Hz, coefficients vary, with C5.50 having the highest at 0.110661, indicating an inconsistent relationship between thickness and absorption at this frequency. At 2000 Hz, the highest coefficient is observed at C5.20 (20 mm) with 0.409134, deviating from the pattern at lower frequencies. Transitioning to 2500 Hz, coefficients are relatively high, and C5.40 (40 mm) displays the highest at 0.341471. At 3000 Hz, there is no sound absorption for all thicknesses (coefficient = 0). For 3500 Hz, sound absorption increases, with the highest coefficient at C5.40 being 0.295546. At 4000 Hz, C5.50 exhibits the highest absorption with a coefficient of 0.133228. At 4500 Hz, no sound absorption is observed across any thickness (coefficient = 0). Finally, at 5000 Hz, coefficients are low, with C5.50 having the highest at 0.089764.

For sample C5 with a 30 mm air gap, there is no simple linear relationship between material thickness and sound absorption. Instead, different thicknesses show varying degrees of effectiveness at different frequencies. At lower frequencies (500 Hz), the thickest material (C5.50) provides the highest absorption. At mid-frequencies (1000 Hz and 1500 Hz), the pattern is less predictable, with thinner materials sometimes showing higher coefficients. The complete lack of absorption at 3000 Hz and 4500 Hz for all thicknesses suggests that these frequencies might correspond to resonant conditions created by the air gap where the material does not dampen sound effectively. The data suggests that material selection for sound insulation with a 30 mm air gap should be based on the specific frequencies of interest, as different thicknesses may be more effective for different frequency ranges. No single thickness provides the best performance across all frequencies.

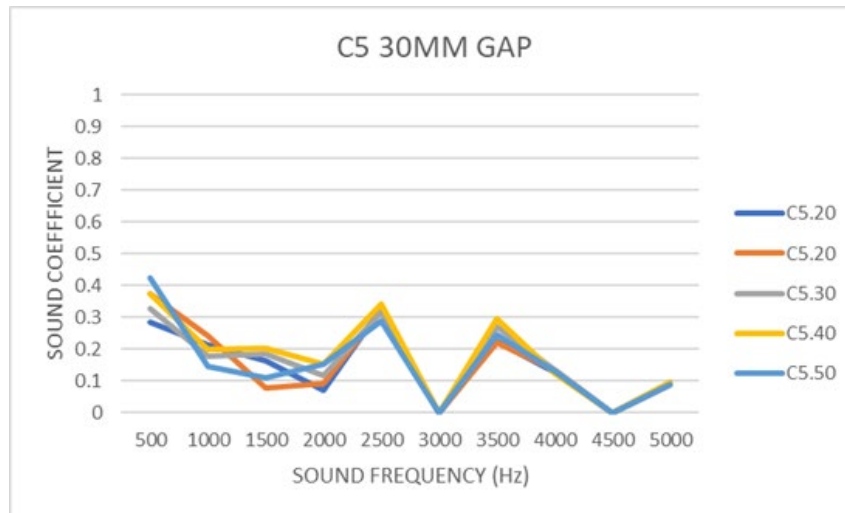


Figure 4.42 Graph of sound coefficient of C5 with 30 mm air gap

4.5.6 Sample F

This experiment will start with the concrete being reinforced with polystyrene foam and the samples were made with different thickness, starting from 10 mm to 50 mm and it will be carried out with no gap, 10 mm air gap, 20 mm air gap and 30 mm air gap. This sample is considered as control sample.

UNIVERSITI TEKNIKAL MALAYSIA MELAKA

4.5.6.1 Sample F sound absorption performance without air gap

Figure 4.43 shows the graph of sound coefficient of F with no air gap. At 500 Hz, the absorption coefficient generally rises with thickness, peaking at F.50 (50 mm) with a coefficient of 0.375208. Moving to 1000 Hz, the trend continues, with the highest absorption at F.30 (30 mm) at 0.390648, but slightly decreases for F.40 and F.50. For 1500 Hz, absorption coefficients are highest for F.20 (20 mm) at 0.117743 and decrease with increasing material thickness. At 2000 Hz, the trend is not consistent, as F.20 shows the highest coefficient at 0.168014. Transitioning to 2500 Hz, coefficients decrease with increasing material thickness, and the highest absorption at F.10 (10 mm) is 0.150517. At

3000 Hz, no sound absorption is observed for any thickness (coefficient = 0). For 3500 Hz, sound absorption increases from zero at 3000 Hz, with the highest coefficient at F.40 (40 mm) being 0.142073. At 4000 Hz, absorption coefficients are somewhat consistent across thicknesses, with a slight peak at F.10. At 4500 Hz, there's no sound absorption (coefficient = 0) for all thicknesses. Finally, at 5000 Hz, absorption coefficients are low, with F.50 showing the highest value at 0.043471. For sample F without an air gap, the relationship between material thickness and sound absorption is complex and varies with frequency. At lower frequencies (500 Hz to 1000 Hz), the absorption tends to increase with thickness, but this trend does not hold consistently at mid-frequencies (1500 Hz to 2500 Hz) where thinner materials sometimes show higher absorption. The absence of sound absorption at 3000 Hz and 4500 Hz across all thicknesses might suggest that these frequencies correspond to resonant frequencies where the material properties do not allow for effective sound damping. At higher frequencies (3500 Hz and 4000 Hz), the absorption is not significantly affected by thickness. At the highest tested frequency (5000 Hz), absorption is minimal across all thicknesses.

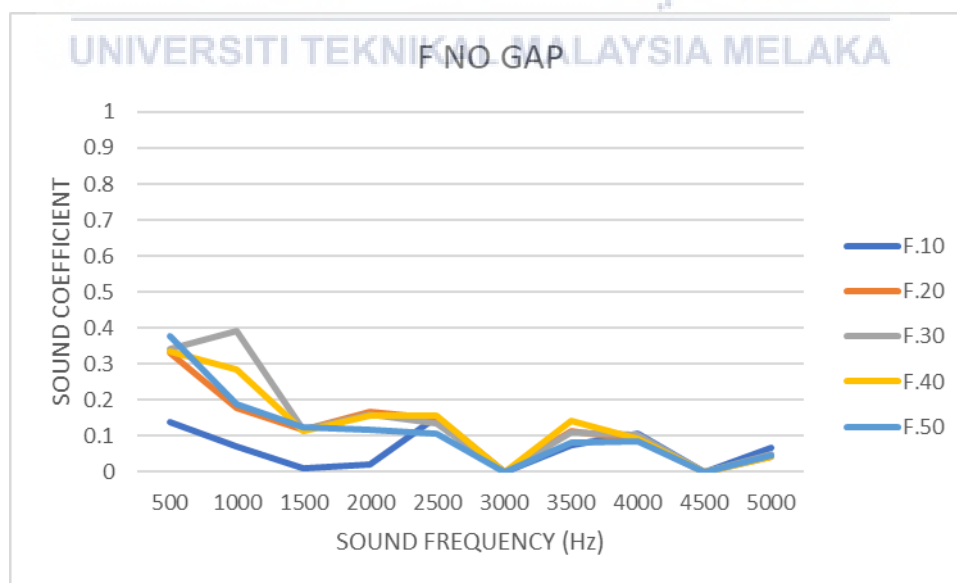


Figure 4.43 Graph of sound coefficient of F with no air gap

4.5.6.2 Sample F sound absorption performance with 10 mm air gap

Figure 4.44 shows the graph of sound coefficient of F with 10 mm air gap. At 500 Hz, the absorption coefficient lacks a clear trend with material thickness, displaying a range of values with the lowest at F.30 and the highest at F.10. Moving to 1000 Hz, coefficients vary, and F.30 exhibits the highest absorption at 0.212449. For 1500 Hz, there's a general increase in absorption with thickness, peaking at F.30 with a coefficient of 0.374185. At 2000 Hz, coefficients again rise with increased thickness, with F.50 showing the highest coefficient at 0.336304. Transitioning to 2500 Hz, the absorption coefficient decreases as material thickness increases, and F.10 has the highest at 0.347344. At 3000 Hz, no sound absorption is observed for any thickness (coefficient = 0). For 3500 Hz, sound absorption increases from zero, with F.10 and F.40 having similar higher coefficients. At 4000 Hz, absorption coefficients are lower than at 3500 Hz, and F.40 shows the highest coefficient at 0.188093. At 4500 Hz, no sound absorption is recorded (coefficient = 0) for all thicknesses. Finally, at 5000 Hz, absorption coefficients are low, with the highest at F.50 being 0.136819. For sample F with a 10 mm air gap, the absorption coefficient varies significantly with frequency and material thickness. At lower frequencies (500 Hz and 1000 Hz), there is no consistent trend relating material thickness to absorption. In the mid-frequency range (1500 Hz to 2000 Hz), thicker materials tend to have higher coefficients, suggesting better absorption with increased thickness. The absence of sound absorption at 3000 Hz and 4500 Hz suggests these frequencies may be resonant frequencies where the material and air gap combination is not effective for sound insulation. At higher frequencies (3500 Hz and 4000 Hz), the absorption is affected by thickness but not in a linear fashion. At the highest tested frequency (5000 Hz), absorption is minimal, although the thickest material (F.50) performs slightly better.

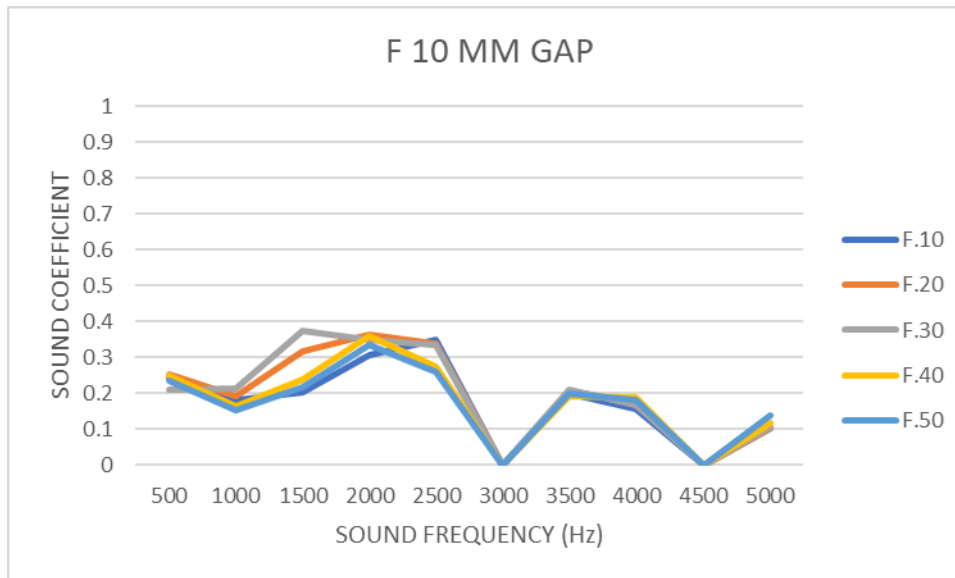


Figure 4.44 Graph of sound coefficient of F with 10 mm air gap

4.5.6.3 Sample F sound absorption performance with 20 mm air gap

Figure 4.45 shows the graph of sound coefficient of F with 20 mm air gap. At 500 Hz, the absorption coefficient generally rises with thickness, reaching its peak at F.50 (50 mm) with a value of 0.261891. Progressing to 1000 Hz, the trend is less clear, with the highest coefficient at F.30 (30 mm) being 0.223651. For 1500 Hz, there's a peak in absorption again at F.30, with a coefficient of 0.332507. At 2000 Hz, absorption coefficients remain high across thicknesses, with F.30 having the highest at 0.366581. Transitioning to 2500 Hz, coefficients are somewhat lower than at 2000 Hz but still relatively high, and F.30 shows the highest at 0.340149. At 3000 Hz, no sound absorption is detected for any thickness (coefficient = 0). For 3500 Hz, sound absorption increases from zero at 3000 Hz, with F.40 (40 mm) displaying the highest coefficient at 0.208941. At 4000 Hz, coefficients decrease compared to 3500 Hz, with F.40 having the highest at 0.220383. At 4500 Hz, there's no sound absorption (coefficient = 0) for all thicknesses. Finally, at 5000 Hz, sound absorption coefficients are low, with F.30 having the highest value at 0.113556. For sample F with a 20 mm air gap, the absorption characteristics are variable and depend on both material thickness

and frequency. In the lower frequencies (500 Hz to 2500 Hz), increased material thickness tends to correlate with higher absorption, with F.30 often having the highest coefficients. However, this trend is not uniform across all frequencies. The lack of absorption at 3000 Hz and 4500 Hz suggests these may be resonant frequencies where the material is ineffective at sound damping due to the air gap's influence. At mid-to-high frequencies (3500 Hz and 4000 Hz), F.40 shows the highest absorption coefficients. At the highest frequency tested (5000 Hz), F.30 provides the most absorption, although the coefficients are quite low across all thicknesses. The data indicates that for sound insulation applications involving a 20 mm air gap, a targeted choice of material thickness based on the frequency of interest is necessary.

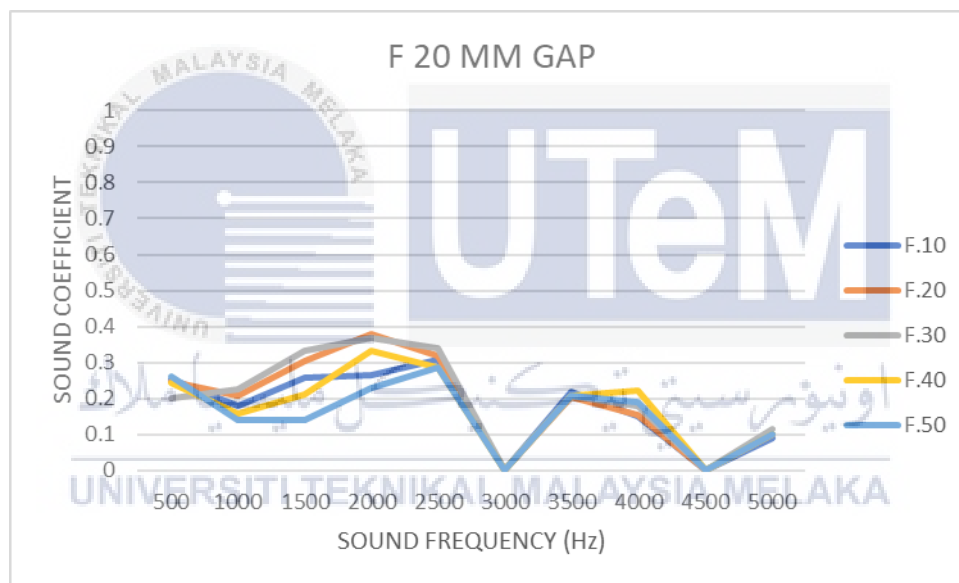


Figure 4.45 Graph of sound coefficient of F with 20 mm air gap

4.5.6.4 Sample F sound absorption performance with 30 mm air gap

Figure 4.46 shows the graph of sound coefficient of F with 30 mm air gap. At 500 Hz, the absorption coefficient peaks at F.10 (10 mm) with 0.261891 and decreases with increasing thickness. Progressing to 1000 Hz, the absorption coefficient lacks consistency with thickness, but F.50 (50 mm) has the highest value at 0.177141. For 1500 Hz, coefficients increase with thickness up to F.30 (30 mm) and then slightly decrease for thicker

samples. At 2000 Hz, F.50 shows the highest absorption coefficient at 0.335292, indicating improved absorption with increased thickness. Moving to 2500 Hz, coefficients decrease as material thickness increases, and F.10 has the highest at 0.286955. At 3000 Hz, no sound absorption is observed for any thickness (coefficient = 0). For 3500 Hz, absorption coefficients are fairly even across different thicknesses, with a slight peak at F.10. At 4000 Hz, coefficients decrease compared to 3500 Hz, with the highest absorption still at F.10 (10 mm). At 4500 Hz, there's no sound absorption (coefficient = 0) for all thicknesses. Finally, at 5000 Hz, sound absorption coefficients are low, with F.50 showing the highest value at 0.132066. For sample F with a 30 mm air gap, the absorption coefficient shows variability dependent on both material thickness and the frequency of the sound. At lower frequencies (500 Hz), the thinnest material (F.10) has the highest absorption coefficient. However, at 1000 Hz and 1500 Hz, the relationship between thickness and absorption is not linear, with the thickest material (F.50) showing the highest absorption at 1000 Hz and F.30 at 1500 Hz. The absence of sound absorption at 3000 Hz and 4500 Hz across all thicknesses might suggest these frequencies are resonant, where the material and air gap combination does not dampen sound effectively. At mid-to-high frequencies (3500 Hz and 4000 Hz), the absorption is relatively uniform across thicknesses, with a slight preference for thinner materials. At the highest frequency tested (5000 Hz), the thickest material (F.50) has a slightly higher coefficient, although the overall absorption remains low.

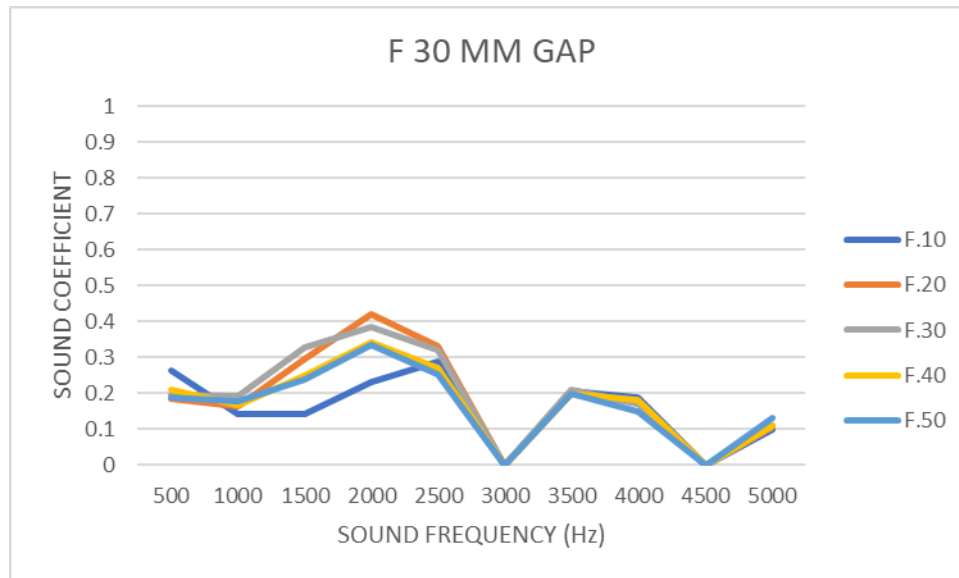


Figure 4.46 Graph of sound coefficient of F with 30 mm air gap

4.5.7 Sample C

This experiment will start with the pure cement and the samples were made with different thickness, starting from 10 mm to 50 mm and it will be carried out with no gap, 10 mm air gap, 20 mm air gap and 30 mm air gap. This sample is considered as control sample.

UNIVERSITI TEKNIKAL MALAYSIA MELAKA

4.5.7.1 Sample C sound absorption performance without air gap

Figure 4.47 shows the graph of sound coefficient of C with no air gap. At 500 Hz, the absorption coefficient exhibits an inconsistent trend with varying thickness, peaking at C.50 (50 mm) with a value of 0.36625. Moving to 1000 Hz, there's a peak for C.40 (40 mm) at 0.286657, but this doesn't follow a clear trend related to thickness. For 1500 Hz, the absorption coefficient is highest for C.20 (20 mm) at 0.306878 and doesn't uniformly increase with thickness. At 2000 Hz, C.50 shows the highest coefficient at 0.265273, indicating better absorption with increased thickness. Transitioning to 2500 Hz, coefficients decrease as material thickness increases, and C.10 has the highest at 0.096642. At 3000 Hz,

no sound absorption is detected across all thicknesses at this frequency (coefficient = 0). For 3500 Hz, sound absorption coefficients are higher, with C.20 showing the highest coefficient at 0.263603. At 4000 Hz, coefficients are relatively consistent across thicknesses, with a slight peak at C.20. At 4500 Hz, there's no sound absorption (coefficient = 0) at this frequency for all thicknesses. Finally, at 5000 Hz, absorption coefficients are generally low, with C.30 having the highest value at 0.201505. For sample C without an air gap, the absorption coefficients vary with frequency and material thickness, without displaying a consistent pattern. At lower frequencies (500 Hz and 1000 Hz), increased material thickness does not consistently result in higher absorption. At mid-frequencies (1500 Hz and 2000 Hz), we observe peaks in absorption that do not correspond with the thickest material. The complete absence of sound absorption at 3000 Hz and 4500 Hz across all thicknesses suggests that these frequencies are resonant, where the material is ineffective at dampening sound. At higher frequencies (3500 Hz and 4000 Hz), the absorption coefficients are not significantly affected by thickness. At the highest tested frequency (5000 Hz), absorption is minimal, although C.30 (30 mm) shows a relatively higher coefficient.

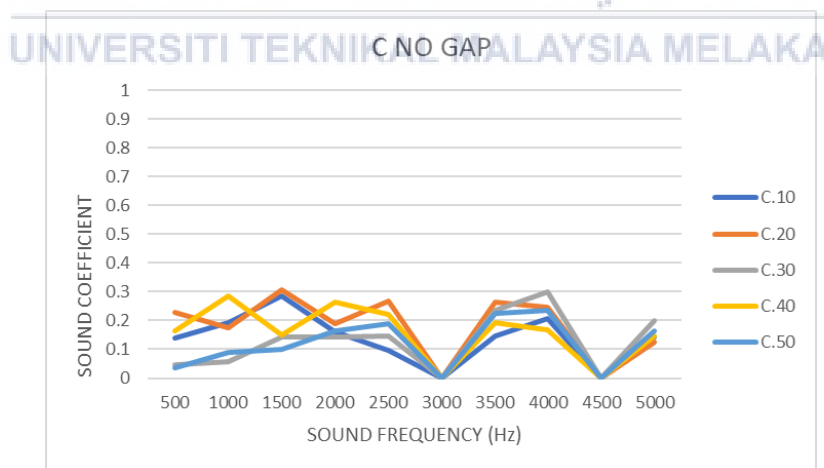


Figure 4.47 Graph of sound coefficient of C no air gap

4.5.7.2 Sample C sound absorption performance with 10 mm air gap

Figure 4.48 shows the graph of sound coefficient of C 10 mm air gap. At 500 Hz, the absorption coefficient peaks at C.50 (50 mm) with a value of 0.317615 and generally decreases as the thickness decreases. Moving to 1000 Hz, C.50 again has the highest coefficient at 0.42797, indicating superior absorption at this thickness. For 1500 Hz, the absorption coefficient peaks at C.20 (20 mm) with 0.483564, revealing an irregular pattern relative to thickness. At 2000 Hz, C.20 maintains the highest absorption coefficient at this frequency with 0.494811. Transitioning to 2500 Hz, the coefficients are relatively high across all thicknesses, and C.40 (40 mm) has the highest at 0.365072. At 3000 Hz, there is no absorption across all thicknesses at this frequency, indicated by coefficients of 0. For 3500 Hz, the coefficients show a diverse pattern, with C.40 displaying the highest coefficient at 0.249692. At 4000 Hz, coefficients are relatively even across thicknesses, with a slight increase for C.30 (30 mm). For 4500 Hz, no sound absorption is detected at this frequency for any thickness, as indicated by coefficients of 0. Finally, at 5000 Hz, the highest absorption coefficient is at C.30 with 0.126688. For sample C with a 10 mm air gap, the absorption coefficients display a complex relationship with both frequency and material thickness. At lower frequencies (500 Hz and 1000 Hz), higher material thickness tends to correlate with higher absorption. However, at 1500 Hz and 2000 Hz, the relationship is not linear, with C.20 showing the highest coefficients, suggesting that other factors may influence the absorption efficiency. The lack of absorption at 3000 Hz and 4500 Hz might be due to resonant frequencies where the combined effect of material properties and the air gap size fails to attenuate the sound. In the mid-frequency range (3500 Hz and 4000 Hz), absorption does not significantly vary with thickness, suggesting

that other factors may play a role in the material's performance. At the highest frequency tested (5000 Hz), C.30 shows the highest absorption, though overall coefficients are low.

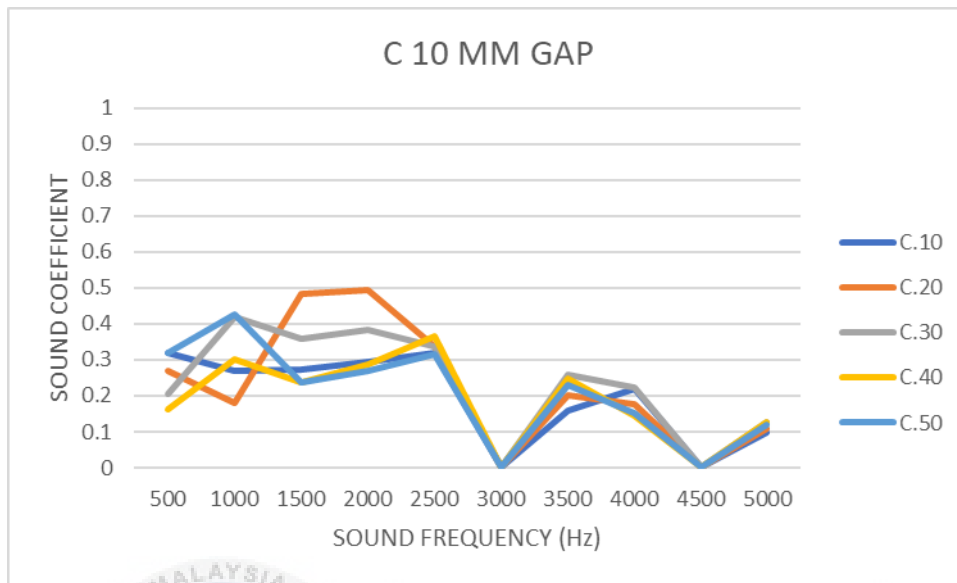


Figure 4.48 Graph of sound coefficient of C 10 mm air gap

4.5.7.3 Sample C sound absorption performance with 20 mm air gap

Figure 4.49 shows the graph of sound coefficient of C 20 mm air gap. There is an anomalous value at the frequency of 2750 Hz, which seems unusually high and out of the typical range for sound absorption coefficients, indicating a possible error or a different scale that does not match the rest of the data. At 500 Hz, the absorption coefficient peaks at C.50 (50 mm) with a value of 0.349016 and decreases as the thickness decreases. Moving to 1000 Hz, C.30 (30 mm) exhibits the highest coefficient at 0.409124, suggesting better absorption with this thickness at this frequency. For 1500 Hz, C.30 maintains the highest absorption coefficient at this frequency with 0.440335. At 2000 Hz, coefficients are relatively high across all thicknesses, and C.20 (20 mm) leads with the highest at 0.48018. Transitioning to 2500 Hz, C.30 shows the highest coefficient at 0.364177. At 3000 Hz, no sound absorption is detected across all thicknesses at this frequency, indicated by coefficients of 0. For 3500 Hz, absorption coefficients are more varied, with C.30 having the highest coefficient at

0.264011. At 4000 Hz, coefficients are fairly consistent across thicknesses, with a slight increase for C.30 at 0.237127. For 4500 Hz, there is no sound absorption at this frequency for any thickness, as indicated by coefficients of 0. Finally, at 5000 Hz, absorption coefficients are low, with C.30 having the highest value at 0.137383. Regarding 2750 Hz, the values listed are anomalously high and likely represent a data entry error or a different unit of measurement not consistent with the sound absorption coefficient scale used for the other frequencies. For sample C with a 20 mm air gap, the absorption coefficients show considerable variation with frequency and material thickness. Generally, C.30 (30 mm) seems to provide the highest absorption across a range of frequencies, particularly in the mid-frequency range (1000 Hz to 2500 Hz). The absence of absorption at 3000 Hz and 4500 Hz could indicate resonant frequencies where the material and air gap combination is ineffective for sound insulation. At higher frequencies (3500 Hz and 4000 Hz), the absorption doesn't vary much with thickness, suggesting that factors other than thickness are influencing the sound absorption properties of the material. At the highest tested frequency (5000 Hz), the absorption is minimal, although C.30 shows the highest coefficient among the tested thicknesses. The values at 2750 Hz should be disregarded or reevaluated, as they do not seem to correlate with the expected range for sound absorption coefficients. The data suggests that C.30 is generally the most effective thickness for sound absorption with a 20 mm air gap across the tested frequencies.

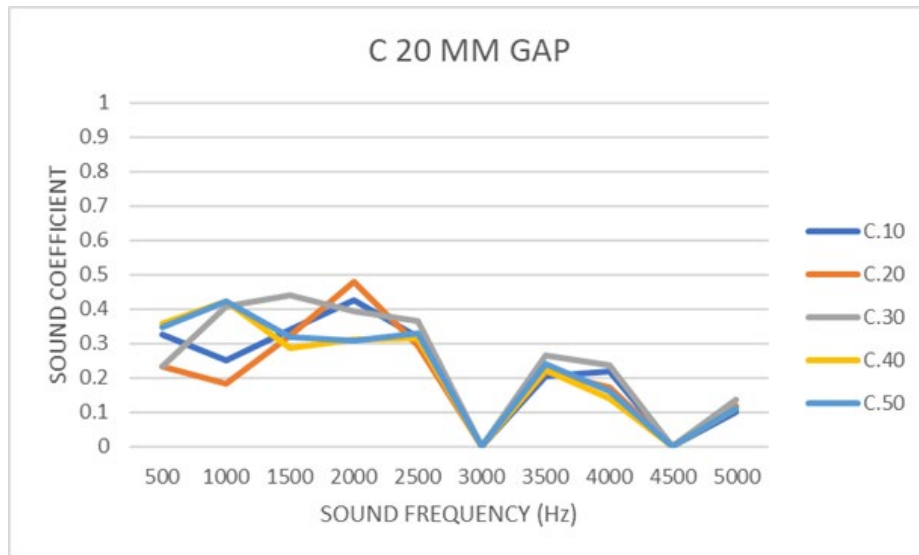


Figure 4.49 Graph of sound coefficient of C 20 mm air gap

4.5.7.4 Sample C sound absorption performance with 30 mm air gap

Figure 4.50 shows the graph of sound coefficient of C 30 mm air gap. At 500 Hz, the highest absorption coefficient is observed at C.50 (50 mm) with 0.37981, suggesting that thicker materials absorb more sound at lower frequencies. Progressing to 1000 Hz, there's a peak at C.40 (40 mm) with 0.454991, indicating that this thickness is most effective at absorbing sound at this frequency. For 1500 Hz, the coefficients are fairly consistent across thicknesses, with a slight peak at C.10 (10 mm) with 0.308302. At 2000 Hz, the highest coefficient is seen at C.20 (20 mm) with 0.490772, revealing an irregular pattern that does not correlate with material thickness. Moving to 2500 Hz, absorption coefficients decrease slightly with increased thickness, but not linearly; C.40 has the highest value at 0.308359. At 3000 Hz, no absorption is detected at this frequency for any thickness, as indicated by coefficients of 0. For 3500 Hz, absorption coefficients increase from C.10 to C.20 but then decrease slightly; C.20 has the highest coefficient at 0.247266. At 4000 Hz, the absorption is not significantly different across the thicknesses, with C.30 showing the highest value at 0.214862. For 4500 Hz, no absorption is detected at this frequency for any thickness, similar

to the 3000 Hz frequency, as indicated by coefficients of 0. Finally, at 5000 Hz, the highest absorption coefficient is at C.10 with 0.102255, but overall, absorption is low at this frequency. For sample C with a 30 mm air gap, the sound absorption properties vary with both frequency and material thickness. At lower frequencies (500 Hz), the thicker materials tend to absorb more sound, while at mid-frequencies (1000 Hz and 1500 Hz), there isn't a clear trend correlating thickness to absorption. There's a notable peak in absorption for C.20 at 2000 Hz, suggesting an optimal thickness for absorption at this frequency. However, the overall trend is non-linear, with no single thickness consistently outperforming others across the frequency range. The absence of absorption at 3000 Hz and 4500 Hz suggests these are resonant frequencies for the material-air gap combination, where sound is not effectively absorbed.

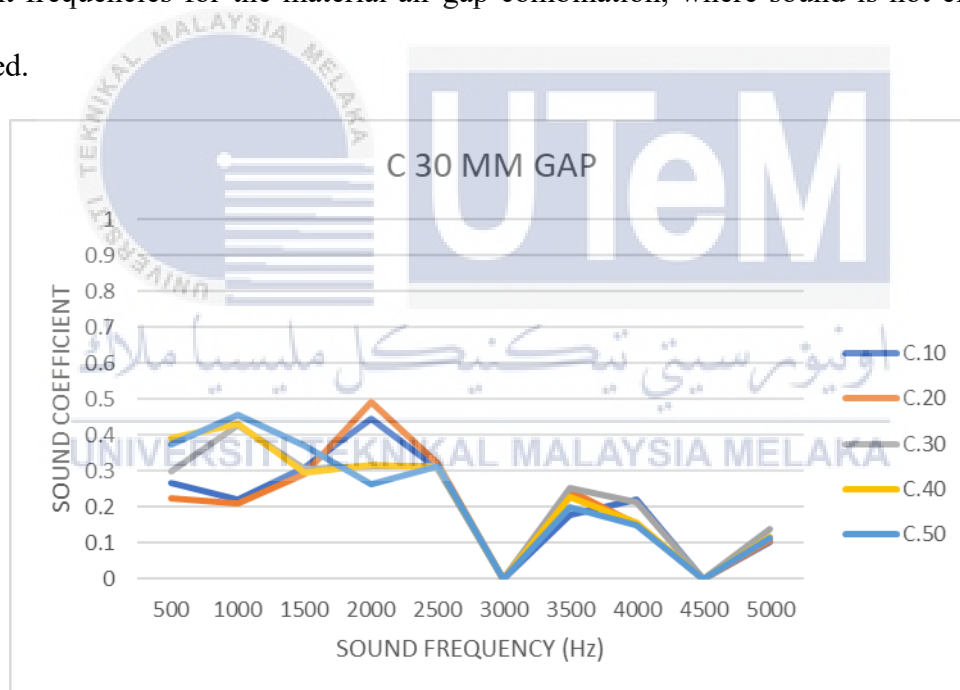


Figure 4.50 Graph of sound coefficient of C 30 mm air gap

4.6 Summary of performance of sound absorption of kenaf core concrete

The sound absorption testing for the samples C, F, C1 through C5 presents an intricate set of results that demonstrate the variability of sound absorption coefficients across different material types and thicknesses, along with variations in air gap sizes.

Sample C exhibited varying absorption performance across the frequency spectrum. Thicker materials demonstrated improved absorption at lower frequencies, but the performance became less predictable at mid to high frequencies. Notably, there was no sound absorption observed at 3000 Hz and 4500 Hz for any thickness.

Similarly, Sample F displayed variable absorption coefficients with no absorption at certain frequencies. The data suggests that the material properties of F, combined with the air gap size, influence its performance, particularly at mid-range frequencies where specific thicknesses perform better than others.

The results for Sample C1 indicated that thicker materials were more effective at lower frequencies, but the effectiveness was not directly proportional to thickness at higher frequencies. The performance across frequencies was notably inconsistent.

Sample C2's absorption coefficients varied with frequency, showing a trend where certain mid-range thicknesses had better absorption capabilities at specific frequencies. Like the other samples, C2 showed no absorption at 3000 Hz and 4500 Hz.

Sample C3 demonstrated peak absorption at certain mid-frequencies, with specific thicknesses showing higher efficiency. The non-linear pattern suggests that optimal sound absorption for C3 is highly frequency-specific.

C4 displayed a complex relationship between thickness and absorption, with some mid-range thicknesses outperforming others at different frequencies. The lack of a clear trend

underscores the importance of matching material properties to the specific sound frequencies that need attenuation.

The performance of C5 across the frequency range was also complex, with no single thickness universally standing out as the most effective. Instead, certain thicknesses were more suited to specific frequencies, emphasizing the need for a tailored approach to sound insulation.

In summary, the sound testing data across all samples indicates that sound absorption is influenced by a combination of material thickness, air gap size, and sound frequency. Lower frequencies generally require thicker materials for effective absorption, while at higher frequencies, the trend is less clear and more dependent on specific material and frequency characteristics. The presence of a non-absorptive response at particular frequencies suggests resonance points where materials are ineffective at sound dampening. Each sample presents a unique profile, emphasizing the importance of carefully matching materials to the acoustic profile of the space and specific sound frequencies that need management. This data can be instrumental in guiding the design of acoustically optimized environments, whether for residential, commercial, or industrial applications.

4.7 The Best Composite Composition for Sound Absorption

The best composite composition for sound absorption is sample C3 and C5 since they often showed higher absorption peaks at multiple points in the frequency spectrum compared to the others. For instance, sample C3 generally displayed higher absorption coefficients at mid-range frequencies, which are often the most problematic in acoustic treatments. Sample C5 also showed notable absorption in the mid-frequency range but with slightly lower coefficients than C3. Therefore, if the goal is to reduce sound across a broad range of

frequencies, particularly in the mid-frequency area, samples C3 or C5 might be the best starting points based on the data available. Figure 4.45 shows the samples of C3 and C5. Based on the data provided for samples C3 and C5, the best thicknesses for sound absorption vary with the frequency range in question. If we are to select a single thickness that performs consistently well across different frequencies, for sample C3, a 30 mm thickness seems to be the most effective. It shows higher sound absorption coefficients at several key frequency points compared to other thicknesses, which suggests that it strikes a good balance between mass and the ability to dampen sound waves.

Similarly, for sample C5, the 30 mm thickness also stands out as providing a consistently higher sound absorption coefficient across the tested frequency spectrum. Although the performance of different thicknesses can vary with specific frequencies, the 30 mm thick material appears to offer a versatile and effective solution for a wide range of frequencies. Therefore, if one were to choose the best composition for sound absorption from the provided options, C3 and C5 with a 30 mm thickness would be recommended based on their overall strong performance. This suggests that these compositions could provide a good level of sound damping for a variety of applications, particularly where mid-frequency sound absorption is desired.

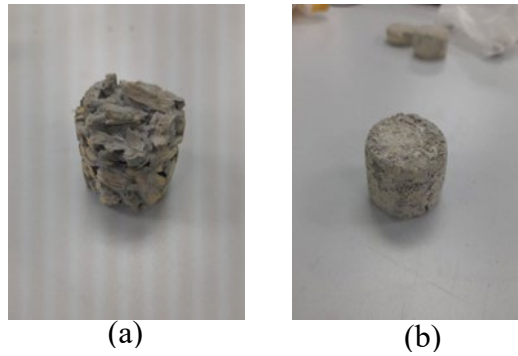


Figure 4.51 The best samples for sound absorption (a) 30 mm thickness of C5 (b) 30 mm thickness of C3

4.8 Summary

After all the related literature by past research has been reviewed, it can be summarized that kenaf fibre has an enormous potential to be a raw material that replaces the current synthetic material. It has been experimentally proven and maintains good sound and great mechanical strength. The use of replacing synthetic with natural materials to protect our climate without abandoning our health concerns. Kenaf fibre has a high potential to solve this problem because it has very low toxicity. It is also interesting to find out that natural kenaf fibre shows better improvement in acoustics and mechanical properties

For the mechanical test the samples, the overall best ratio that gives well performance towards each testing is sample 20 mm kenaf core (C5) and concrete. This is because the small size of kenaf core gives more interfacial bonding of the composites when mixing with the concrete. Furthermore, when compared with the control samples, this ratio considered as potential application in concrete in replacing other materials because of the high performance in flexural and compression strength.

As for the acoustic test, the sample's sound absorption coefficient with different thickness of 10 mm, 20 mm, 30 mm, 40 mm and 50 mm thickness were observed using impedance tube testing. There were three types of sound wave frequency produced which is low frequency with a range of 0 to 1000 Hz and it is represent with redline, medium frequency with a range of 1200 Hz to 2400 Hz represent with green line and high frequency with a range of 2500 Hz to 5000 represent with the blue line. Figure 4.46 shows the illustration of sound absorption of the sample with the thickness of 30 mm. It is experimentally proven that natural fibre is a better sound absorber than synthetic material. Sample C5 with 30 mm thickness and C3 with 30 mm thickness shows better results than C and F which is pure cement and polystyrene fo0.314966am respectively. Sample C5.30 shows a sound coefficient of 0.334663 at 500 Hz, 0.314199 at 2000 Hz and 0.314966 at 2500 Hz in low, medium and high frequency meanwhile C3.3o shows a sound coefficient of 0.405105 at 500 Hz, 0.313739 at 2000 Hz and 0.313739 at 2500 Hz an this is the value when there is no air gap. In summary, at the lower frequency of 500 Hz, C3 shows a substantial improvement over C with a 34.75% increase in the sound absorption coefficient. C5 also shows improvement but to a lesser extent, with an 11.32% increase. At the mid and higher frequencies of 2000 Hz and 2500 Hz, both C3 and C5 do not show an improvement over F; in fact, there's a slight decrease in performance at 2000 Hz. However, at 2500 Hz, both compositions show an increase over F, with C5 showing a slightly higher percentage improvement than C3.

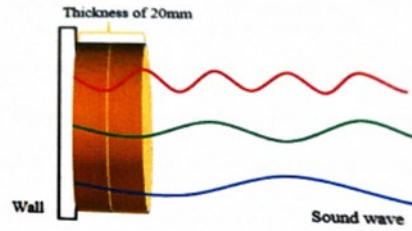


Figure 4.52 Illustration of sound absorption of the sample with a 30 mm thickness sample.

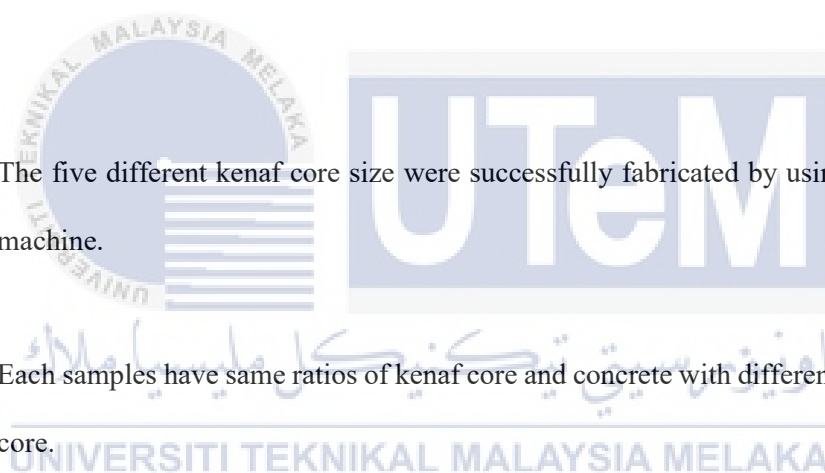
The expected result that can be determined from this research is the best kenaf core size with a good sound absorption. When selecting the best kenaf core size for an acoustical panel in concrete, the specific dimensions provided can be considered which are 10 mm, 20 mm, 30 mm, 20 mesh and 40 mesh. A kenaf core size of 10 mm would provide a relatively fine texture. It may offer moderate sound absorption properties, especially for high-frequency sounds. This size is suitable if the environment has limited space or if the panel is designed to be compact. With a slightly larger kenaf core size of 20 mm, it can improve sound absorption compared to the 10 mm. This size may strike a balance between acoustic performance and panel thickness, making it suitable for various applications. A kenaf core size of 30 mm would offer further enhanced sound absorption properties compared to the previous sizes. It allows for more kenaf material in the panel, which can improve low-frequency sound absorption. This size is expected to be ideal. Similar to the 20 mesh, 40 mesh refers to a finer particle size distribution. It is likely to provide improved acoustic performance compared to coarser options, especially in terms of high-frequency sound absorption. So, the expected result is the 30 mm size will be the most suitable

CHAPTER 5

CONCLUSION AND RECOMMENDATIONS

5.1 Conclusion

This study presents an overview of kenaf fibre's potential to be the raw material that can replace the existing polystyrene foam reinforced concrete. The reinforcement used was kenaf fibre with a constant of 300 g in all the samples but the thickness of the samples are from a range of 10 mm thickness to 50 mm thickness. The first objective is to fabricate the acoustical panel made from different size of kenaf core with cement using 3d printing mould. The following is a summary of conclusions:

- 
- a) The five different kenaf core size were successfully fabricated by using a 3D printing machine.
 - b) Each samples have same ratios of kenaf core and concrete with different sizing of kenaf core.

This research's second objective was to investigate the composite composition for acoustic and mechanical performance. The significant conclusion for this objective as follows :

- a) From the overall compressive strength performance analysis, while cement (C) has the highest performance in compression tests, the reinforced samples like C5 show considerable improvements with a compressive strength of 0.44 M over the foam sample (F) since C5 has over 131.58% improvement in strength compared to Foam at 30 mm thickness

- b) From the overall flexural performance analysis, C3 shows a significant improvement over Foam with a flexural strength of 2.84 MPa (F), being 178.43% stronger in flexural strength at 30 mm thickness
- c) From the overall sound absorption performance, the best size of kenaf core is C5 for lower frequency which is at 500 Hz it has the peak sound coefficient of 0.388719 which is 27.75% better than polystyrene foam at no air gap
- d) From the overall sound absorption performance, the best size of kenaf core is C3 for mid-range frequency which is at 1500 Hz it has the peak sound coefficient of 0.290442. which is 37.75% better than polystyrene foam at no air gap.

This research's third objective was to propose the best composite size for optimum performance that best for acoustical panel. The following points emerged from the present investigation.

- a) The kenaf core size of 20 mm (C5) is the best based on sound absorption performance and mechanical strength performance
- b) Kenaf core sized of 20 mm (C5) and 10 mm (C3) shows the best performance for sound absorption with 30 mm thickness
- c) Kenaf core sized of 20 mm (C5) shows the best performance for mechanical strength performance

- d) The evidence from this study suggests that kenaf fibre can replace the current concrete that is mixed with polystyrene foam.

5.2 Recommendations

This research has thrown up many questions in need for further investigations related to this field of study. Hence, there are few recommendations suggestions for upcoming research. The following are recommendations proposed;

- a) The fabrication process, which is the development of the sample, need to be improved by changing the method of mixing the concrete and kenaf core , drying method, curing process for further investigation.
- b) The experimental testing for sound absorption test was suggested for further studies
- c) Study on the behaviour of different temperature towards the performance acoustic panel

5.3 Sustainability Element

Sustainability is the capacity to meet the current demands without undermining future generation's ability to meet their own needs. Sustainability is critical in our everyday lives. Sustainable development has involved the redistribution of the product to the atmosphere

during the creation of the product and resource extraction until the end of the product life cycle. The fabricated composite material can indeed be viewed as a sustainable commodity due to the easy-to-access manufacturing material factor, the decrease in the amount of matrix used, and the improvement in cost efficiency.

One of the factors to be considered is that the manufacturing material was easily reachable. Kenaf core was easily accessible since the kenaf plant became a commercial plant promoted by the Malaysian government to replace the tobacco plantation. As a result, the kenaf core used as reinforcement has wholly fulfilled the principle of sustainability due to its simple accessibility. Besides the ease of kenaf core availability, promoting nationally generated natural fibre in product development may also lead to a better future by boosting the country's economy. When the kenaf core itself is manufactured locally; the price is lower than the other natural fibres.

Another factor will be that fabricated composite material may also be classified as a green product. The explanation beyond it would be the volume of the kenaf core used, and polyester fibre was 1:3. With the kenaf core used as a reinforcement for concrete, the amount of polyester fibre as a matrix required for composite manufacturing can be decreased, and the amount of waste produced for the environment and landfill can be reduced. Besides, the fabricated component's cost can be reduced by minimizing the amount of matrix used in the manufacture of the product.

In a nutshell, kenaf core as reinforcement for the development of kenaf core concrete was a sustainable product because of the ease of the kenaf core can be obtained. The ratio of the

kenaf core used was 1:3 in the fabrication composite and the higher cost was more effective due to its sustainability and properties than commercializing the product.

5.4 Commercial Value and Potential

These findings provide the following insights for future research development of panel application. The reason for using only kenaf core and concrete is to produce an eco-friendly product that has a best fire test performance but low in cost. Kenaf fiber is accessible and can be found locally, and the fiber show high potential for fire resistance panel application development since they excel in fire performance test. Kenaf fiber can also reduce the manufacturing process costs as the synthetic material cost becomes higher and higher due to the market demand. The only drawbacks are that it lacks a lightweight compared to polystyrene, but kenaf fiber is an environmentally friendly material. They are also biodegradable and takes only about four to six months to decay while the polystyrene is a non-biodegradable material that will take up to 500 years to degrade that will only end up as a pile waste before it can decompose.

5.5 Research Achievement

This research focuses specifically on the development of kenaf core concrete, A memory token is taken and shown in Figure 5.2. The accomplishment that have been accomplished by this research include:

- a) Gold Award Winner for participant in ITEX 2023 on 11-12 May 2023 held at KLCC, Malaysia



Figure 5.1 Memory of ITEX 2023



REFERENCES

Abdalla JA, Thomas BS, Hawileh RA. Use of hemp, kenaf and bamboo natural fiber in cement-based concrete. *Materials Today: Proceedings*. 2022 Jan 1;65:2070-2.

Abdollah MFB, Shuhimi FF, Ismail N, Amiruddin H. and Umehara, N., 2015. Selection and verification of kenaf fibres as an alternative friction material using weighted decision matrix method. *Materials & Design*, 67, pp.577-582

Abdullah S, Tajuddin R.M. Thermal Gravimetric Analysis (Tga) of Kenaf Core and Its Cellulose for Membrane Fabrication. In *InCIEC 2015: Proceedings of the International Civil and Infrastructure Engineering Conference 2016* (pp. 667-677). Springer Singapore.

Afzal MZ, Ibrahim AK, Xu Y, Niyitanga S, Li Y, Li D, Yang X, Zhang L. Kenaf (*hibiscus cannabinus* L.) breeding. *Journal of Natural Fibers*. 2022 Nov 2;19(11):4063-81.

Alexander M, Beushausen H. Durability, service life prediction, and modelling for reinforced concrete structures—review and critique. *Cement and Concrete Research*. 2019 Aug 1;122:17-29.

Al-Mamun M, Rafii MY, Misran AB, Berahim Z, Ahmad Z, Khan MM, Oladosu Y, Arolu F. Kenaf (*Hibiscus Cannabinus* L.): A Promising Fiber Crop with Potential for Genetic Improvement Utilizing Both Conventional and Molecular Approaches. *Journal of Natural Fibers*. 2023 Dec 31;20(1):2145410.

Arenas JP, Crocker MJ. Recent trends in porous sound-absorbing materials. *Sound & vibration*. 2010 Jul 12;44(7):12-8.

Arjmandi R, Yıldırım I, Hatton F, Hassan A, Jefferies C, Mohamad Z, Othman N. Kenaf fibers reinforced unsaturated polyester composites: A review. *Journal of Engineered Fibers and Fabrics*. 2021 Aug;16:15589250211040184.

Asdrubali, Francesco, and Giulio Pispola. "Acoustical optimization of a roller blind box." Proc. ICSV13, Vienna, Austria (2006).

Asyraf MZ, Suriani MJ, Ruzaidi CM, Khalina A, Ilyas RA, Asyraf MR, Syamsir A, Azmi A, Mohamed A. Development of Natural Fibre-Reinforced Polymer Composites Ballistic Helmet Using Concurrent Engineering Approach: A Brief Review. *Sustainability*. 2022 Jun 9;14(12):7092.

Baghban, Mohammad Hajmohammadian, and Reza Mahjoub. "Natural kenaf fiber and LC3 binder for sustainable fiber-reinforced cementitious composite: a review." *Applied Sciences* 10, no. 1 (2020): 357.

Bajaber MA, Hakeem IY. UHPC evolution, development, and utilization in construction: A review. *Journal of Materials Research and Technology*. 2021 Jan 1;10:1058-74.

Chandramouli K, Pannirselvam N, NagaSaiPardhu DV, Anitha V. Experimental investigation on banana fibre reinforced concrete with conventional concrete. *International Journal of recent Technology and Engineering*. 2019 Mar;7(6S).

Chin DD, Yahya MN, Din NB, Ong P. Acoustic properties of biodegradable composite micro-perforated panel (BC-MPP) made from kenaf fibre and polylactic acid (PLA). *Applied Acoustics*. 2018 Sep 1;138:179-87.

Clyne, Trevor William, and Derek Hull. *An introduction to composite materials*. Cambridge university press, 2019.

Dasgupta A. Retrofitting of concrete structure with fiber reinforced polymer. *International Journal*. 2018;4(9):42-9.

David Müzel, Sarah, Eduardo Pires Bonhin, Nara Miranda Guimarães, and Erick Siqueira Guidi. "Application of the finite element method in the analysis of composite materials: A review." *Polymers* 12, no. 4 (2020): 818.

de Azevedo, Afonso RG, Markssuel Teixeira Marvila, Bassam A. Tayeh, Daiane Cecchin, Artur Camposo Pereira, and Sergio Neves Monteiro. "Technological performance of açai natural fibre reinforced cement-based mortars." *Journal of Building Engineering* 33 (2021): 101675.

Dong C. Review of natural fibre-reinforced hybrid composites. *Journal of Reinforced Plastics and Composites*. 2018 Mar;37(5):331-48.

Fadzlita MT, Yeo KB, Choong WH, Melvin M. Absorption Coefficient of Acoustic Coir Fibre Panel and Effects of Varying Percentage of Perforated Plates. *Journal of Applied Sciences*. 2014 Dec;14(22):3106-9.

Giwa Ibrahim SA, Karim R, Saari N, Wan Abdullah WZ, Zawawi N, Ab Razak AF, Hamim NA, Umar RU. Kenaf (*Hibiscus cannabinus* L.) seed and its potential food applications: a review. *Journal of food science*. 2019 Aug;84(8):2015-23.

Harmaen AS, Paridah MT, Jawaid M, Fariz AM, Asmawi B. Effect of Silica Aerogel on Polypropylene Reinforced with Kenaf Core Fiber for Interior Automotive Components. *In Kenaf Fibers and Composites* 2018 Jun 14 (pp. 81-92). CRC Press.

Ilyas RA, Sapuan SM, Ibrahim R, Abral H, Ishak MR, Zainudin ES, Asrofi M, Atikah MS, Huzaifah MR, Radzi AM, Azammi AM. Sugar palm (*Arenga pinnata* (Wurmb.) Merr) cellulosic fibre hierarchy: A comprehensive approach from macro to nano scale. *Journal of Materials Research and Technology*. 2019 May 1;8(3):2753-66.

Jayasuriya A, Shibata ES, Chen T, Adams MP. Development and statistical database analysis of hardened concrete properties made with recycled concrete aggregates. *Resources, Conservation and Recycling*. 2021 Jan 1;164:105121.

Jawaid, M., Thariq, M. and Saba, N. eds., 2018. Structural health monitoring of biocomposites, fibre-reinforced composites and hybrid composites.

Jirawattanasomkul T, Ueda T, Likitlersuang S, Zhang D, Hanwiboonwat N, Wuttiwannasak N, Horsangchai K. Effect of natural fibre reinforced polymers on confined compressive strength of concrete. *Construction and Building Materials*. 2019 Oct 30;223:156-64.

Judawisastra, H., Sukmawati, A., Zaidi, S. Z. J., & Harito, C. (2022). Sustainable Sound Absorber from Nonwoven Fabric of Natural Biduri Fibers (*Calotropis gigantea*) with Polyester Binder. *Journal of Natural Fibers*, 19(16), 12791-12804.

Kamal, I.B., 2014. Kenaf for biocomposite: an overview. *Journal of Science and Technology*, 6(2).

Karim R, Noh NA, Ibadullah WZ, Zawawi N, Saari N. Kenaf (*Hibiscus cannabinus* L.) seed extract as a new plant-based milk alternative and its potential food uses. In *Milk Substitutes- Selected Aspects 2020* Oct 14. IntechOpen.

Kinnane, O., Reilly, A., Grimes, J., Pavia, S. and Walker, R., 2016. Acoustic absorption of hemp-lime construction. *Construction and building materials*, 122, pp.674-682.

Kishore SE, Sujithra R, Dhatreyi B. A review on latest acoustic noise mitigation materials. *Materials Today: Proceedings*. 2021 Jan 1;47:4700-7.

Kumar P, Roy R. Study and experimental investigation of flow and flexural properties of natural fiber reinforced self compacting concrete. *Procedia Computer Science*. 2018 Jan 1;125:598-608.

Kurinjimalar, R., Vimala, S., Silambarasan, M. and Chinnasami, S., 2021. A Review on Coir fibre Reinforced Composites with Different Matrix.

Li F, Liu Y, Leng J. Progress of shape memory polymers and their composites in aerospace applications. *Smart Materials and Structures*. 2019 Sep 23;28(10):103003.

Li VC. Engineered cementitious composites (ECC): bendable concrete for sustainable and resilient infrastructure. Springer; 2019 Apr 30.

Li Y, Su Y, Tan KH, Zheng X, Sheng J. Pore structure and splitting tensile strength of hybrid Basalt–Polypropylene fiber reinforced concrete subjected to carbonation. *Construction and Building Materials*. 2021 Aug 23;297:123779.

Lim ZY, Putra A, Nor MJ, Yaakob MY. Sound absorption performance of natural kenaf fibres. *Applied Acoustics*. 2018 Jan 15;130:107-14.

Malviya RK, Singh RK, Purohit R, Sinha R. Natural fibre reinforced composite materials: Environmentally better life cycle assessment–A case study. *Materials Today: Proceedings*. 2020 Jan 1;26:3157-60.

Mohanty AR, Fatima S. Noise control using green materials. *Sound and Vibration*. 2015 Feb 1;49(2):13-5.

Mokhothu, T.H. and John, M.J., 2017. Bio-based coatings for reducing water sorption in natural fibre reinforced composites. *Scientific reports*, 7(1), p.13335.

Muthukumar N, Thilagavathi G, Neelakrishnan S, Poovaragan PT. Sound and thermal insulation properties of flax/low melt PET needle punched nonwovens. *Journal of Natural Fibers*. 2019 Feb 17;16(2):245-52.

Ngo TD. Introduction to composite materials. *Composite and Nanocomposite Materials—From Knowledge to Industrial Applications*. 2020 Feb 25.

Ngo TD. Introduction to composite materials. *Composite and Nanocomposite Materials—From Knowledge to Industrial Applications*. 2020 Feb 25.

Noryani M, Sapuan SM, Mastura MT. Multi-criteria decision-making tools for material selection of natural fibre composites: A review. *Journal of Mechanical Engineering and Sciences*. 2018 Mar 1;12(1):3330.

OBAKIN OA, OLADUNMOYE OM. IMPACT STRENGTH OF KENAF FIBER AND CORN COB ASH ROOFING TILES FOR SUSTAINABLE HOUSING DEVELOPMENT. *Journal of Basic and Applied Research International*. 2020 Aug 1:33-8.

Okuda, N. and Sato, M., 2004. Manufacture and mechanical properties of binderless boards from kenaf core. *Journal of wood science*, 50, pp.53-61.

Peças P, Carvalho H, Salman H, Leite M. Natural fibre composites and their applications: a review. *Journal of composites science*. 2018 Nov 17;2(4):66.

Qasim OA. A review paper on specimens size and shape effects on the concrete properties. *International Journal of Recent Advances in science and technology*. 2018;5(3):13-25.

Rajak DK, Pagar DD, Kumar R, Pruncu CI. Recent progress of reinforcement materials: a comprehensive overview of composite materials. *Journal of Materials Research and Technology*. 2019 Nov 1;8(6):6354-74.

Rajak DK, Pagar DD, Menezes PL, Linul E. Fiber-reinforced polymer composites: Manufacturing, properties, and applications. *Polymers*. 2019 Oct 12;11(10):1667.

Raju A, Shanmugaraja M. Recent researches in fiber reinforced composite materials: A review. *Materials Today: Proceedings*. 2021 Jan 1;46:9291-6.

Rizkalla, S., Dawood, M. And Shahawy, M., 2015. FRP for Transportation and Civil Engineering Infrastructre: Reality and Vision.

Rubino, Felice, Antonio Nisticò, Fausto Tucci, and Pierpaolo Carlone. "Marine application of fiber reinforced composites: a review." *Journal of Marine Science and Engineering* 8, no. 1 (2020): 26.

Saad, M.J. and Kamal, I., 2012. Kenaf core particleboard and its sound absorbing properties. *Journal of Science and Technology*, 4(2), pp. 22-34.

Sadrmanesh V, Chen Y. Simulation of tensile behavior of plant fibers using the discrete element method (DEM). *Composites Part A: Applied Science and Manufacturing*. 2018 Nov 1;114:196-203.

Sahu P, Gupta MK. A review on the properties of natural fibres and its bio-composites: Effect of alkali treatment. *Proceedings of the Institution of Mechanical Engineers, Part L: Journal of Materials: Design and Applications*. 2020 Jan;234(1):198-217.

Samaei SE, Berardi U, Taban E, Soltani P, Mousavi SM. Natural fibro-granular composite as a novel sustainable sound-absorbing material. *Applied Acoustics*. 2021 Oct 1;181:108157.

Sadrmanesh V, Chen Y. Bast fibres: structure, processing, properties, and applications. *International Materials Reviews*. 2019 Oct 3;64(7):381-406.

Sanjay MR, Madhu P, Jawaid M, Senthamarai kanna n P, Senthil S, Pradeep S. Characterization and properties of natural fiber polymer composites: A comprehensive review. *Journal of Cleaner Production*. 2018 Jan 20;172:566-81.

Saravanan N, Buvaneshwari M. Experimental Investigation on Behaviour of Natural Fibre Concrete (Sisal Fibre). *Cellulose*. 2018;54:66.

Shahar FS, Sultan MT, Shah AU, Safri SN. A short review on the extraction of kenaf fibers and the mechanical properties of kenaf powder composites. *InIOP Conference Series: Materials Science and Engineering* 2019 Nov 1 (Vol. 670, No. 1, p. 012028). IOP Publishing.

Satyanarayana KG, Sukumaran K, Mukherjee PS, Pavithran C, Pillai SG. Natural fibre-polymer composites. *Cement and Concrete composites*. 1990 Jan 1;12(2):117-36.

Siakeng, R., Jawaid, M., Ariffin, H., Sapuan, S.M., Asim, M. and Saba, N., 2019. Natural fiber reinforced polylactic acid composites: A review. *Polymer Composites*, 40(2), pp.446-463.

Solahuddin, B.A., 2022, January. A critical review on experimental investigation and finite element analysis on structural performance of kenaf fibre reinforced concrete. In *Structures* (Vol. 35, pp. 1030-1061). Elsevier.

Summerscales, J., Dissanayake, N.P., Virk, A.S. and Hall, W., 2010. A review of bast fibres and their composites. Part 1–Fibres as reinforcements. *Composites Part A: Applied Science and Manufacturing*, 41(10), pp.1329-1335.

Taban E, Soltani P, Berardi U, Putra A, Mousavi SM, Faridan M, Samaei SE, Khavanin A. Measurement, modeling, and optimization of sound absorption performance of Kenaf fibers for building applications. *Building and Environment*. 2020 Aug 1;180:107087.

Taheri S. A review on five key sensors for monitoring of concrete structures. *Construction and Building Materials*. 2019 Apr 20;204:492-509.

Taiwo EM, Yahya K, Haron Z. Potential of using natural fiber for building acoustic absorber: A review. In *Journal of Physics: Conference Series* 2019 Aug 1 (Vol. 1262, No. 1, p. 012017). IOP Publishing.

Tran KQ, Satomi T, Takahashi H. Tensile behaviors of natural fiber and cement reinforced soil subjected to direct tensile test. *Journal of Building Engineering*. 2019 Jul 1;24:100748.

Van Damme H. Concrete material science: Past, present, and future innovations. *Cement and Concrete Research*. 2018 Oct 1;112:5-24.

Wangler T, Roussel N, Bos FP, Salet TA, Flatt RJ. Digital concrete: a review. *Cement and Concrete Research*. 2019 Sep 1;123:105780.

Xu, Q. and Chang, G.K., 2014. Experimental and numerical study of asphalt material geospatial heterogeneity with intelligent compaction technology on roads. *Construction and Building Materials*, 72, pp.189-198.

Yahya MN, Sambu M, Latif HA, Junaid TM. A study of acoustics performance on natural fibre composite. In IOP Conference Series: Materials Science and Engineering 2017 Aug 1 (Vol. 226, No. 1, p. 012013). IOP Publishing.

Yang T, Hu L, Xiong X, Petru M, Noman MT, Mishra R, Militký J. Sound absorption properties of natural fibers: A review. *Sustainability*. 2020 Oct 14;12(20):8477.

Yang T, Hu L, Xiong X, Petru M, Noman MT, Mishra R, Militký J. Sound absorption properties of natural fibers: A review. *Sustainability*. 2020 Oct 14;12(20):8477.

Yang T, Hu L, Xiong X, Petru M, Noman MT, Mishra R, Militký J. Sound absorption properties of natural fibers: A review. *Sustainability*. 2020 Oct 14;12(20):8477.

Yap ZS, Khalid NH, Haron Z, Khu WH, Yeak SH, Amran M. Rock wool-reinforced concrete: Physico-mechanical properties and predictive modelling. *Journal of Building Engineering*. 2022 Nov 1;59:105128.

Yusuff I, Sarifuddin N, Ali AM. A review on kenaf fiber hybrid composites: Mechanical properties, potentials, and challenges in engineering applications. *Progress in Rubber, Plastics and Recycling Technology*. 2021 Feb;37(1):66-83.

Zhou C, Cai L, Chen Z, Li J. Effect of kenaf fiber on mechanical properties of high-strength cement composites. *Construction and Building Materials*. 2020 Dec 10;263:121007.

Zhu, X., Kim., Wang, Q. and Wu, Q., 2013. Recent advances in the sound insulation properties of bio-based materials. *BioResources*, 9(1), pp. 1764-1786

APPENDICES

GANTT CHART FOR PSM 1

APPENDIX A

No	Task	Status	Week													
			1	2	3	4	5	6	7	8	9	10	11	12	13	14
1	Supervisor Selection and Registered PSM Title	Plan														
		Actual														
2	Briefing of PSM title	Plan														
		Actual														
3	Module 1: Research Design And Planning	Plan														
		Actual														
4	Discuss Problem Statement And Objective For Chapter 1	Plan														
		Actual														
5	Drafting And Writing Chapter 1	Plan														
		Actual														
6	Module 2: Final Year Project Literature Review	Plan														
		Actual														
7	Drafting And Writing Chapter 2	Plan														
		Actual														
8	Module 3: Research Methodology	Plan														
		Actual														
9	Drafting And Writing Chapter 3	Plan														
		Actual														
10	Drafting And Writing Chapter 4 (Expected Results)	Plan														
		Actual														
11	Recheck And Submit Chapter 1,2, 3, And 4	Plan														
		Actual														
12	Preparation And Presentation of PSM 1	Plan														
		Actual														

GANTT CHART FOR PSM 2

APPENDIX B

Task Project		Gantt Chart For PSM 2															
		Status	Week														
			1	2	3	4	5	6	7	8	9	10	11	12	13	14	
Discussion planning task with supervisor	Plan																
	Actual																
Cutting mold	Plan																
	Actual																
Raw material preparation	Plan																
	Actual																
Fabrication process	Plan																
	Actual																
Cutting sample	Plan																
	Actual																
Testing sample	Plan																
	Actual																
Analysis of the data	Plan																
	Actual																
Draft and writing of Chapter 4	Plan																
	Actual																
Submission of chapter 4	Plan																
	Actual																
Draft and writing of Chapter 5	Plan																
	Actual																
Submission of Chapter 5	Plan																
	Actual																
Submission draft report PSM 2	Plan																
	Actual																
Last correction of the report	Plan																
	Actual																
Submission of report to supervisor and panels	Plan																
	Actual																
Preparation of slide andr presentation of PSM 2	Plan																
	Actual																

SHAZMIN BINTI SHAHRULZAMAN_B092010457

ORIGINALITY REPORT

17%

SIMILARITY INDEX

11%

INTERNET SOURCES

11%

PUBLICATIONS

6%

STUDENT PAPERS

PRIMARY SOURCES

1	www.mdpi.com Internet Source	1%
2	Submitted to Universiti Teknikal Malaysia Melaka Student Paper	1%
3	digitalcollection.utm.edu.my Internet Source	1%
4	eprints.usm.my Internet Source	1%
5	www.researchgate.net Internet Source	1%
6	Submitted to University of Dundee Student Paper	<1%
7	David, N. V., M. N. Zainal, and M. J. M. Nor. "Determination of the Effects of Air Gap and Hind Support on the Sound Absorption Coefficient of Biobased and Foam Materials", Volume 12 Vibration Acoustics and Wave Propagation, 2012. Publication	<1%

8	worldwidescience.org Internet Source	<1 %
9	Musli Nizam Yahya, Desmond Daniel Vui Sheng Chin. "A Review on the Potential of Natural Fibre for Sound Absorption Application", IOP Conference Series: Materials Science and Engineering, 2017 Publication	<1 %
10	clausiuspress.com Internet Source	<1 %
11	dspace.tul.cz Internet Source	<1 %
12	Submitted to Pusan National University Library Student Paper	<1 %
13	Submitted to University Tun Hussein Onn Malaysia Student Paper	<1 %
14	Submitted to Fr Gabriel Richard High School Student Paper	<1 %
15	Tidarut Jirawattanasomkul, Tamon Ueda, Suched Likitlersuang, Dawei Zhang et al. "Effect of natural fibre reinforced polymers on confined compressive strength of concrete", Construction and Building Materials, 2019 Publication	<1 %

16	publisher.uthm.edu.my Internet Source	<1 %
17	www.utm.my Internet Source	<1 %
18	www.hindawi.com Internet Source	<1 %
19	Manish Raj, Shahab Fatima, Naresh Tandon. "A study of areca nut leaf sheath fibers as a green sound-absorbing material", Applied Acoustics, 2020 Publication	<1 %
20	umpir.ump.edu.my Internet Source	<1 %
21	S.E. Kishore, R. Sujithra, B. Dhatreyi. "A review on latest acoustic noise mitigation materials", Materials Today: Proceedings, 2021 Publication	<1 %
22	bioresources.cnr.ncsu.edu Internet Source	<1 %
23	coek.info Internet Source	<1 %
24	ebin.pub Internet Source	<1 %
25	Ankit Jain, Cheruku Sandesh Kumar, Yogesh Shrivastava. "Fabrication and Machining of	<1 %

Fiber Matrix Composite through Electric Discharge Machining: A short review",
Materials Today: Proceedings, 2022

Publication

26	Ancuța Elena Tiuc, Ovidiu Nemeș, Horatiu Vermesan, Adina Cristina Toma. "New sound absorbent composite materials based on sawdust and polyurethane foam", Composites Part B: Engineering, 2018 Publication	<1 %
27	c.coek.info Internet Source	<1 %
28	"Pineapple Leaf Fibers", Springer Science and Business Media LLC, 2020 Publication	<1 %
29	Sezgin Ersoy, Haluk Küçük. "Investigation of industrial tea-leaf-fibre waste material for its sound absorption properties", Applied Acoustics, 2009 Publication	<1 %
30	agronomy.emu.ee Internet Source	<1 %
31	Desmond Daniel Vui Sheng Chin, Musli Nizam Bin Yahya, Nazli Bin Che Din, Pauline Ong et al. "Sound Absorption Performance of Micro-Perforated Panel (MPP) Made from Biodegradable Composite (<i>Hibiscus</i>	<1 %

Cannabinus+PLA) Material", Key Engineering Materials, 2018

Publication

32

Submitted to Imperial College of Science, Technology and Medicine

<1%

Student Paper

33

eprints.uthm.edu.my

<1%

Internet Source

34

"Green Biocomposites", Springer Science and Business Media LLC, 2017

<1%

Publication

35

Arun Raju, M. Shanmugaraja. "Recent researches in fiber reinforced composite materials: A review", Materials Today: Proceedings, 2020

<1%

Publication

36

"Acoustic Textiles", Springer Science and Business Media LLC, 2016

<1%

Publication

37

Submitted to Manipal University

<1%

Student Paper

38

Ebrahim Taban, Parham Soltani, Umberto Berardi, Azma Putra et al. "Measurement, modeling, and optimization of sound absorption performance of Kenaf fibers for building applications", Building and Environment, 2020

<1%

Publication

39	etheses.whiterose.ac.uk Internet Source	<1 %
40	www.tandfonline.com Internet Source	<1 %
41	link.springer.com Internet Source	<1 %
42	www.techscience.com Internet Source	<1 %
43	Abdul Latif, Hanif, Musli Nizam Yahya, Mohamed Najib Rafiq, Mathan Sambu, Mohd Imran Ghazali, and Mohamed Nasrul Mohamed Hatta. "A Preliminary Study on Acoustical Performance of Oil Palm Mesocarp Natural Fiber", Applied Mechanics and Materials, 2015. Publication	<1 %
44	eprints.utm.my Internet Source	<1 %
45	Abhishek Sadananda Madival, Deepak Doreswamy, Raviraj Shetty. "A review on the physical and mechanical properties of natural fiber reinforced composites and its machinability using abrasive waterjet machining", Materials Today: Proceedings, 2023 Publication	<1 %

46	Z.Y. Lim, A. Putra, M.J.M. Nor, M.Y. Yaakob. "Sound absorption performance of natural kenaf fibres", Applied Acoustics, 2018 Publication	<1 %
47	dokumen.pub Internet Source	<1 %
48	"Aging Effects on Natural Fiber-Reinforced Polymer Composites", Springer Science and Business Media LLC, 2022 Publication	<1 %
49	Submitted to University of Surrey Student Paper	<1 %
50	mSPACE.lib.umanitoba.ca Internet Source	<1 %
51	hdl.handle.net Internet Source	<1 %
52	riunet.upv.es Internet Source	<1 %
53	Submitted to Universiti Kebangsaan Malaysia Student Paper	<1 %
54	Submitted to Universiti Tenaga Nasional Student Paper	<1 %
55	dSPACE.lib.cranfield.ac.uk Internet Source	<1 %

hasselbom.com.php54.levonline.com

56	Internet Source	<1 %
57	mdpi-res.com Internet Source	<1 %
58	"Handbook of Epoxy/Fiber Composites", Springer Science and Business Media LLC, 2022 Publication	<1 %
59	Submitted to Salah College of Technology Student Paper	<1 %
60	www.intechopen.com Internet Source	<1 %
61	InCIEC 2014, 2015. Publication	<1 %
62	Md Azree Othuman Mydin, Mohd Nasrun Mohd Nawii, Ruba A. Odeh, Anas A. Salameh. "Potential of Biomass Frond-Fiber on Mechanical Properties of Green Foamed Concrete", Sustainability, 2022 Publication	<1 %
63	Yi Jiang, Tung-Chai Ling, Caijun Shi, Shu-Yuan Pan. "Characteristics of steel slags and their use in cement and concrete—A review", Resources, Conservation and Recycling, 2018 Publication	<1 %
64	www.amazon.se	

	Internet Source	<1 %
65	"Vegetable Fiber Composites and their Technological Applications", Springer Science and Business Media LLC, 2021 Publication	<1 %
66	Ashafi'e Mustafa, Mohd Fadzli Bin Abdollah, Fairuz Fazillah Shuhimi, Nurhidayah Ismail, Hilmi Amiruddin, Noritsugu Umehara. "Selection and verification of kenaf fibres as an alternative friction material using Weighted Decision Matrix method", Materials & Design, 2015 Publication	<1 %
67	Submitted to City University of Hong Kong Student Paper	<1 %
68	www.clinicaltrialsregister.eu Internet Source	<1 %
69	ejournal.indo-intellectual.id LAYSIA MELAKA Internet Source	<1 %
70	unsworks.unsw.edu.au Internet Source	<1 %
71	"Hybrid Fiber Composites", Wiley, 2020 Publication	<1 %
72	Submitted to Universiti Teknologi Malaysia Student Paper	<1 %

73	Submitted to University of Cape Town Student Paper	<1 %
74	nova.newcastle.edu.au Internet Source	<1 %
75	İbrahim Can Kaymaz, Alperen Doğru, Miray Batıkan Kandemir, Mehmet Özgür Seydibeyoğlu. "Investigations of the Friction and Wear Resistance of the Natural Fiber-Reinforced Polyamide Composites", Wiley, 2024 Publication	<1 %
76	Aamir Mahmood, Muhammad Tayyab Noman, Miroslava Pechočiaková, Nesrine Amor et al. "Geopolymers and Fiber-Reinforced Concrete Composites in Civil Engineering", Polymers, 2021 Publication	<1 %
77	Submitted to Universiti Malaysia Perlis Student Paper	<1 %
78	eprints.usq.edu.au Internet Source	<1 %
79	penerbit.uthm.edu.my Internet Source	<1 %
80	"Structural Health Monitoring System for Synthetic, Hybrid and Natural Fiber	<1 %

Composites", Springer Science and Business Media LLC, 2021

Publication

81	Submitted to Brunel University Student Paper	<1 %
82	Ebrahim Taban, Ali Khavanin, Abdolreza Ohadi, Azma Putra, Ahmad Jonidi Jafari, Mohammad Faridan, Ardalan Soleimanian. "Study on the acoustic characteristics of natural date palm fibres: Experimental and theoretical approaches", Building and Environment, 2019 Publication	<1 %
83	Submitted to Kingston University Student Paper	<1 %
84	Motoe Ando, Masatoshi Sato. "Evaluation of the self-bonding ability of sugi and application of sugi powder as a binder for plywood" Journal of Wood Science, 2010 Publication	<1 %
85	Submitted to Newcastle College, Tyne & Wear Student Paper	<1 %
86	mts.intechopen.com Internet Source	<1 %
87	1library.net Internet Source	<1 %

88	Detao Liu, Kunfeng Xia, Wenxiong Chen, Rendang Yang, Bin Wang. "Preparation and design of green sound-absorbing materials via pulp fibrous models", Journal of Composite Materials, 2011 Publication	<1%
89	Pouya Hassani, Parham Soltani, Mohammad Ghane, Mohammad Zarrebini. "Porous resin-bonded recycled denim composite as an efficient sound-absorbing material", Applied Acoustics, 2021 Publication	<1%
90	accedacris.ulpgc.es Internet Source	<1%
91	cait.rutgers.edu Internet Source	<1%
92	perpustakaan.poltekkes-malang.ac.id Internet Source	<1%
93	Aruna Subasinghe, Arcot A. Somashekar, Debes Bhattacharyya. "Effects of wool fibre and other additives on the flammability and mechanical performance of polypropylene/kenaf composites", Composites Part B: Engineering, 2018 Publication	<1%
94	Cellulose Fibers Bio- and Nano-Polymer Composites, 2011.	<1%

95	Submitted to Higher Education Commission Pakistan Student Paper	<1 %
96	www.ncbi.nlm.nih.gov Internet Source	<1 %
97	B.U. Anyanwu, G.O. Olayinka, D.T. Ezeokeke, O.S. Fayomi, O.O. Oluwole. " Effect of Kenaf Core Fibre () as one of the Dispersing Phases in Brake Pad Composite Production ", Journal of Physics: Conference Series, 2019 Publication	<1 %
98	Chunheng Zhou, Liping Cai, Zongping Chen, Junhua Li, Sheldon Q. Shi. "Effect of kenaf fiber on mechanical properties of high-strength cement composites", Construction and Building Materials, 2020 Publication	<1 %
99	Manufacturing of Natural Fibre Reinforced Polymer Composites, 2015.AYSIA MELAKA Publication	<1 %
100	Md Al-Mamun, Mohd Y. Rafii, Azizah Binti Misran, Zulkarami Berahim et al. " Kenaf (L.): A Promising Fiber Crop with Potential for Genetic Improvement Utilizing Both Conventional and Molecular Approaches ", Journal of Natural Fibers, 2022 Publication	<1 %

101	Submitted to Nottingham Trent University Student Paper	<1 %
102	Mohamed Ali Elkasaby, Utkarsh, Nabeel Ahmed Syed, Ghaus Rizvi, Atef Mohany, Remon Pop-Iliev. "Evaluation of electro-spun polymeric nanofibers for sound absorption applications", AIP Publishing, 2020 Publication	<1 %
103	Submitted to Queensland University of Technology Student Paper	<1 %
104	"Lignocellulosic Composite Materials", Springer Science and Business Media LLC, 2018 Publication	<1 %
105	Submitted to Asian Institute of Technology Student Paper	<1 %
106	Submitted to International Islamic University Malaysia Student Paper	<1 %
107	Mlando Basel Mvubu, Rajesh Anandjiwala, Asis Patnaik. "Effects of air gap, fibre type and blend ratio on sound absorption performance of needle-punched non-woven fabrics", Journal of Engineered Fibers and Fabrics, 2019 Publication	<1 %

108	Submitted to Universiti Malaysia Pahang Student Paper	<1 %
109	Submitted to University College Technology Sarawak Student Paper	<1 %
110	eprints.utar.edu.my Internet Source	<1 %
111	etd.aau.edu.et Internet Source	<1 %
112	ro.uow.edu.au Internet Source	<1 %
113	0-www-mdpi-com.brum.beds.ac.uk Internet Source	<1 %
114	F.U.S.M. Saad, N. Salim, R. Roslan. "Physical and mechanical properties of kenaf/seaweed reinforced polypropylene composite" Materials Today: Proceedings, 2021 Publication	<1 %
115	N M Azzmi, J M Yatim, D Mazlan, Norhidayah Md Ulang, S Z Hashim, N A S Kamarudin. "Effect of reduction of heat using Kenaf fibrous pulverised fuel ash concrete in hydration process", IOP Conference Series: Materials Science and Engineering, 2021 Publication	<1 %

116	Seyed Ehsan Samaei, Umberto Berardi, Ebrahim Taban, Parham Soltani, Seyed Mohammad Mousavi. "Natural fibro-granular composite as a novel sustainable sound-absorbing material", Applied Acoustics, 2021 Publication	<1 %
117	Submitted to University of Brighton Student Paper	<1 %
118	Submitted to University of the Sunshine Coast Student Paper	<1 %
119	Submitted to Vilnius Gediminas Technical University Student Paper	<1 %
120	acikbilim.yok.gov.tr Internet Source	<1 %
121	chinawebshop.su Internet Source	<1 %
122	1library.co Internet Source	<1 %
123	F S Shahr, M T H Sultan, A U M Shah, S N A Safri. "A short review on the extraction of kenaf fibers and the mechanical properties of kenaf powder composites", IOP Conference Series: Materials Science and Engineering, 2019 Publication	<1 %

124	Nur-Ushafa Mazumder, Rashed Al Mizan, Mohammad Irfan Iqbal. "Advances and applications of biofiber-based polymer composites", Elsevier BV, 2022 Publication	<1 %
125	P. Soltani, R. Mirzaei, E. Samaei, M. NourMohammadi, S. Gharib, D. D. Abdi, E. Taban. "Sound absorption characteristics of aluminosilicate fibers", International Journal of Environmental Science and Technology, 2022 Publication	<1 %
126	Ramesh, M.. "Kenaf (Hibiscus cannabinus L.) fibre based bio-materials: A review on processing and properties", Progress in Materials Science, 2016. Publication	<1 %
127	channeli.in Internet Source	<1 %
128	ijsret.com Internet Source	<1 %
129	ncsu.edu Internet Source	<1 %
130	patents.google.com Internet Source	<1 %
131	sutir.sut.ac.th:8080 Internet Source	<1 %

		<1 %
132	Abir Khan, S.M. Sapuan, Vasi Uddin Siddiqui, E.S. Zainudin, M.Y.M. Zuhri, M.M. Harussani. "A review of recent developments in kenaf fiber/polylactic acid composites research", International Journal of Biological Macromolecules, 2023 Publication	<1 %
133	Mengtao Liang, Huagen Wu, Jiankang Liu, Yuqi Shen, Guanghua Wu. "Improved sound absorption performance of synthetic fiber materials for industrial noise reduction: a review", Journal of Porous Materials, 2022 Publication	<1 %
134	Mokgaotsa Jonas Mochane, Teboho Clement Mokhena, Emmanuel Rotimi Sadiku, S. S. Ray, T. G. Mofokeng. "Chapter 2 Green Polymer Composites Based on Polylactic Acid (PLA) and Fibers", Springer Science and Business Media LLC, 2019 Publication	<1 %
135	Pradyut Anand, Anand Kumar Sinha, Puja Rajhans. "Study on Mechanical and Durability Properties of Aerated Concrete Block Containing Construction and Demolition Waste with Aluminium Stearate Powder Along with Alkaline Solution and Considering	<1 %

Accelerated Curing Tank", Iranian Journal of
Science and Technology, Transactions of Civil
Engineering, 2023

Publication

136 Thinesh Sharma Balakrishnan, Mohamed
Thariq Hameed Sultan, Farah Syazwani
Shahar, Adi Azriff Basri et al. "Fatigue and
Impact Properties of Kenaf/Glass-Reinforced
Hybrid Pultruded Composites for Structural
Applications", Materials, 2024

Publication

137 Submitted to Universiti Teknologi MARA <1 %
Student Paper

138 afinia.com <1 %
Internet Source

139 dspace.lboro.ac.uk <1 %
Internet Source

140 eprints.utem.edu.my <1 %
Internet Source

141 ikpress.yolasite.com <1 %
Internet Source

142 library.ctr.utexas.edu <1 %
Internet Source

143 ml.scribd.com <1 %
Internet Source

vuir.vu.edu.au

144	Internet Source	<1%
145	www.lidsen.com Internet Source	<1%
146	E.A. Darwish, Mohamad Midani. "The potential of date palm midribs-based fabric acoustic panels for sustainable interior design", <i>Ain Shams Engineering Journal</i> , 2022 Publication	<1%
147	H.N. Dhakal, Z.Y. Zhang, R. Guthrie, J. MacMullen, N. Bennett. "Development of flax/carbon fibre hybrid composites for enhanced properties", <i>Carbohydrate Polymers</i> , 2013 Publication	<1%
148	Md Zobair Al Mahmud, Md Didarul Islam, S.M. Fazle Rabbi. "Analysis of epoxy composites reinforced with jute, banana, and coconut fibers and enhanced with Rubik's layer: Tensile, bending, and impact performance evaluation", <i>Journal of the Mechanical Behavior of Biomedical Materials</i> , 2023 Publication	<1%
149	Rubén Maderuelo-Sanz, Francisco José García-Cobos, Francisco José Sánchez-Delgado, María Isabel Mota-López et al.	<1%

"Mechanical, thermal and acoustical evaluation of biocomposites made of agricultural waste for ceiling tiles", Applied Acoustics, 2022

Publication

150 S Gokulkumar, PR Thyla, L Prabhu, S Sathish. "Measuring Methods of Acoustic Properties and Influence of Physical Parameters on Natural Fibers: A Review", Journal of Natural Fibers, 2019

Publication

151 S. Mohd Izwan, S.M. Sapuan, M.Y.M. Zuhri, A.R. Mohamed. "Thermal Stability and Dynamic Mechanical Analysis of Benzoylation Treated Sugar Palm/Kenaf Fiber Reinforced Polypropylene Hybrid Composites", Polymers, 2021

Publication

152 S. Thirumalvalavan, N. Senthilkumar, B. Deepanraj, L. Syam Sundar. "Assessment of mechanical properties of flax fiber reinforced with Delrin polymer composite", Materials Today: Proceedings, 2023

Publication

153 Shuang Su, Yuan Gao, Xinghai Zhou, Xiaoqing Xiong, Ying Wang, Lihua Lyu. "Structure of Waste Hemp Stalks and Their Sound Absorbing Properties", Polymers, 2022

Publication

154	Smita Salunkhe, Chetan Patil, Chetan M. Thakar. "Exploring the potential of natural materials as eco-friendly sound absorbers", Materials Today: Proceedings, 2023 Publication	<1 %
155	Tidarut Jirawattanasomkul, Suched Likitlersuang, Nattamet Wuttiwannasak, Tamon Ueda, Dawei Zhang, Thanakit Voravutvityaruk. "Effects of Heat Treatment on Mechanical Properties of Jute Fiber-Reinforced Polymer Composites for Concrete Confinement", Journal of Materials in Civil Engineering, 2020 Publication	<1 %
156	Submitted to University of Edinburgh Student Paper	<1 %
157	Xiuhong Li, Yujie Peng, Youqi He, Chupeng Zhang, Daode Zhang, Yong Liu. "Research Progress on Sound Absorption of Electrospun Fibrous Composite Materials", Nanomaterials, 2022 Publication	<1 %
158	businessdocbox.com Internet Source	<1 %
159	core.ac.uk Internet Source	<1 %

160	etd.astu.edu.et Internet Source	<1 %
161	pdfcoffee.com Internet Source	<1 %
162	vdocuments.mx Internet Source	<1 %
163	vtechworks.lib.vt.edu Internet Source	<1 %
164	"Handbook of Ecomaterials", Springer Nature, 2019 Publication	<1 %
165	"Second RILEM International Conference on Concrete and Digital Fabrication", Springer Science and Business Media LLC, 2020 Publication	<1 %
166	Jamal A. Abdalla, Blessen Skariah Thomas, Rami A. Hawileh. "Use of hemp, kenaf and bamboo natural fiber in cement-based concrete", Materials Today: Proceedings, 2022 Publication	<1 %
167	K. M. Rakesh, Ramachandracharya Srinidhi, S. Gokulkumar, K. S. Nithin et al. "Experimental Study on the Sound Absorption Properties of Finger Millet Straw, Darbha, and Ripe Bulrush Fibers", Advances in Materials Science and Engineering, 2021 Publication	<1 %

168	M.S. Khan, A. Fuzail Hashmi, M. Shariq, S.M. Ibrahim. "Effects of incorporating fibres on mechanical properties of fibre-reinforced concrete: A review", Materials Today: Proceedings, 2023 Publication	<1 %
169	M.T. Fadzlita, K.B. Yeo, W.H. Choong, M. Melvin. "Absorption Coefficient of Acoustic Coir Fibre Panel and Effects of Varying Percentage of Perforated Plates", Journal of Applied Sciences, 2014 Publication	<1 %
170	R. Dharmaraj, B. SivaKumar. "A feasibility study on cement with addition of Prosopis Juliflora ash as in concrete", Materials Today: Proceedings, 2020 Publication	<1 %
171	Said Bousshine, Mohamed Ouakarrouch, Abdelmajid Bybi, Najma Laaroussi, Mohammed Garoum, Amine Tilioua. "Acoustical and thermal characterization of sustainable materials derived from vegetable, agricultural, and animal fibers", Applied Acoustics, 2022 Publication	<1 %
172	Wong, I.L.. "A review of transparent insulation systems and the evaluation of payback period	<1 %

for building applications", Solar Energy, 200709

Publication

173 "Structural Integrity and Monitoring for Composite Materials", Springer Science and Business Media LLC, 2023

Publication

174 Ancauța Elena Tiuc, Ovidiu Nemeș, Horațiu Vermeșan, Adina Cristina Toma. "New sound absorbent composite materials based on sawdust and polyurethane foam",

Composites Part B: Engineering, 2019

Publication

175 Desmond Daniel Vui Sheng Chin, Musli Nizam Bin Yahya, Nazli Bin Che Din, Pauline Ong. "Acoustic properties of biodegradable composite micro-perforated panel (BC-MPP) made from kenaf fibre and polylactic acid (PLA)", Applied Acoustics, 2018

Publication

176 Jianli Liu, Xinjin Liu, Yan Xu, Wei Bao. "The acoustic characteristics of dual-layered porous nonwovens: a theoretical and experimental analysis", The Journal of The Textile Institute, 2014

Publication

177 Mark Alexander, Hans Beushausen. "Durability, service life prediction, and

<1 %

modelling for reinforced concrete structures – review and critique", Cement and Concrete Research, 2019

Publication

178

Veronika Gumanová, Lýdia Sobotová, Tibor Dzuro, Miroslav Badida, Marek Moravec. "Experimental Survey of the Sound Absorption Performance of Natural Fibres in Comparison with Conventional Insulating Materials", Sustainability, 2022

Publication

<1%

